Nama Jurnal : Mechanical Engineering for Society and Industry (MESI)

Judul Artikel : Improving the thermal efficiency of fin-tube heat exchangers by optimizing geometric parameters of curved rectangular winglet vortex generators

Penulis : **Dan Mugisidi,** Oktarina Heriyani, Amir Khalid, Ahmed Rahmani.

Status Penulis : Penulis ke 1, Koresponden.

Volume : Volume 6 No. 1 (2026)

Peringkat : Q3

Properties Q3

https://www.scimagojr.com/journalsearch.php?q=21101176033&tip=sid&clean=0

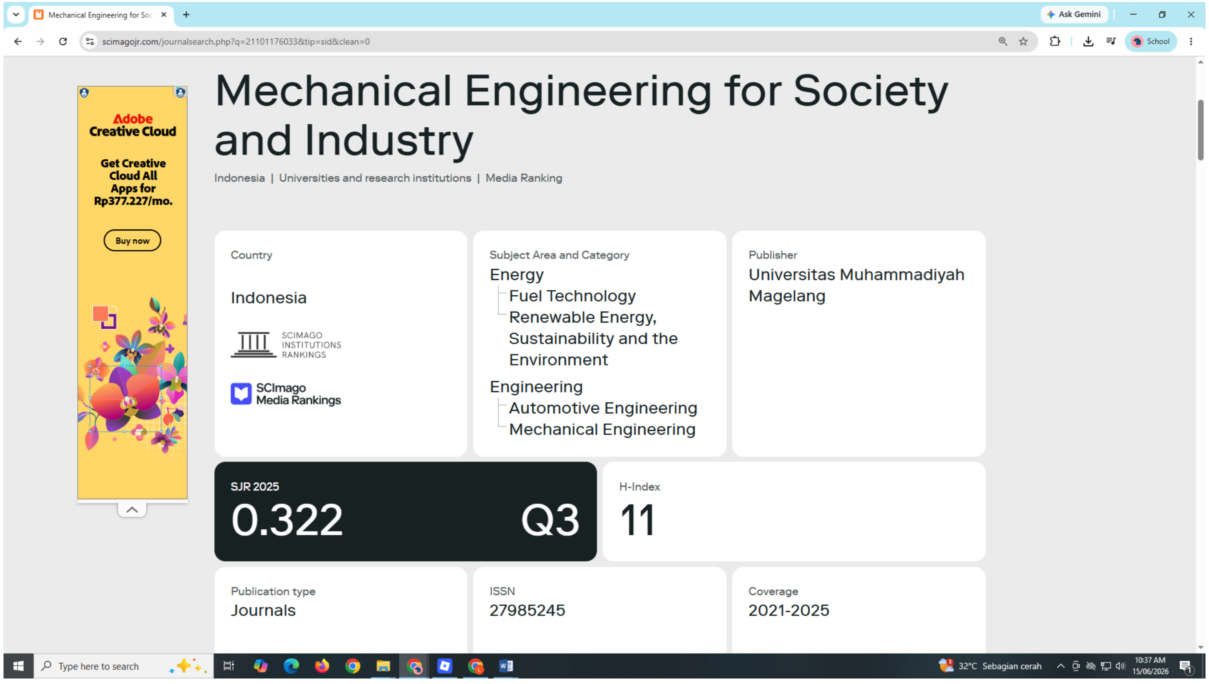

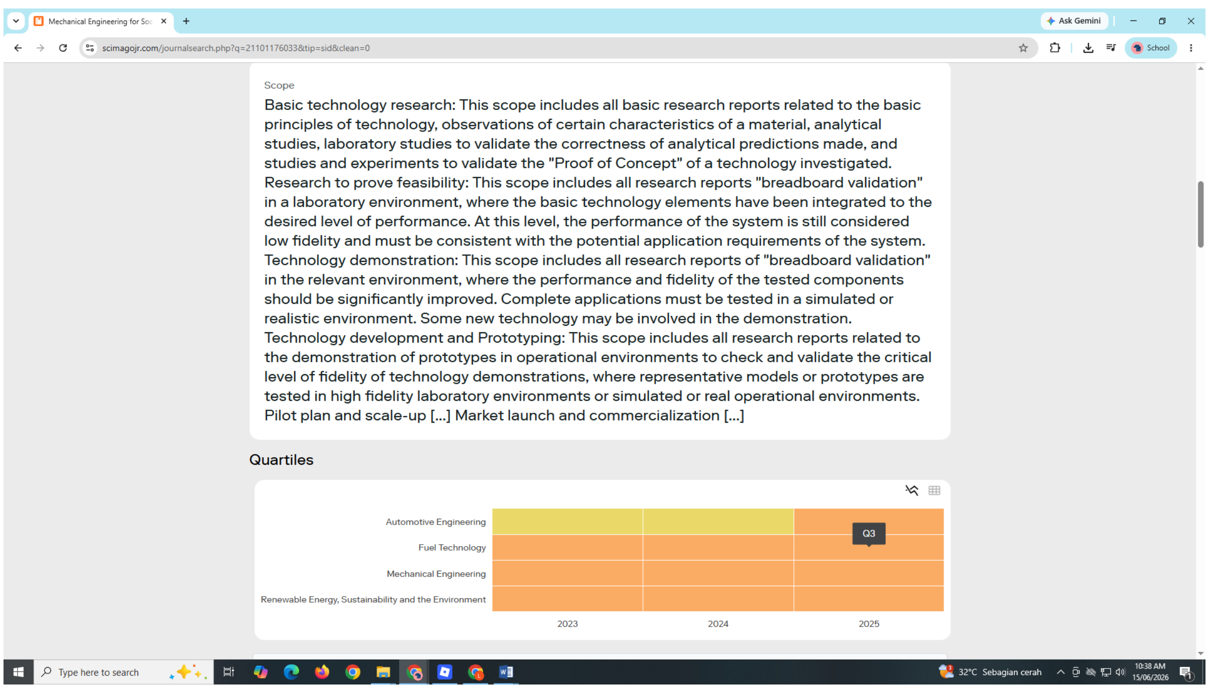

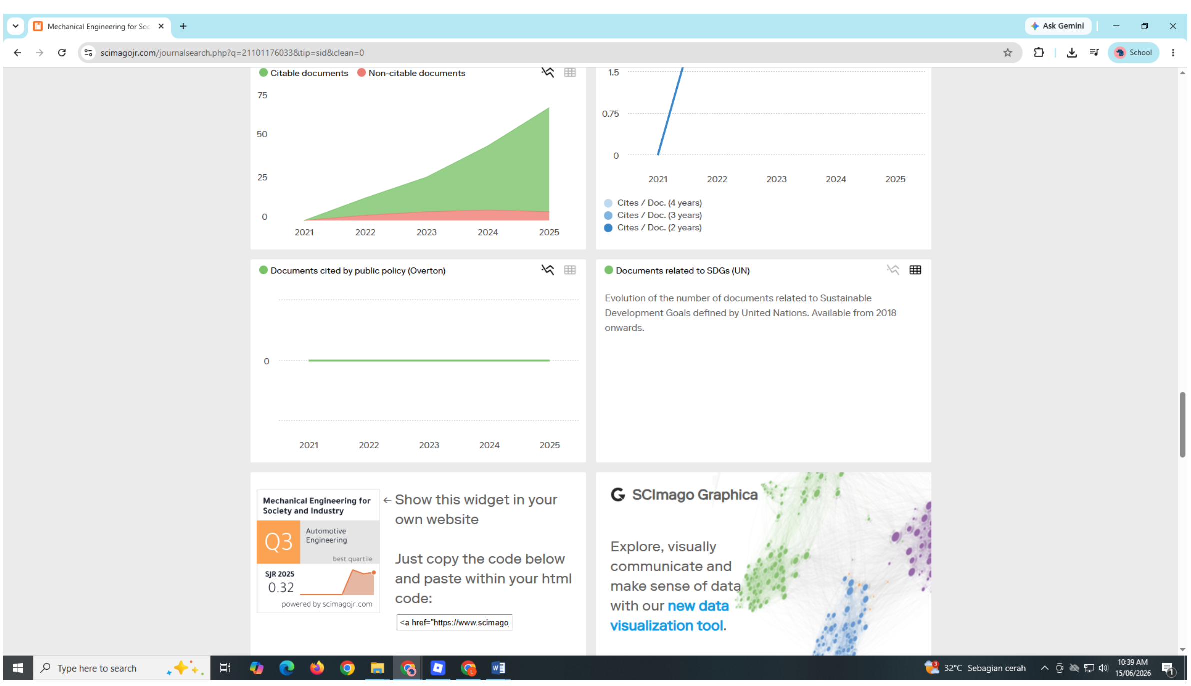

Link Journal

https://journal.unimma.ac.id/mesi/index

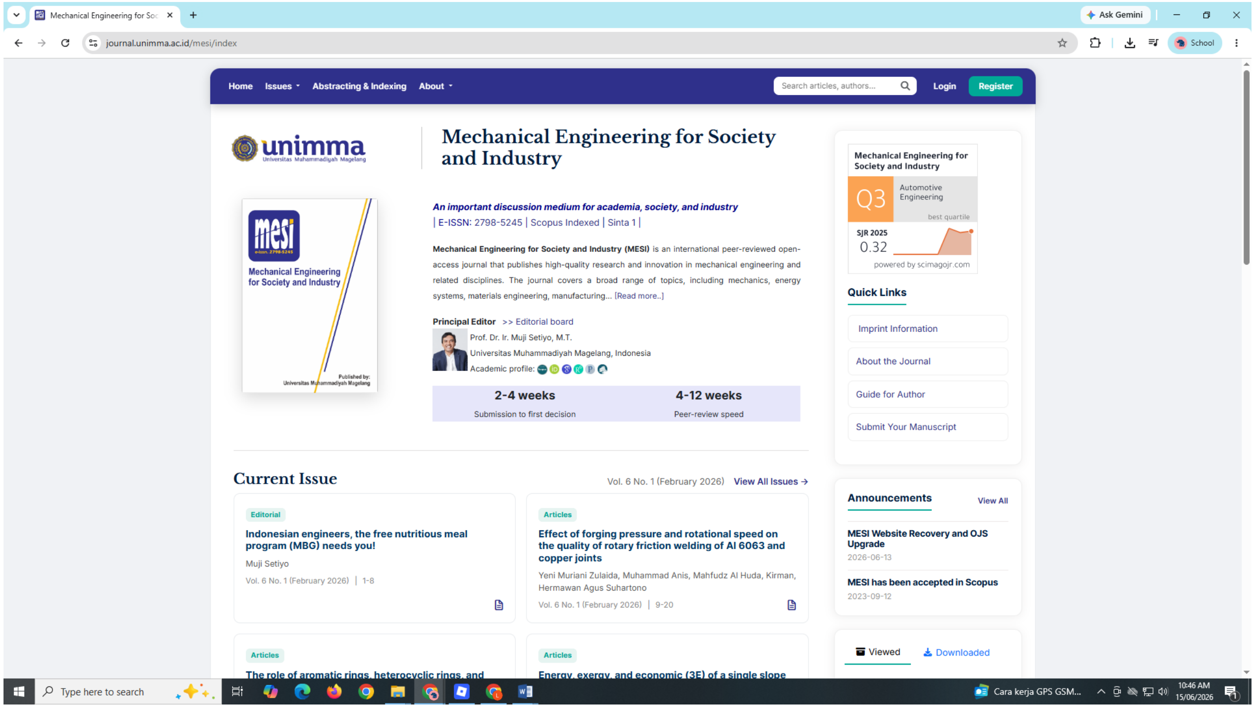

Link Editorial Board

https://journal.unimma.ac.id/mesi/editorialteam

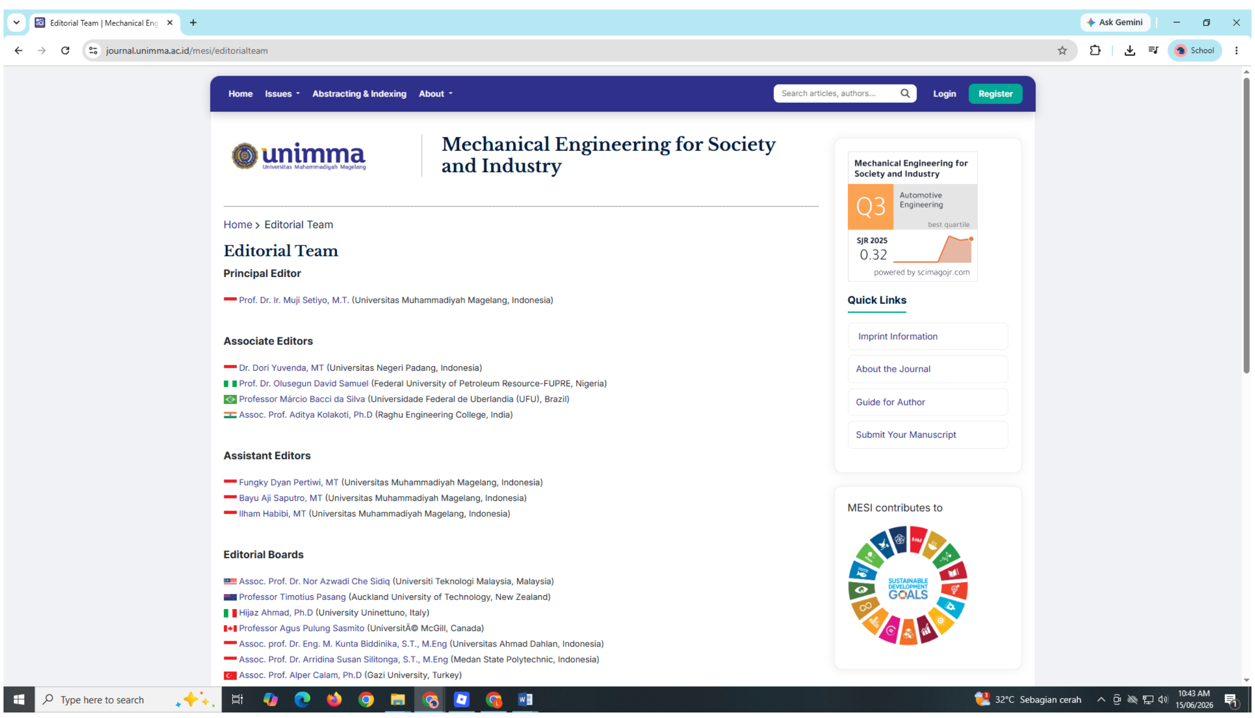

Daftar Isi

https://journal.unimma.ac.id/mesi/issue/view/666

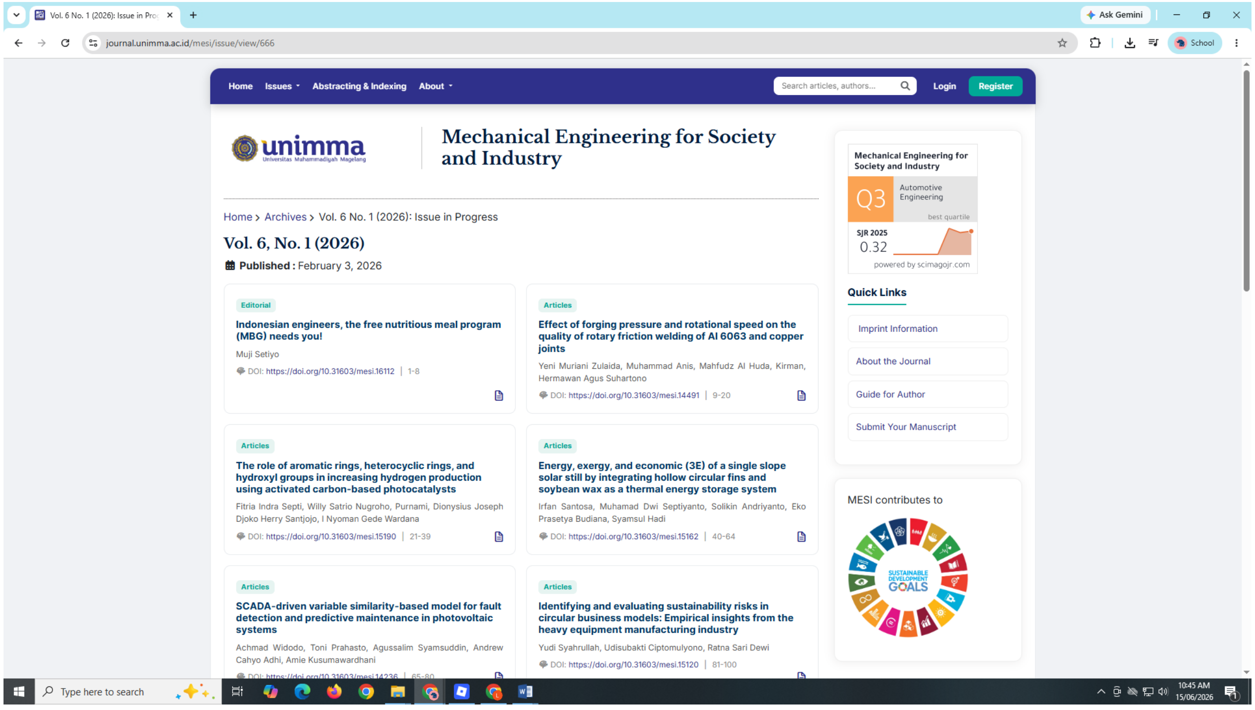

Link Artikel

https://journal.unimma.ac.id/mesi/article/view/15393

BUKTI KORESPONDENSI

Notifications

[MESI] Editor Decision

2026-02-19 02:19 PM

Dan Mugisidi, Oktarina Heriyani, Amir Khalid, Ahmed Rahmani:

We have reached a decision regarding your submission to Mechanical Engineering for Society and Industry, "Improving the Thermal Efficiency of Fin-tube Heat Exchangers by Optimizing Geometric Parameters of Curved Rectangular Winglet Vortex Generators".

Our decision is: **Revisions Required**

Please revise your manuscript carefully, the revision process requires two major documents:

-
    - The first is the revised manuscript highlighting all the modifications made following the recommendations received from the reviewers (example of the revised manuscript).
    - The second is a letter listing the authors’ responses illustrating they have addressed all the concerns of the reviewers and editors (example of response letter).

These two documents should be drafted carefully. The authors of the manuscript can agree or disagree with the comments of the reviewers and are not always obliged to implement their recommendations, but they should in all cases provide a well-argued justification for their course of action.

You are expected to return the revised paper no later than **2 weeks** from your receiving this notification.

Notifications

[MESI] Editor Decision

2026-02-19 02:19 PM

Dan Mugisidi, Oktarina Heriyani, Amir Khalid, Ahmed Rahmani:

We have reached a decision regarding your submission to Mechanical Engineering for Society and Industry, "Improving the Thermal Efficiency of Fin-tube Heat Exchangers by Optimizing Geometric Parameters of Curved Rectangular Winglet Vortex Generators".

Our decision is: **Revisions Required**

Please revise your manuscript carefully, the revision process requires two major documents:

- The first is the revised manuscript highlighting all the modifications made following the recommendations received from the reviewers (example of the revised manuscript).
- The second is a letter listing the authors' responses illustrating they have addressed all the concerns of the reviewers and editors (example of response letter).

These two documents should be drafted carefully. The authors of the manuscript can agree or disagree with the comments of the reviewers and are not always obliged to implement their recommendations, but they should in all cases provide a well-argued justification for their course of action.

You are expected to return the revised paper no later than **2 weeks** from your receiving this notification.

Notifications

[MESI] Editor Decision

2026-02-19 02:19 PM

Dan Mugisidi, Oktarina Heriyani, Amir Khalid, Ahmed Rahmani:

We have reached a decision regarding your submission to Mechanical Engineering for Society and Industry, "Improving the Thermal Efficiency of Fin-tube Heat Exchangers by Optimizing Geometric Parameters of Curved Rectangular Winglet Vortex Generators".

Our decision is: **Revisions Required**

Please revise your manuscript carefully, the revision process requires two major documents:

-
    - The first is the revised manuscript highlighting all the modifications made following the recommendations received from the reviewers (example of the revised manuscript).
    - The second is a letter listing the authors' responses illustrating they have addressed all the concerns of the reviewers and editors (example of response letter).

These two documents should be drafted carefully. The authors of the manuscript can agree or disagree with the comments of the reviewers and are not always obliged to implement their recommendations, but they should in all cases provide a well-argued justification for their course of action.

You are expected to return the revised paper no later than **2 weeks** from your receiving this notification.

Revised Manuscript

Participants Edit

Fungky Dyan Pertiwi (fungkydyan)

Dan Mugisidi (dmugisidi)

Messages

Note	From
Dear Editor Please kindly to find the revised manuscript Best Regards	dmugisidi Mar 05
Dear Author, Kindly check the manuscript using an appropriate plagiarism detection tool and ensure that the similarity index is below 15%. If the similarity exceeds this threshold, please revise the relevant sections accordingly before resubmitting the manuscript. Thank you for your attention.	fungkydyan Mar 16
Dear Editor Dear Editor, please kindly note that the similarity result is 15%, which meets the required threshold.	dmugisidi Mar 23

Revised Manuscript

Participants Edit

Fungky Dyan Pertiwi (fungkydyan)

Dan Mugisidi (dmugisidi)

Messages

Note	From
Dear Editor Please kindly to find the revised manuscript Best Regards	dmugisidi Mar 05
Dear Author, Kindly check the manuscript using an appropriate plagiarism detection tool and ensure that the similarity index is below 15%. If the similarity exceeds this threshold, please revise the relevant sections accordingly before resubmitting the manuscript. Thank you for your attention.	fungkydyan Mar 16
Dear Editor Dear Editor, please kindly note that the similarity result is 15%, which meets the required threshold.	dmugisidi Mar 23

Revised Manuscript

Participants Edit

Fungky Dyan Pertiwi (fungkydyan)

Dan Mugisidi (dmugisidi)

Messages

Note	From
Dear Editor Please kindly to find the revised manuscript Best Regards	dmugisidi Mar 05
Dear Author, Kindly check the manuscript using an appropriate plagiarism detection tool and ensure that the similarity index is below 15%. If the similarity exceeds this threshold, please revise the relevant sections accordingly before resubmitting the manuscript. Thank you for your attention.	fungkydyan Mar 16
Dear Editor Dear Editor, please kindly note that the similarity result is 15%, which meets the required threshold.	dmugisidi Mar 23

Dear editors and reviewers,

Thank you for your essential suggestions regarding our manuscript. We attach the revised manuscript through this journal system. We have marked the revised manuscript with yellow color for reviewer #A, blue color for reviewer #B, blue color for All reviewer.

<u>REVIEWER A</u>

1) Many studies have been conducted in this field. Specifically, what distinguishes the current work from other manuscript? The novelty of the manuscript has not been adequately articulated.

2) The introduction requires fundamental revision. The presented literature review is extremely weak.

3) The manuscript requires a comprehensive revision in terms of both stylistic and literary quality.

4) Please express the boundary conditions in mathematical form.

5) For the convergence assessment of the numerical solution, have only the residuals been checked?

6) An in-depth discussion about the results should be provided.

7) The Conclusions section needs to be improved, presenting a better discussion based on results.

8) In the manuscript, merely describing the trends of the figures is insufficient; a physical interpretation and analysis of the figures must be provided.

9) Including figures depicting flow streamlines could be beneficial.

10) The numerical solution methodology should be clearly presented.

11) Is a thermal enhancement factor of 1.075 cost-effective? Is it economically feasible considering the manufacturing costs of the vortex generator?

Our Response

1) We sincerely thank the reviewer for this important comment. We acknowledge that the novelty and distinguishing contributions of the manuscript were not sufficiently emphasized in the previous version. In the revised manuscript, we have carefully clarified and explicitly articulated the unique contributions of this study.

Specifically, the novelty of the present work lies in:

1. The integrated parametric investigation of both geometric perforation (hole width) and positional configuration (radial distance), which have predominantly been examined independently in previous studies.
2. The development of a performance-based geometric optimization framework that evaluates the coupled thermal–hydraulic effects of these two design variables.
3. The application of this framework to Circular Ring Winglet Vortex Generators (CRWVGs), for which systematic optimization studies remain limited.

In addition, we have revised the Introduction (line 28 Page 3 to line 10 page 4) to clearly define the research gap and added a dedicated paragraph explicitly stating the novelty and main contributions of the study. We believe these revisions now clearly distinguish our work from existing literature.

2) Thank you for this valuable comment. We fully acknowledge that the previous version of the Introduction did not sufficiently establish the scientific background and research gap. In the revised manuscript, we have fundamentally restructured the Introduction section.

Specifically, we have:

1. Expanded the literature review by incorporating recent and high-impact studies published in the last 5–7 years and synthesizing them into a coherent and well-structured narrative that provides a stronger theoretical foundation for the study.
2. Clearly identified the research gap and limitations in prior studies.
3. Explicitly highlighted the novelty and contribution of our work.

These revisions can be found in Pages 2–4 of the revised manuscript. We believe that the Introduction is now significantly improved and provides a stronger theoretical and contextual foundation for the study.

3) We sincerely thank the reviewer for this constructive comment. In response, the manuscript has undergone a comprehensive language revision to improve clarity, coherence, and overall academic style. The entire text has been carefully proofread and professionally edited by a native English speaker (or professional language editing service) to ensure grammatical accuracy, consistency in terminology, and improved readability.

We believe that these revisions have substantially enhanced the stylistic and literary quality of the manuscript. A professional English editing certificate has been obtained and can be provided upon request.

4) We thank the Reviewer for this constructive comment. In the revised manuscript (Section 2.3), the boundary conditions have been explicitly expressed in mathematical form, with all symbols clearly defined, to improve clarity and numerical reproducibility. The applied boundary conditions are summarized as follows:

Inlet (velocity inlet)

$$\mathbf{u} = (u_{in}, 0,0), T = T_{in}$$

where $\mathbf{u}$ is the velocity vector, $u_{in}$is the uniform inlet velocity, and $T_{in}$is the inlet air temperature.

Outlet (pressure outlet)

$$p = p_{out}$$

$$\frac{\partial \mathbf{u}}{\partial n} = 0, \frac{\partial T}{\partial n} = 0$$

where p_{out} is the reference outlet pressure and $n$denotes the outward normal direction at the outlet boundary.

Solid walls (tube, fins, and vortex generators)

$$\mathbf{u} = 0$$

$$T = T_w$$

where $T_w$is the constant wall temperature imposed on the tube surface.

Periodic boundaries (transverse/spanwise direction)

$$\phi(x, y, z) = \phi(x, y, z + P)$$

where ϕrepresents the dependent flow variables (velocity components, pressure, and temperature), and $P$is the periodic pitch length, as shown in pages 6 – 7.

5) We thank the Reviewer for this important comment. The convergence of the numerical solution was not evaluated solely based on residual reduction. A comprehensive convergence assessment combining residual-based, physical-based, and grid-independence criteria was employed to ensure numerical accuracy and physical reliability, in page 8.

First, the normalized residuals of the governing equations were monitored throughout the iterative process. Convergence was assumed when the residuals of continuity and momentum equations decreased below 10^{-6}, while a stricter criterion of $10^{-8}$was imposed for the energy equation, due to the heat-transfer-focused nature of the present study.

Second, in addition to residual monitoring, several global physical quantities were tracked to confirm solution stability. These quantities include the average Nusselt number (Nu_{avg}), friction factor (f), and outlet bulk temperature (T_{out}). The solution was considered physically converged only when the relative variation of these parameters over 500 successive iterations satisfied:

$$\left| \frac{\phi^{(n)} - \phi^{(n-500)}}{\phi^{(n)}} \right| < 0.1\%$$

where ϕrepresents Nu_{avg}, f, or T_{out}, and $n$denotes the current iteration.

Furthermore, a grid independence study was performed using four progressively refined grids, ranging from 600,641 to 915,422 elements. The relative differences in both $Nu_{avg}$and $f$between the two finest grids were found to be less than 0.1%, confirming that the numerical results are independent of mesh resolution. Details of the grid independence test are provided in Table 1 of the revised manuscript.

6) We sincerely thank the Reviewer for this valuable comment. In the revised manuscript, the Results and Discussion section has been substantially expanded to provide a deeper quantitative and physical interpretation of the numerical findings rather than merely describing observed trends. The revisions have been incorporated in the revised manuscript (Pages 11–18).

Specifically, the enhancement in heat transfer is now analyzed in relation to the vortex generation mechanism induced by the CRW-VGs. The results show that the maximum normalized Nusselt number (Nu/Nu_0) occurs at an angular position of $120°$, reaching **1.140** for the 0.25H hole width and **1.19** for the 0.5H hole width. These correspond to heat transfer enhancements of approximately **14%** and **19%**, respectively, compared to the baseline configuration. This improvement is attributed to stronger longitudinal vortices and intensified jet-induced mixing, which thin the thermal boundary layer and increase the local temperature gradient at the tube surface.

The friction characteristics were also analyzed quantitatively. At $\alpha = 120°$and $r/R = 1.25$, the normalized friction factor (f/f_0) reaches **1.193** for the 0.25H hole width and **1.165** for the 0.5H hole width, indicating increased momentum dissipation due to stronger vortex formation and flow separation. However, at moderate angular positions ($60°$–$90°$), the friction factor decreases, demonstrating a more favorable balance between mixing intensity and flow resistance.

Furthermore, the influence of radial placement was clarified. Increasing the radial distance from $r/R = 1.25$to 1.5 reduces the friction factor while slightly decreasing heat transfer enhancement, indicating that vortex–wake interaction weakens as the CRW-VGs move farther from the tube surface.

To provide a comprehensive thermo-hydraulic evaluation, the Thermal Enhancement Factor (TEF) was analyzed. The maximum TEF values of **1.075** (0.25H) and **1.064** (0.5H) were obtained at $\alpha = 120°$and $r/R = 1.25$. These values indicate overall performance improvements of approximately **7.5%** and **6.4%**, respectively, when both heat transfer augmentation and pressure drop penalties are considered simultaneously.

Additionally, the velocity, pressure, and temperature contours were reinterpreted to explain the physical mechanisms governing these trends. The jet flow emerging from the perforated CRW-VGs mitigates wake recirculation behind the tube, weakens stagnation regions, and promotes longitudinal vortex development. At moderate angular positions, coherent vortices enhance convective transport efficiently. At larger angles, excessive flow separation increases pressure loss, explaining the observed thermo-hydraulic trade-off.

The variation of Nu/Nu_0 with angle demonstrates a strong dependence on vortex stability and secondary flow development generated by the CRW-VGs. At lower angles (30°–60°), the winglets induce relatively weak longitudinal vortices, resulting in moderate boundary layer disruption and limited heat transfer enhancement. As the angle approaches 75°–90°, the vortex structure becomes less coherent, and partial flow recirculation reduces mixing efficiency, leading to the observed minimum in Nu/Nu_0. The maximum enhancement occurring near 120° indicates the formation of stable and well-developed longitudinal vortices that intensify cross-stream mixing and effectively thin the thermal boundary layer, thereby maximizing heat transfer. Beyond this angle (135°–150°), excessive flow separation and vortex breakdown reduce vortex coherence, diminishing thermal performance despite increased flow disturbance.

The influence of hole width further clarifies the underlying flow mechanisms. A smaller hole width (0.25H) generates more concentrated and energetic vortices, producing sharper peaks in Nu/Nu_0 due to stronger shear layer interaction and localized boundary layer thinning around the tube surface. In contrast, a larger hole width (0.5H) allows partial flow penetration through the perforation, which weakens the vortex core strength but promotes more stable and distributed secondary flows, resulting in smoother performance trends. Additionally, increasing the radial distance to r/R = 1.5 enhances the interaction between the induced vortices and the tube wake region, improving momentum and thermal energy exchange. These combined effects confirm that the heat transfer enhancement is governed by the balance between vortex strength, flow stability, and boundary layer disruption, with 120° representing the most effective configuration for vortex-induced thermal augmentation.

7) Thank you for your valuable comment. We agree that the previous version of the Conclusions section was relatively concise and did not sufficiently elaborate on the interpretation of the results. In the revised manuscript, the Conclusions section has been substantially improved by:

1. Providing a clearer synthesis of the main findings.
2. Adding a deeper discussion linking the results to the research objectives.
3. Highlighting the scientific contribution and practical implications of the study.

We believe these revisions have strengthened the discussion and improved the overall quality of the Conclusions section.

8) We sincerely thank the Reviewer for this constructive comment. In the revised manuscript, the discussion of all figures has been substantially strengthened to provide detailed physical interpretations rather than merely describing graphical trends.

Specifically, the velocity, pressure, and temperature contours (Figures 7–12) are now analyzed in terms of vortex generation, jet-induced mixing, boundary layer disruption, wake suppression, and flow separation behavior. The discussion explicitly links these flow phenomena to the quantitative variations observed in the normalized Nusselt number (Nu/Nu_0), friction factor (f/f_0), and Thermal Enhancement Factor (TEF).

For example, the maximum heat transfer enhancement at $\alpha = 120°$, where Nu/Nu_0reaches 1.140 (0.25H) and 1.19 (0.5H), is now explained by the formation of stronger longitudinal vortices and intensified jet interaction from the perforated CRW-VGs, which thin the thermal boundary layer and increase the wall temperature gradient. Similarly, the corresponding rise in friction factor (up to $f/f_0 = 1.193$and 1.165) is interpreted as a consequence of increased momentum dissipation and localized flow separation at higher angular positions.

Additionally, the reduction of friction factor at moderate angles (60°–90°) is physically explained by smoother wake behavior and weaker separation zones, as evidenced by the velocity and pressure contours. The temperature distributions are also interpreted to demonstrate how wake suppression and vortex–boundary layer interaction contribute to enhanced convective heat transfer.

9) Including figures depicting flow streamlines could be beneficial.

10) We sincerely thank the Reviewer for this valuable comment. We agree that the numerical solution methodology should be presented in a clearer and more structured manner to ensure transparency and reproducibility. Accordingly, the revised manuscript has been substantially improved in Sections 2.1–2.5 to explicitly describe the complete numerical procedure, including the physical modeling assumptions, discretization strategy, turbulence modeling, convergence criteria, grid independence analysis, and validation process (Pages 9 – 10).

The numerical methodology employed in this study is summarized as follows:

1. **Numerical Approach**

   The three-dimensional steady-state governing equations of mass, momentum, and energy were solved using the Finite Volume Method (FVM). The airflow was assumed to be incompressible, Newtonian, and turbulent with constant thermophysical properties.

2. **Turbulence Model**

   Turbulence effects were modeled using the shear stress transport (SST) k–ω model. This model was selected due to its proven capability in accurately predicting adverse pressure gradients and flow separation phenomena, which are expected in fin-tube heat exchangers equipped with curved rectangular winglet vortex generators (CRW-VGs).

3. **Discretization Scheme and Pressure–Velocity Coupling**

The convective terms of the momentum and energy equations were discretized using a second-order upwind scheme to improve numerical accuracy. Pressure–velocity coupling was handled using the SIMPLE algorithm to ensure stable and accurate convergence.

4. **Grid Strategy and Mesh Independence**

   A non-uniform mesh was generated with refined inflation layers near the tube and vortex generator surfaces to properly resolve velocity and thermal boundary layers. A grid independence study was conducted using four progressively refined meshes ranging from 600,641 to 915,422 cells. The variation in the average Nusselt number and friction factor between the two finest meshes was less than 0.1%, confirming mesh-independent results. Therefore, the mesh consisting of 822,157 cells was adopted for all simulations.

5. **Convergence Criteria**

   Convergence was achieved when the residuals of continuity and momentum equations were reduced below 10^{-5}, and the energy equation residual was reduced below 10^{-6}. In addition to residual monitoring, global performance parameters such as the average Nusselt number and pressure drop were monitored to ensure physical stability of the solution.

6. **Model Validation**

   The numerical model was validated against the reference data reported by Oh et al. The deviation of the predicted Nusselt number ranged between 2%–6%, while the deviation in friction factor ranged between 4%–8%. These deviations fall within acceptable limits, confirming the reliability of the adopted numerical methodology.

11) We sincerely thank the Reviewer for highlighting the importance of evaluating the economic relevance of the obtained Thermal Enhancement Factor (TEF).

In the present study, the maximum TEF achieved is approximately **1.075**, which corresponds to a **7.5% net improvement in thermo-hydraulic performance under constant fan power conditions**. By definition,

$$TEF = \frac{Nu/Nu_0}{(f/f_0)^{1/3}}$$

A TEF value greater than unity indicates that the enhancement in heat transfer outweighs the associated increase in flow resistance when evaluated under equal fan power input. Therefore, the obtained TEF confirms that the perforated CRW-VG configuration provides a thermodynamic advantage without imposing a disproportionate pressure penalty.

It is important to note that in air-side fin-and-tube heat exchangers, even moderate improvements in overall performance (5–10%) can be practically significant. A 7.5% enhancement may result in:

- Reduction in required heat transfer surface area for the same cooling capacity,
- Lower fan operating time to reach target thermal conditions,
- Potential reduction in system energy consumption over long-term operation,
- Improved compactness of the heat exchanger core.

Regarding manufacturing feasibility, the proposed curved rectangular winglet vortex generators (CRW-VGs) are passive devices fabricated from thin sheet material and integrated directly into the fin structure. The addition of perforations can be achieved using standard stamping or punching processes that are already common in fin production lines. Consequently, the incremental manufacturing cost is expected to be minimal, particularly in large-scale production.

Furthermore, the perforated configuration contributes to mitigating excessive pressure rise compared to solid vortex generators, thereby reducing the burden on the fan system. This balance between heat transfer enhancement and controlled pressure penalty supports the economic viability of the design.

REVIEWER B

1. The manuscript requires professional English proofreading. Several sentences contain grammatical errors and awkward phrasing that affect clarity and readability. A thorough language revision is strongly recommended before further consideration.
2. Some paragraphs throughout the manuscript are too short and fragmented, which disrupts the logical flow of the discussion. The authors are advised to merge related short paragraphs where appropriate to improve coherence and readability.
3. Symbols such as Nu/Nuo, f/fo, and r/R are not consistently formatted in terms of subscripts and notation. The manuscript would benefit from a dedicated Nomenclature section that clearly defines all symbols and ensures consistency throughout the paper.
4. The statement “While studies like that of Oh et al.,” is incomplete and not properly cited. Please revise the sentence structure and ensure that the citation is formatted correctly and clearly linked to the corresponding reference.

5. The quality of Figure 1 needs improvement. Some text and dimensional labels are not clearly visible, which makes it difficult to interpret the geometry and parameters. Please provide a higher-resolution figure with clearly readable annotations.
6. Figure 1 appears to contain three different illustrations. However, the manuscript does not clearly explain the differences between these subfigures. Please clarify in detail what each subfigure represents and how they differ from one another.
7. Please carefully re-examine the governing equations section. The equations are not clearly presented and appear incomplete. All conservation equations should be explicitly written and consistent with the stated assumptions and turbulence model.
8. After conducting the Grid Independence Test (GIT), which mesh configuration was ultimately selected for the final simulations? Please clearly state the selected number of elements and justify the choice.
9. There is a serious inconsistency in Section 3.2. The manuscript reports maximum TEF values of 1.075 and 1.064, but later states that TEF exceeds 1.5 at $\alpha = 120°$. This numerical inconsistency raises concerns about data reliability. The authors must verify the results, re-check Figure 13, and correct the reported maximum TEF values.
10. References [7] and [23] appear to be identical. Similarly, references [18] and [21], as well as [20] and [22], seem to be duplicated. Please carefully review and correct the reference list to eliminate redundancy.
11. The reported maximum TEF value of approximately 1.07 represents only about a 7% improvement. In the heat exchanger enhancement literature, TEF improvements typically range from 1.2 to 1.5. The authors should justify the engineering significance of this relatively modest enhancement, particularly considering the added manufacturing complexity of perforated vortex generators.

Our Response

1. Thank you for the constructive suggestion. The manuscript has been carefully proofread and edited by a professional English language editing service to enhance clarity, grammatical accuracy, and readability. All identified language issues have been corrected in the revised manuscript.
2. Thank you for the insightful comment. The manuscript has been carefully revised to improve logical flow and coherence. Short and fragmented paragraphs have been merged where appropriate to enhance readability and ensure smoother transitions between related ideas. We believe the overall structure and discussion are now more cohesive in the revised version.

3. Thank you for the valuable suggestion. All symbols and notations have been carefully standardized throughout the manuscript to ensure consistency in subscripts and formatting. In addition, a dedicated Nomenclature section has been added on Page 24 to clearly define all symbols and parameters used in the study.
4. Thank you for the careful observation. The citation has also been corrected and properly formatted to clearly correspond to the appropriate reference in the reference list. The revised sentence now provides a complete and coherent comparison within the context of related studies.
5. Thank you for your thoughtful comment. We sincerely appreciate your attention to detail. In response, we have carefully revised Figure 1 to enhance both its visual quality and readability. We are pleased to provide a higher-resolution version, with all dimensional labels, symbols, and annotations enlarged and reformatted for better clarity.
6. Thank you for this valuable comment. We have revised the description of Figure 1 to clearly explain the content and differences of each subfigure. The revised manuscript now explicitly describes the purpose of each subfigure in the figure caption and within the main text to ensure that readers can clearly distinguish between the global domain, the vortex generator geometry, and the perforation-related parameters. This clarification has been incorporated in the revised version of the manuscript.
7. Thank you for the careful observation. The Governing Equations section has been thoroughly revised to ensure clarity and completeness. All conservation equations, including continuity, momentum, and energy equations, are now explicitly written and properly formatted. The equations have also been aligned with the stated assumptions of steady-state, incompressible, and turbulent flow conditions. In addition, the description of the SST turbulence model has been clarified to ensure consistency with the numerical methodology. The revised equations are now clearly presented in Section 2.2 of the manuscript.
8. Thank you for the important comment. A grid independence test was conducted using four progressively refined meshes ranging from 600,641 to 915,422 elements. The relative deviations of Nu_avg and f between the two finest meshes were below 0.1%, confirming mesh independence. Based on this analysis, the mesh with **822,157 elements** was selected for all final simulations, as it provides an optimal balance between numerical accuracy and computational efficiency. This clarification has been clearly stated in Section 2.4 of the revised manuscript.
9. Thank you for identifying this inconsistency. The TEF values have been carefully re-verified against Figure 13. The correct maximum TEF values are 1.075 (0.25H) and 1.064 (0.5H), and the previous erroneous statement has been removed. The revised Section 3.3 is now fully consistent with the graphical data, and all numerical values have been thoroughly checked to ensure reliability.

10. Thank you for carefully reviewing the reference list. We have thoroughly re-examined all cited works to ensure accuracy and eliminate any potential redundancy. Unintended duplicate entry was identified and has now been removed. The reference list has been corrected, and the numbering has been updated accordingly throughout the manuscript. We confirm that all remaining references are distinct and correctly cited.
11. Thank you for this important comment. We acknowledge that the maximum TEF value obtained in the present study (≈1.075) represents a moderate enhancement compared to some studies reporting TEF values in the range of 1.2–1.5. However, it is important to note that many of those higher TEF values are achieved under conditions involving significantly increased pressure penalties or more aggressive geometric modifications.

    In the present work, the objective was not to maximize vortex intensity alone, but to achieve a balanced thermo-hydraulic optimization under practical air-side operating conditions. For fin-and-tube heat exchangers operating with low-density air, even a 5–10% improvement under constant fan power conditions is considered practically meaningful, as it can reduce required heat transfer surface area, improve compactness, or lower long-term energy consumption.

    Furthermore, the proposed perforated CRW-VGs are integrated into the fin structure and can be manufactured using conventional stamping or punching processes, resulting in minimal additional manufacturing complexity. Therefore, the moderate TEF enhancement obtained represents a realistic and economically viable performance improvement rather than an over-optimized configuration with excessive pressure penalties.

    This clarification has been emphasized in Section 3.4 of the revised manuscript.

Scribendi

Certificate of Editing and Proofreading

This certifies that a version of the document titled

Improving the Thermal Efficiency of Fin-tube Heat Exchangers by Optimizing Geometric Parameters of Curved Rectangular Winglet Vortex Generators

authored by

Dan Mugisidi

was edited and/or proofread by Scribendi as order number

1071792

for clarity, consistency, and correctness according to the requirements and guidelines specified by the client.

March 4, 2026

Scribendi Inc

SCRIBENDI INC.
405 RIVERVIEW DRIVE
CHATHAM, ON N7M 0N3 CANADA
+1 (519) 351 1626

www.scribendi.com

Improving the Thermal Efficiency of Fin-tube Heat Exchangers by Optimizing Geometric Parameters of Curved Rectangular Winglet Vortex Generators

Dan Mugisidi[1,*], Oktarina Heriyani[1], Amir Khalid[2], Ahmed Rahmani[3]

[1]Department of Mechanical Engineering, Faculty of Industrial and Informatics Technology, Universitas Muhammadiyah Prof DR HAMKA, Jakarta, Indonesia

[2]Faculty of Mechanical and Manufacturing Engineering, Universiti Tun Hussein Onn Malaysia, Batu Pahat, Johor, Malaysia

[3]Sustainable Development and Environmental Protection Laboratory, Larbi Ben M'hidi University, Oum El Bouaghi, 04000, Algeria

*Corresponding author, e-mail: dan.mugisidi@uhamka.ac.id

Abstract

Thermal efficiency is a fundamental criterion in the design and operation of heat exchangers because it provides a clear view of the thermal behaviour and reliability of the system. Integrating vortex generators (VGs) with heat exchangers often increases turbulence and enhances the heat transfer rate but at the cost of increased pressure drops. *This study aims to maximise the thermal enhancement factor (TEF) in fin–tube heat exchangers by optimising the radial distance, hole width and angular position of curved rectangular winglet vortex generators (CRW-VGs).* Computational fluid dynamics analysis is utilised to investigate how variations in radial distance and hole width influence CRW-VG performance. Parameters such as TEF, Nusselt number ratio, friction factor ratio and flow regime were examined. The results show that smaller radial distances suppress mixing vortices and enhance TEF, while larger hole widths generate strong jet flows and increase heat transfer rates. The highest TEF of 1.075 is achieved at an angular position of 120°, a hole width of 0.5 H and a radial distance of 1.25. The study reveals that optimising the geometric parameters of VGs is proven satisfactory for enhancing heat transfer performance and minimising pressure drop.

Keywords: curved rectangular winglet, heat transfer enhancement, hole width, radial distance, vortex generator

Improving the Thermal Efficiency of Fin-tube Heat Exchangers by Optimizing Geometric Parameters of Curved Rectangular Winglet Vortex Generators

1. Introduction

Thermal efficiency is a crucial aspect in the design and operation of heat exchanger systems, playing an essential role in various industrial applications, such as power generation, cooling and chemical processing [1]. The need for better heat exchange in these systems with more compact designs has resulted in much research on this topic.

Air is the common working fluid in fin–tube heat exchangers. Similar to all gases, air has relatively poor thermophysical properties for heat transfer [2]. This limitation prompted researchers to enhance the effectiveness of heat transfer systems to increase energy efficiency while lowering production costs. Enhancing the air-side heat transfer of these equipment has been the subject of several theoretical, numerical and experimental investigations. A proven effective solution is the integration of vortex generators (VGs). These small devices are designed to enhance aerodynamic performance, flow control and heat transfer in forced draft cooling towers [3]. VGs improve thermal performance by inducing subsidiary currents, disrupting interface region development and promoting fluid dispersion near the walls. The longitudinal vortices generated by VGs allow reduced stagnation zones behind the tubes [4], increase turbulence intensity and well fluid mixing [5]. Increasing turbulence often enhances the heat transfer rate but at the cost of increased pressure drops. Therefore, optimising heat transfer and reducing fluid flow resistance have become the primary focus.

Previous studies have demonstrated that both the placement and geometric configuration of VGs significantly influence the thermal–hydraulic performance of fin–tube heat exchangers. Positioning VGs near the centre of the tube has been shown to provide more effective heat transfer enhancement compared with inlet or outlet placements, primarily due to the stronger interaction between the generated vortices and the tube wake region [6], [7]. In addition, smaller VG geometries operating at lower Reynolds numbers have been reported to further improve heat exchange performance [8].

Geometric optimisation of the heat exchanger structure also plays an important role in determining overall performance. The optimal combination of a larger fin pitch and a smaller tube diameter has been experimentally identified as providing improved fluid flow characteristics [9].

However, increasing the fin pitch can reduce the Nusselt number (Nu) and the wall friction factor (f) because of weakened vorticity formation and enhanced turbulent energy dissipation [10]. Furthermore, numerical investigations have shown that combining concave and convex VG surfaces generates stronger longitudinal vortices, resulting in an enhancement of the heat transfer rate of approximately 14.4% [11].

Operational parameters, such as VG location and angle of attack (AoA), further determine heat transfer effectiveness. Higher attack angles, particularly when VGs are positioned farther from the tube, can substantially increase heat transfer rates [12]. Conversely, smaller angles may be advantageous in certain configurations by directing colder fluid towards weak wake regions [13]. An AoA of 45° has consistently been identified as providing superior thermal enhancement compared with other angles [14], [15]. Furthermore, increasing the number of staggered VGs enhances the thermal enhancement factor (TEF) by accelerating flow and promoting fluid mixing in the wake region [16], [17]. These configurations are commonly arranged in common flow up, common flow down (CFD) or hybrid arrangements to optimise performance.

In rectangular channel systems, geometric parameters, such as winglet aspect ratio and channel height (H), have been identified as the dominant factors affecting heat transfer performance [18], [19]. Increasing duct height significantly alters vortex development, especially when VGs are mounted on opposing walls, thereby enhancing overall flow dynamics and heat transfer efficiency. Heat exchange performance is also highly sensitive to VG position and geometry [20], with even minor geometric changes producing noticeable variations in performance [21], [22].

Among the various structural innovations, perforated VGs have emerged as a promising approach for improving thermal performance [23]. Perforated rectangular winglets have been reported to increase the Nu by approximately 3.91–5.52 times, achieving a maximum thermal performance factor of 2.01 [24]. Similarly, double perforated inclined elliptic turbulators have demonstrated Nu enhancements of up to 217.4% [25]. These improvements are attributed to jet flows generated through perforations, which disrupt recirculation zones and intensify fluid mixing, thereby enhancing thermal exchange efficiency [26], [27], [28].

Despite these substantial advancements, existing studies predominantly emphasise external geometric modifications, placement strategies and angle of attack variations. Although perforating the VG surface can either enhance or deteriorate heat transfer performance, depending on the hole size, number and placement, because it changes the vortex strength and the pressure drop [29], systematic investigations of hollow rectangular winglet VGs remain limited. More importantly, the geometric perforation parameter (hole width) and the positional parameter (radial distance from the tube) have largely been examined independently. Consequently, the coupled interaction between these two design variables and their combined influence on thermal–hydraulic performance has not been comprehensively evaluated. This lack of integrated parametric analysis restricts the development of optimised hollow VG configurations capable of simultaneously maximising heat transfer enhancement and minimising pressure drop penalties. To overcome this limitation, this study proposes a performance-based geometric optimisation framework for circular ring winglet vortex generators (CRW-VGs) in fin–tube heat exchangers, focusing on radial distance and hole width as key design variables.

The coupled effects of radial distance (r/R = 1.25 and 1.5) and hole width (0.25 *H* and 0.5 *H*) are systematically analysed using high-fidelity CFD simulations. Performance is evaluated through integrated metrics, including the TEF, Nu/Nu_0, friction factor ratio (f/f_0) and flow structure characterisation. By integrating geometric sensitivity analysis with unified thermo-hydraulic evaluation and mechanistic interpretation of vortex dynamics, this study identifies the optimal configuration that maximises heat transfer while minimising pressure drop, providing both quantitative assessment and mechanistic insight for a compact heat exchanger design.

2. Methodology

2.1 Physics Model

Figure 1 shows the geometric details of a heat exchanger with three rows of staggered tubes. The VGs employed in this study take the form of a rectangular curved winglet design characterised by the geometry depicted in Fig. 1. Figure 1(a) presents the overall configuration of the fin–tube heat exchanger and the computational domain employed in the CFD simulations. The three-dimensional (3D) schematic depicts the staggered tube arrangement and the direction of airflow. The top view specifies the tube pitches: the transverse pitch, PT = 2.25 D and the longitudinal pitch, PL = 6.75 D, where D denotes the outer tube diameter. The side view defines H as the vertical distance between two adjacent fins. The dashed rectangular region marks the representative segment selected from the complete heat exchanger geometry for numerical modelling. The tube radius, R = D/2, serves as the reference length for positioning analysis. Figure 1(b) shows the detailed geometry of the CRW-VG. The winglet length in the streamwise direction is 2 H, which is twice that of H. The winglet height is 0.9 H, providing a small clearance from the fin surface to prevent excessive blockage. Perforated configurations use circular holes with diameters of 0.5 *H* and *0.25 H*, representing the large, medium and small perforation cases, respectively, examined in the parametric study. All geometric dimensions are normalised by H for geometric similarity and scalable comparison.

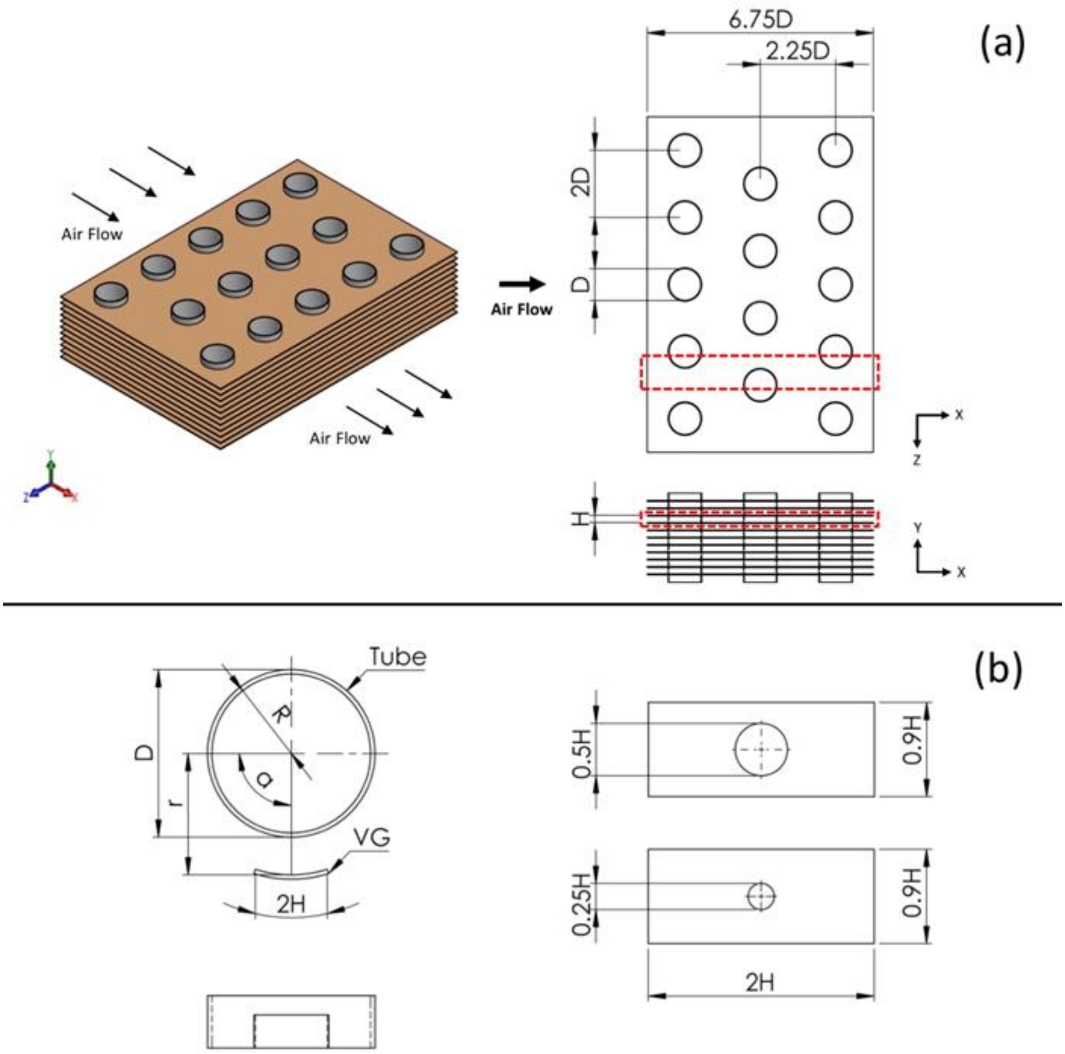

Fig. 1. Schematic illustration and the main dimensions of the studied VG (a) the overall configuration of the fin–tube heat exchanger, (b) detailed geometry of the CRW-VG

This model serves as a pivotal component in our experimental setup, aimed at investigating its effects on enhancing fluid dynamics and heat transfer processes. The geometry of the VGs, as illustrated in the figure, showcases its distinctive features and potential to induce vortices and modify the flow field. Due to its efficacy in improving the performance of various thermal systems, such VG configurations have been widely studied [19], making them ideal candidates for our research endeavours. By using this specific design, this study aims to elucidate the VGs' impact on the efficiency and effectiveness of heat transfer mechanisms within our experimental apparatus.

The main dimensions refer to Oh and Kim's previous investigation [30]: diameter D = 32 mm, length L = 6.75, longitudinal pitch P_L = 2.25D, transverse pitch (P_T) = 2D, H = 7 mm, length of the section with radius 2 H and corner radius 60°. The hole widths of the CRW-VGs are 0.25 H and 0.5 H, with a VG height of 0.9 H. The angular position (α) indicates the angle measured in an anticlockwise manner from the lengthwise orientation of the tube to the line linking the CRW-VGs to the central point of the tube, (r) denotes the distance measured radially from this central point, and R represents the radius of the tube. The investigation of these parameters was carried out using variations in position angles (α): 30°, 45°, 60°, 75°, 90°, 105°, 120°, 135° and 150° with r/R = 1.25 and 1.5.

2.2 Governing Equation

The flow conditions in the system under investigation are assumed to be incompressible, indicating that changes in density due to pressure variations are negligible and do not significantly alter the fluid's behaviour. In the fin tube heat exchanger, a Newtonian fluid with a constant stream is employed. The conservation equations for mass, momentum and energy are expressed as follows:

$$\nabla \cdot \vec{V} = 0 \tag{1}$$

$$\rho\left(\vec{V} \cdot \nabla\right)\vec{V} = -\nabla p + \mu\nabla^2\vec{V} \tag{2}$$

$$\rho\vec{V} \cdot \nabla h = \nabla \cdot (k\nabla T) \tag{3}$$

The notation in the equation above equations, namely $\vec{V}$, ρ, p, h, k, μ, and T involved are the velocity vector, air density, static pressure, thermal conductivity of air, dynamic viscosity, and static temperature, respectively.

The heat transfer performance (TEF) is formulated as follows [31],

$$TEF = (Nu/Nu_0)/(f/f_0)^{1/3} \tag{4}$$

where the Nusselt number (Nu) and friction factor (f) are formulated as follows.

$$Nu = hL_c/k \tag{5}$$

$$f = 2\Delta pH/(\rho U_c^2\ L) \tag{6}$$

2.3 Computational domain and Boundary Conditions

Figure 2 illustrates the computational domain of the fin–tube heat exchanger equipped with CRW-VGs. The domain represents the lateral arrangement, flow direction and fin pitch orientation. Owing to geometric uniformity and cyclic configuration, the computational region is defined as half of the transverse pitch (P_T/2) in the x-direction and one full pitch length in the z-direction. This periodic simplification significantly reduces computational costs while preserving the essential flow and heat transfer characteristics.

To ensure an accurate representation of the physical system, steady-state and incompressible flow assumptions are adopted. The domain is extended sufficiently in the streamwise direction to allow proper flow development and to avoid undesirable numerical or physical instabilities.

Boundary Conditions

At the inlet, a uniform velocity profile and a constant temperature are specified:

$$\mathrm{u} = (u_{in}, 0,0), T = T_{in} \tag{7}$$

where u is the velocity vector, u_{in} is the inlet air velocity, and T_{in} is the inlet air temperature.

At the outlet, a constant reference pressure is prescribed:

$$p = p_{out} \tag{8}$$

together with zero-gradient conditions for velocity and temperature:

$$\frac{\partial \mathrm{u}}{\partial n} = 0, \frac{\partial T}{\partial n} = 0 \tag{9}$$

where n denotes the outward normal direction to the outlet boundary.

For all solid surfaces, including the tube, fins, and CRW-VGs, the no-slip condition is applied:

$$\mathrm{u} = 0 \tag{10}$$

A constant wall temperature is imposed on the tube surface:

$$T = T_w \tag{11}$$

where $T_w$is the prescribed tube wall temperature.

Due to the periodicity of the geometry in the transverse and spanwise directions, periodic boundary conditions are employed:

$$\phi(x, y, z) = \phi(x, y, z + P) \tag{12}$$

where ϕ represents the dependent flow variables (velocity components, pressure and temperature), and Pdenotes the periodic pitch length.

These boundary conditions ensure physically consistent flow development and reliable prediction of heat transfer and fluid flow characteristics within the computational domain.

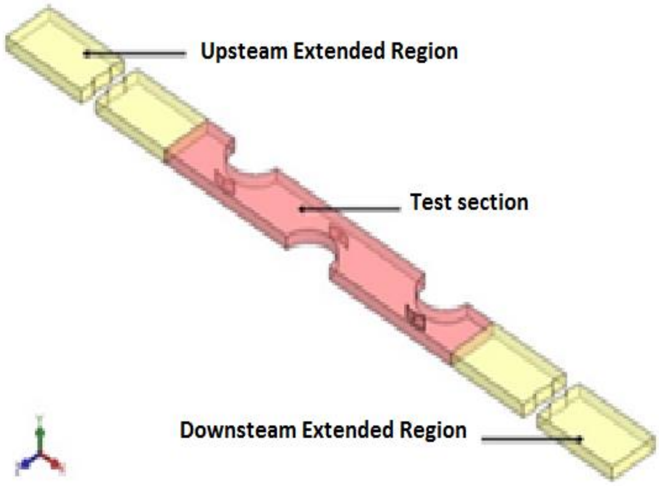

Fig. 2. Computational domain

Matching boundary conditions are established in the x orientation amid the algorithmic region, while cyclic restrictions are established on both the higher and lower surfaces in the upriver and downriver orientations. The wing region incorporated into the CRW-VGs serves as a barrier, and the tube is subjected to constraints at this enclosure. These conditions ensure stable flow patterns within the algorithmic region, preventing undesired turbulence or instability. Moreover, the no-slip conditions and consistent surface temperature facilitate precise control and optimise the flow dynamics around the wing region and tube enclosure.

2.4 Convergence Assessment

The convergence of the numerical solution was assessed using a combination of residual-based, physical-based and grid-independence criteria to ensure numerical accuracy and physical reliability.

The normalised residuals of the governing equations were monitored during the iterative process. Convergence was assumed when the residuals of the continuity and momentum equations decreased below 10^{-6}, while a stricter threshold of $10^{-8}$was imposed for the energy equation due to the heat transfer-oriented nature of the present study.

In addition to residual monitoring, several global physical quantities were continuously tracked, including the average Nusselt number ($Nu_{\_avg}$), f and outlet bulk temperature (T_{out}). The solution was considered physically converged only when the relative variation in these parameters over 500 successive iterations was satisfied:

$$\left| \frac{\phi^{(n)} - \phi^{(n-500)}}{\phi^{(n)}} \right| < 0.1\% \quad (13)$$

where ϕrepresents $Nu_{\_avg}$, f, or T_{out}, and ndenotes the iteration number.

Furthermore, a grid independence study was conducted using four progressively refined meshes ranging from 600,641 to 915,422 elements. The relative deviations of $Nu_{\_avg}$ and f between the two finest meshes were below 0.1%, confirming mesh independence. This value is well within the commonly accepted convergence range of 1%–2% [32]. Thus, the grid with 822,157 elements was adopted for all subsequent simulations to achieve an optimal balance between numerical accuracy and computational efficiency.

2.5 Grid independence test

A grid independence test was carried out for numerical analysis. The computational grid was bifurcated into two parts, specifically the region adjacent to the VGs and the rest of the area. The non-conformal interface approach was implemented between these two zones. To ensure accuracy in analysis and attain optimal grid quality, grid generation employed inflation techniques in the tube vicinity and VGs. As illustrated in Fig. 3, the cell geometry utilised around the VGs is tetrahedral because the element can precisely capture arbitrary flow around the complex geometry of the VG [33] and is directly relevant to finely detailed VGs. Four different grid sizes are considered in Table 1 to list the number of cells.

Table 1 Grid independence test.

Number of grids	$Nu_{\_avg}$	f
600,641	16.55447	0.09671
715,421	16.70175	0.09603
822,157	16.79783	0.09551
915,422	16.80972	0.09549

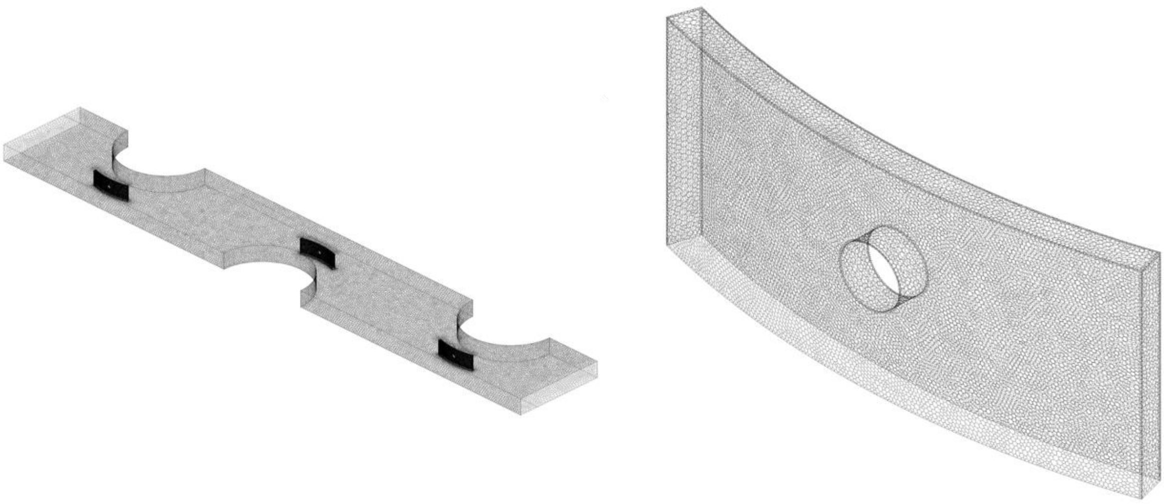

Fig. 3. Computational grid test

2.6 Numerical Solution Methodology

Numerical simulations were performed under steady-state conditions using the finite volume method to solve the 3D governing equations of mass, momentum and energy. Airflow was assumed to be incompressible, Newtonian and turbulent, with constant thermophysical properties.

Turbulence effects were modelled using the shear stress transport (SST) k–ωmodel, which combines the robustness of the k–ωformulation near the wall with the freestream independence of the k–εmodel in the outer region. This model is particularly suitable for predicting adverse pressure gradients and flow separation occurring in fin–tube heat exchangers equipped with CRW-VGs.

The governing equations were discretised using a second-order upwind scheme for the convective terms of momentum and energy equations to enhance numerical accuracy. Pressure–velocity coupling was achieved using the SIMPLE algorithm. Spatial discretisation was applied consistently across the computational domain to ensure numerical stability.

A non-uniform computational grid was employed, with mesh refinement and inflation layers applied near the tube and VG surfaces to accurately capture velocity and thermal boundary layers. A grid independence study was conducted using four mesh resolutions, as detailed in Table 1. The variation in Nu_avg and f between the two finest meshes was less than 0.1%, indicating mesh-independent results. Consequently, the mesh with 822,157 cells was selected for all simulations as an optimal compromise between accuracy and computational cost.

2.6 Validation

The convergence of the numerical solution was ensured by monitoring the normalised residuals of the governing equations. The convergence criteria were set to $10^{-5}$for continuity and momentum equations and $10^{-6}$for the energy equation. In addition to residual reduction, global quantities, such as Nu_avg and pressure drop, were monitored to confirm the physical convergence of the solution.

The simulation model adopted in this study was based on a previously validated configuration [30], which serves as a reference case for assessing the reliability of the numerical method. Turbulent flow was modelled using the k–ω SST model in conjunction with the governing Equations (1)–(3). This model is well known for accurately predicting adverse pressure gradients and flow separation, making it suitable for complex flow simulations in fin–tube heat exchangers equipped with curved VGs.

The numerical results were validated against published experimental data [30], as illustrated in Fig. 4. The comparison showed good agreement, with deviations of 2%–6% for Nu and 4%–8% for f, and an overall error below 9%. These results confirm the reliability of the present numerical methodology for predicting heat exchanger performance.

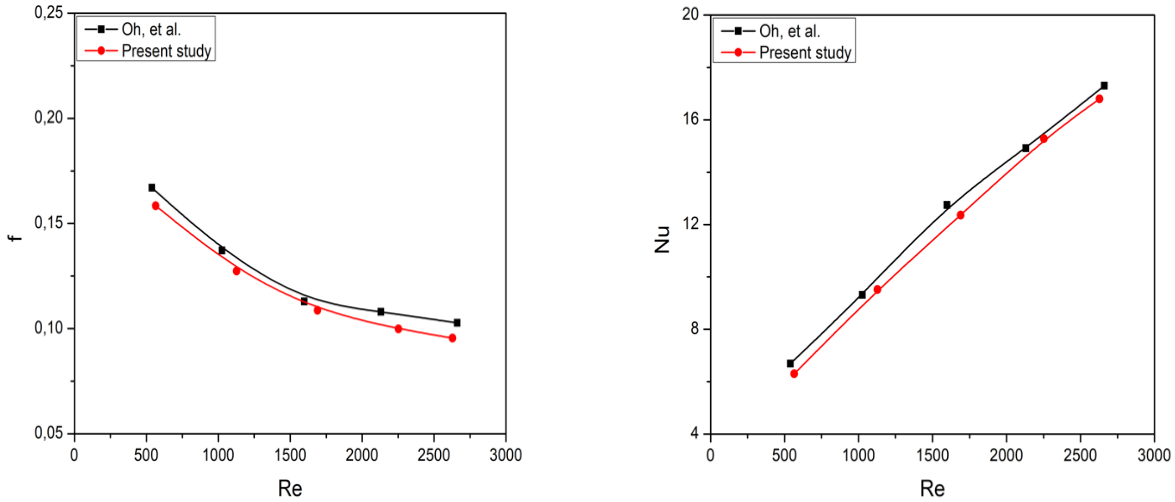

(a) (b)

Fig. 4. Numerical validation results (a) f (b) Nu

3. Results

3.1 Influence of geometry and radial distance on the $\mathrm{Nu/Nu_0}$ and $\mathrm{f/f_0}$ values

The assessment of heat transfer performance can be observed from the resulting Nu/Nu_0 value. The comparison between Nu and Nu_o (Nusselt number under reference conditions) provides insight into heat transfer efficiency. Deviations in Nu/Nu_o signify alterations in the thermal performance of the observed system, as shown in Fig. 5 (i.e. (a) is 0.25 H and (b) is 0.5 H). Figures 5 and 6 demonstrate the coupled relationship between heat transfer enhancement and flow resistance as a function of the attack angle, hole width and radial position of the CRW-VGs. As shown in Fig. 5, the variation in Nu/Nu_0 strongly depends on vortex stability and secondary flow development. At lower angles (30°–60°), moderate longitudinal vortices are generated, resulting in limited boundary layer disruption and moderate heat transfer enhancement. However, as indicated in Fig. 6, this regime is accompanied by only a slight increase in f, reflecting a moderate disturbance level within the flow field.

When the angle approaches 75°–90°, both Nu/Nu_0 (Figure 5) and f/f_0 (Figure 6) reach relatively low values. This behaviour indicates a weakened and less coherent vortex structure, in which reduced mixing leads to minimal heat transfer enhancement and lowered flow resistance. The reduction in heat transfer in this region is mainly attributed to the reduced effective contact area for heat transfer, intensified rotational motion and the formation of lateral vortices on the surface of the perforated VGs [34], which dissipate energy without significantly enhancing boundary layer thinning.

A significant change occurs at 120°: a maximum Nu/Nu_0 (Fig. 5) and a pronounced increase in f/f_0 (Fig. 6). This correspondence confirms that strong and stable longitudinal vortices are formed at this angle, intensifying cross-stream mixing and effectively thinning the thermal boundary layer. However, enhanced vortex strength also increases shear stress and energy dissipation, leading to higher pressure penalties. This regime represents a high-disturbance, high-enhancement condition in which heat transfer improvement is achieved at the expense of increased friction losses.

At larger angles (135°–150°), both Nu/Nu_0 and f/f_0 decrease, suggesting vortex breakdown and excessive flow separation. Although flow disturbance remains present, the loss of vortex coherence reduces effective mixing and pressure buildup.

The influence of hole width and radial distance further clarifies the thermo-hydraulic interaction. The smaller hole width (0.25 *H*) produces more concentrated vortices and sharper enhancement peaks in Fig. 5 and relatively controlled friction increases in Fig. 6. By contrast, the larger hole width (0.5 *H*) allows partial flow penetration through the perforation, promoting distributed secondary flows that increase energy dissipation and friction levels while slightly moderating heat transfer gains. Similarly, increasing the radial distance to r/R = 1.5 strengthens the vortex–wake interaction, enhancing Nu/Nu_0 but also elevating f/f_0 because of the intensified momentum exchange.

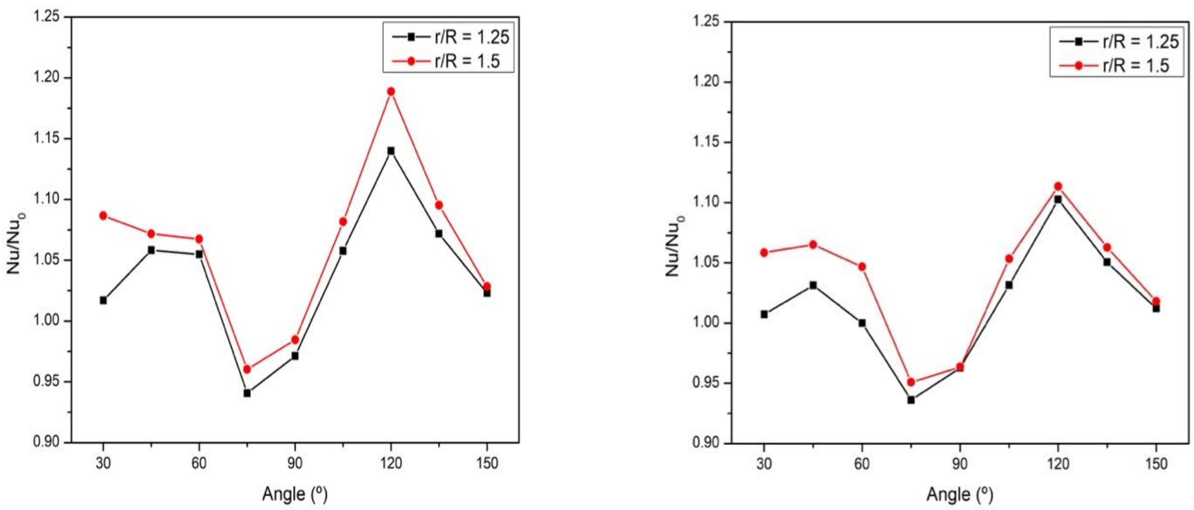

(a) (b)

Fig. 5. The effect Nu/Nu_o (a) hole width CRW-VGs 0.25*H* (b) hole width CRW-VGs 0.5*H*

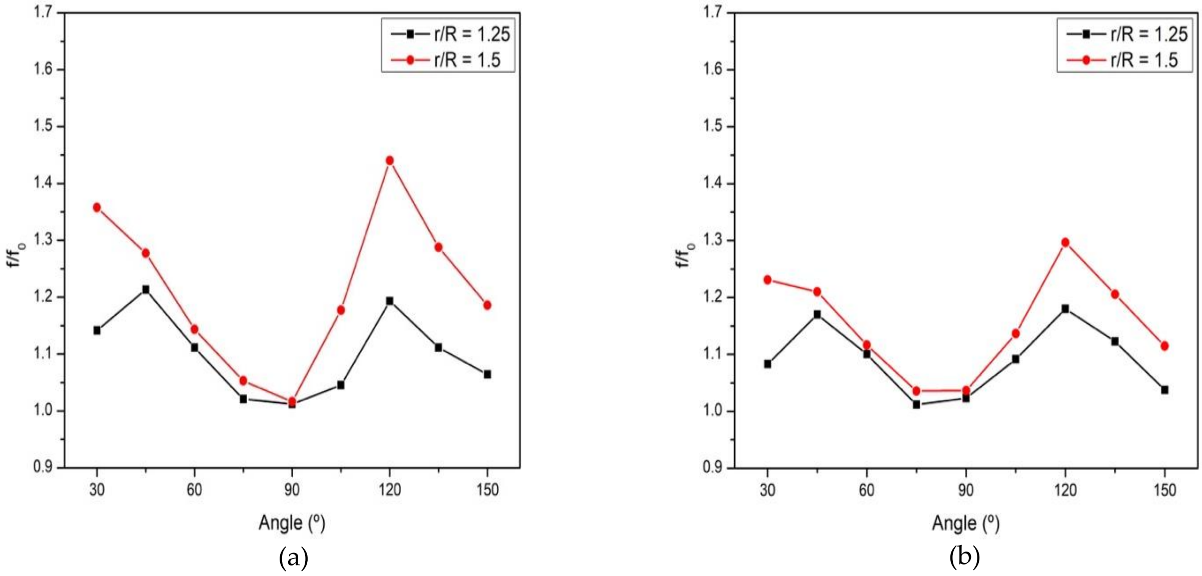

Fig. 6. The effect of position angle on the friction factor (a) hole width CRW-VGs 0.25*H* (b) hole width CRW-VGs 0.5*H*

Overall, the combined analysis of Figs. 5 and 6 confirms that the thermo-hydraulic performance is governed by the balance between vortex intensity, boundary layer disruption and flow resistance. The angle of 120° emerges as the most effective configuration in terms of heat transfer enhancement, although its practical suitability must be evaluated through an integrated metric, such as the TEF, to ensure that the gain in heat transfer justifies the associated pressure penalty.

3.2 Flow Field and Thermal Field Interpretation

Reducing f with an increase in Nu using holes can reduce the pressure drop. As Nu and f are parameters of the TEF, the heat transfer performance can be determined, as discussed above, by looking at the contour changes in speed, temperature and pressure in Figs. 7, 8, 9, 10, 11 and 12. Figures 7–12 reveal that the thermo-hydraulic performance of the CRW-VGs is governed not merely by geometric variation but primarily by the stability regime of the generated longitudinal vortices. Three distinct flow regimes can be identified as the attack angle (α) increases: (i) weak vortex regime (30°–60°), (ii) coherent vortex amplification regime (75°–120°) and (iii) vortex breakdown regime (135°–150°).

In the weak vortex regime, velocity contours (Figs. 7–8) indicate limited secondary flow development and only a partial disruption of the boundary layer. The generated vortices are insufficient to induce the deep penetration of core flow towards the heated surface.

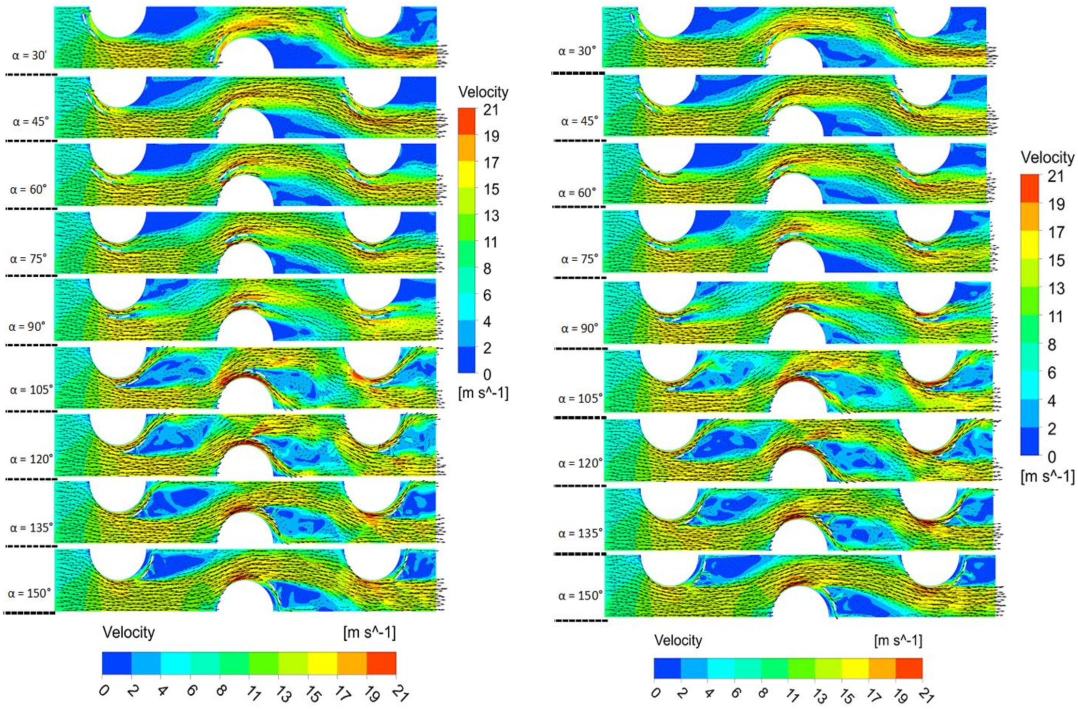

(a) (b)

Fig. 7. Velocity contour *r*/*R* 1.25 (a) hole width 0.25*H* (b) hole width 0.5*H*

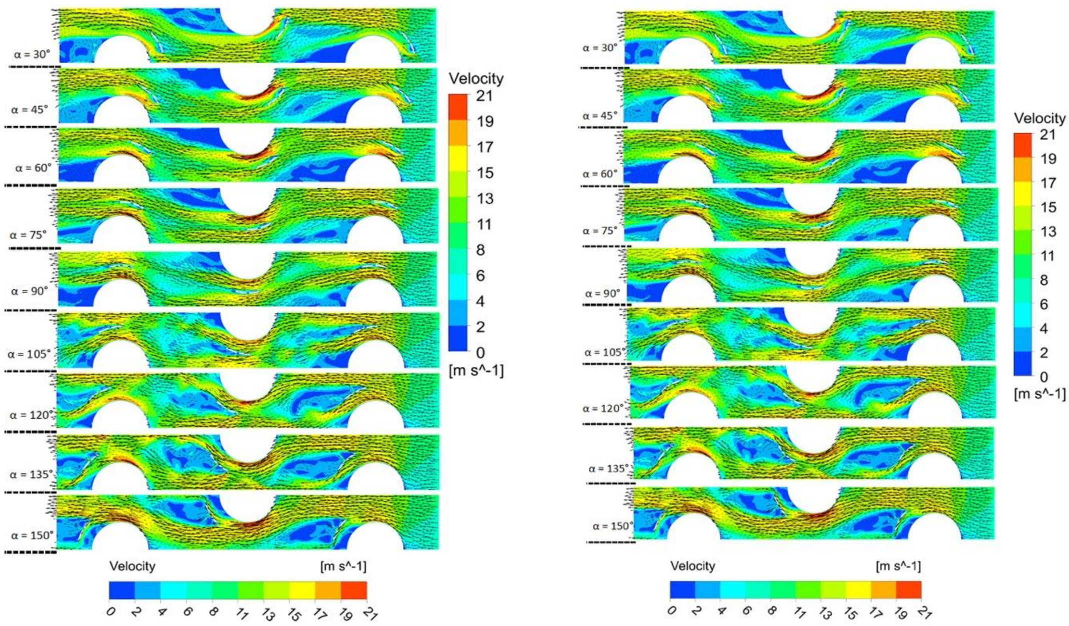

(a) (b)

Fig. 8. Velocity contour r/R 1.5 (a) hole width 0.25*H* (b) hole width 0.5*H*

Consequently, the temperature contours (Figs. 11–12) show a relatively thick thermal boundary layer and non-uniform temperature stratification. The pressure contours (Figs. 9–10) display moderate upstream–downstream gradients, indicating limited energy dissipation and relatively small pressure penalties. However, as fluids move swiftly, they have fewer opportunities for prolonged interaction, resulting in smaller pressure drops [35]. This explains why lower attack angles, despite smoother flow behaviour, do not generate substantial convective enhancement.

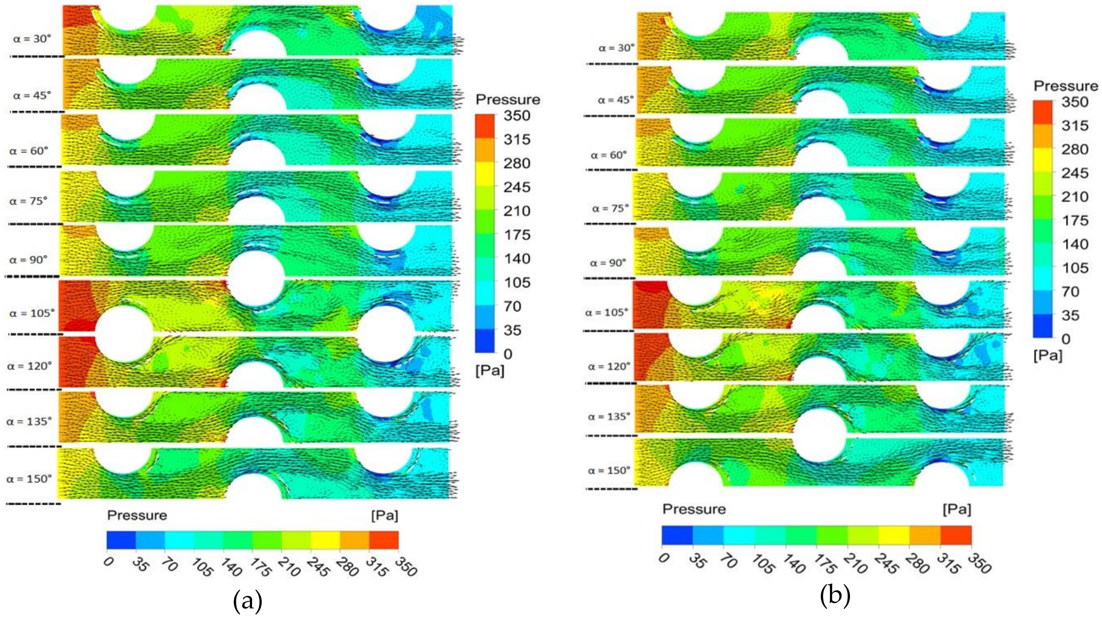

Fig. 9. Pressure drop contour r/R 1.25 (a) hole width 0.25H (b) hole width 0.5H

A fundamentally different behaviour emerges in the coherent vortex amplification regime ($\alpha \approx 105°–120°$). In this range, the velocity field exhibits highly organised longitudinal vortices with an intensified cross-stream momentum exchange. The vortices transport high-momentum core fluid towards the heated wall while ejecting low-momentum near-wall fluid outward, significantly thinning the thermal boundary layer. The temperature distribution becomes more uniform, thus confirming enhanced convective transport. Simultaneously, the pressure field exhibits the most pronounced gradients, reflecting maximal shear production and vortex strength.

Nevertheless, the perforated configuration introduces an additional mechanism. As depicted in Figs. 9 and 10, the jet stream emanating from the orifice of the CRW-VGs has the potential to alleviate stagnation flow, consequently reducing the pressure drop [36], [37], [38]. This jet-induced acceleration redistributes local pressure peaks and mitigates excessive recirculation behind the VG, thereby partially compensating for the pressure penalty associated with strong vortex generation. Therefore, this regime represents a critical transition state in which vortex strength and structural coherence are maximised, while perforation-induced jet flow moderates stagnation-related losses.

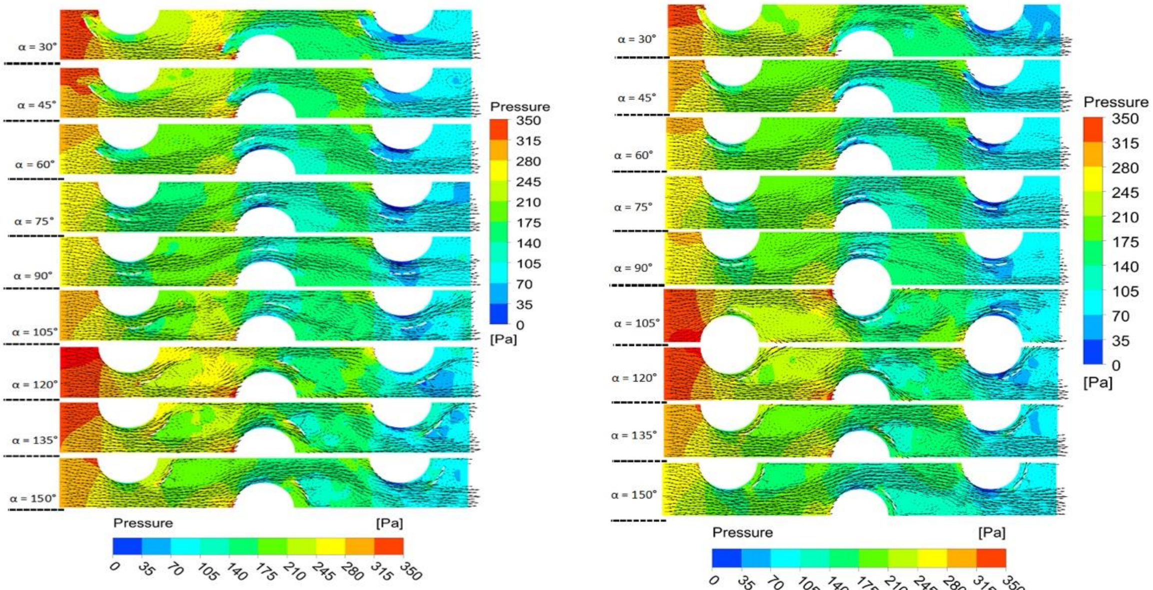

(a) (b)

Fig. 10. Pressure drop contour *r*/*R* 1.5 (a) hole width 0.25*H* (b) hole width 0.5*H*

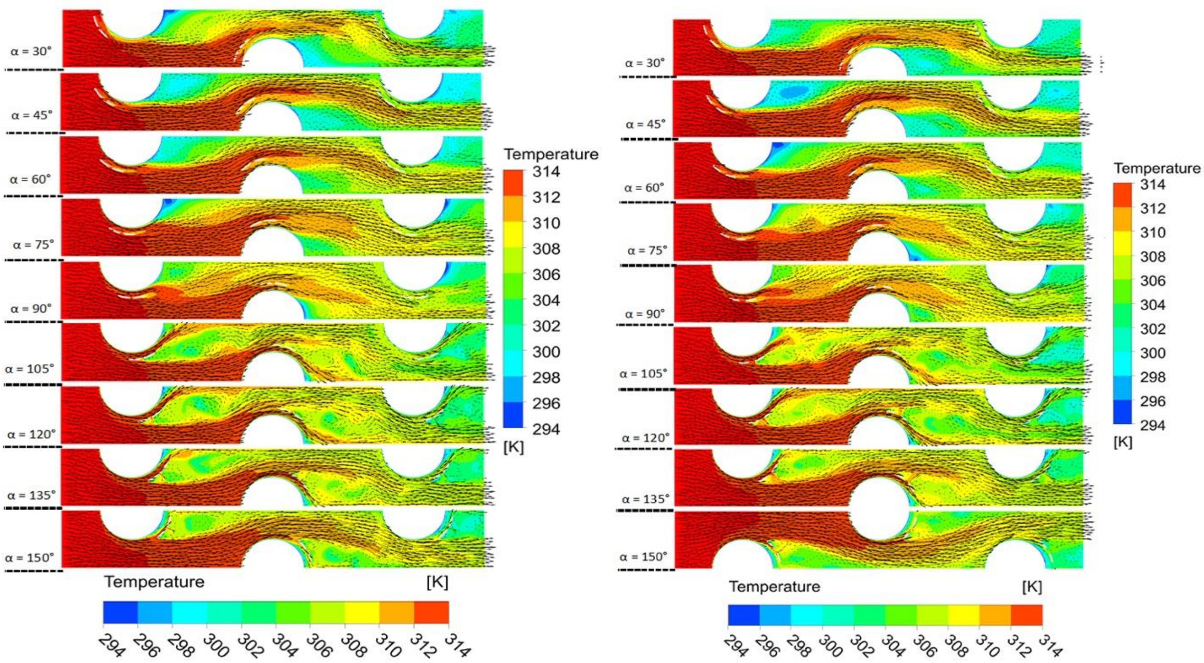

(a) (b)

Fig. 11. Temperature contour *r*/*R* 1.25 (a) hole width 0.25*H* (b) hole width 0.5*H*

When $\alpha \geq 135°$, the system enters a vortex breakdown regime. Although apparent disturbance increases, velocity contours reveal fragmented and unstable vortical structures. The pressure distribution becomes spatially irregular, indicating that kinetic energy is increasingly dissipated through chaotic separation rather than organised secondary motion. As a result, temperature contours show reduced effectiveness in boundary layer thinning, despite intensified disturbance.

This demonstrates that excessive geometric forcing shifts the system from a structured convective enhancement to instability-driven dissipation.

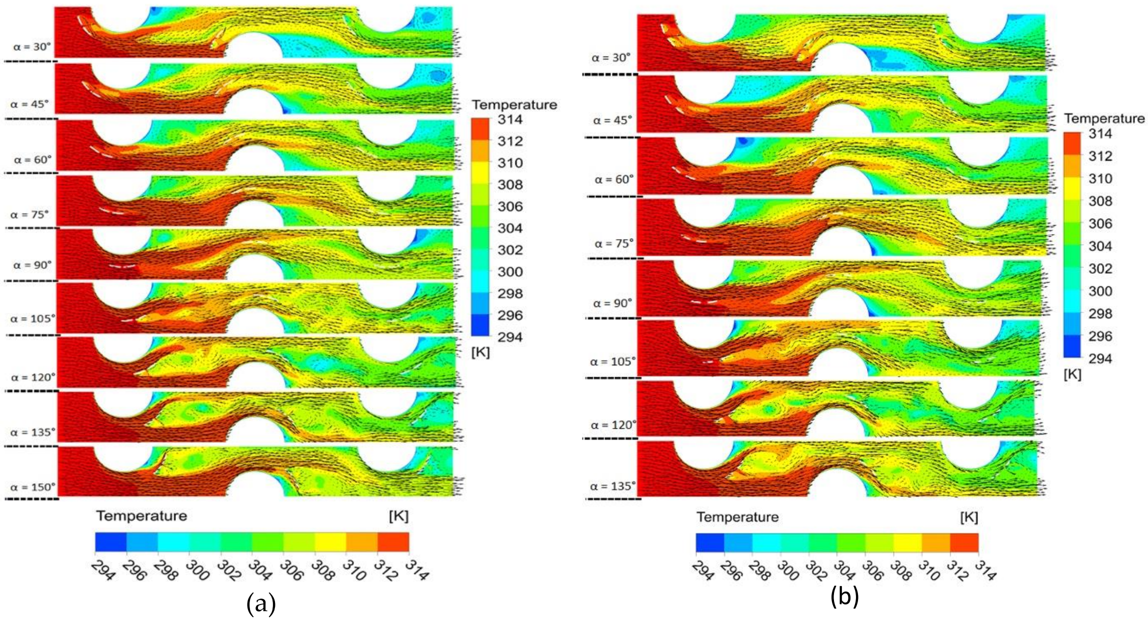

Fig. 12. Temperature contour r/R 1.5 (a) hole width $0.25H$ (b) hole width $0.5H$

The geometric parameters further modulate these mechanisms. An increasing radial position to r/R = 1.5 enhances the wake–vortex interaction and prolongs vortex persistence, intensifying the heat transfer but also elevating the pressure penalties. Similarly, a smaller hole width (0.25 H) generates concentrated vortices and sharper shear layers, thereby promoting a stronger boundary layer disruption. By contrast, a larger hole width (0.5 H) allows for greater flow penetration through the perforation, redistributing vortex energy and stabilising the pressure field, thereby offering a more balanced thermo-hydraulic response.

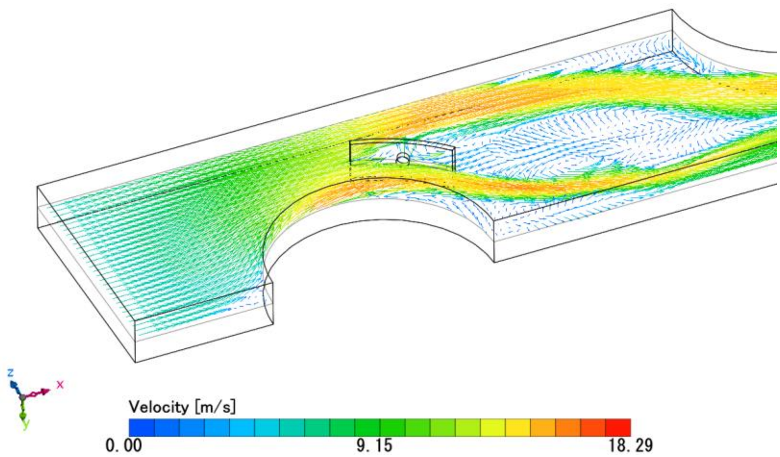

Fig. 13. Streamline velocity $\alpha = 120°$, r/R = 1.25, hole width = 0.5H

Overall, the results demonstrate that thermo-hydraulic optimization is governed by vortex coherence rather than vortex magnitude alone. The optimal configuration ($\alpha \approx 105°–120°$) corresponds to the condition where organized secondary flow production is maximized, stagnation effects are partially mitigated by jet-induced flow through perforations, and instability-driven energy dissipation has not yet dominated the system. This mechanistic interpretation advances the understanding of perforated vortex generators by identifying vortex stability and jet–wake interaction as the primary control parameters governing performance. As illustrated in Fig. 13, the streamline and velocity contours reveal a coherent high-velocity core developing along the inner wall of the curved channel, accompanied by jet-induced momentum injection from the perforations into the wake region. This mechanism promotes thermal boundary layer thinning through enhanced near-wall acceleration while simultaneously suppressing large-scale recirculation that would otherwise increase frictional losses. The interaction between curvature-driven Dean vortices and the longitudinal vortices generated by the VG further intensifies transverse momentum exchange, improving convective transport uniformity along the heated surface. Consequently, the heat transfer augmentation achieved within the optimal angular range is not merely a function of vortex strength, but rather of sustained vortex organization and controlled jet–wake stabilization, which collectively ensure enhanced Nusselt number performance with moderated pressure penalties.

3.3 Influence of geometry and radial distance on thermal enhancement factor

The variation in the TEF with the r/R ratio at different angular positions is presented in Figs. 13(a) and 13(b) for hole widths of 0.25 H and 0.5 H, respectively. For both configurations, r/R = 1.25 consistently produces higher TEF values than r/R = 1.5, with the most pronounced improvement occurring at $\alpha = 120°$. The maximum TEF reaches 1.075 for 0.25 H and 1.064 for 0.5 H. This trend indicates that a shorter radial distance provides a more favourable balance between heat transfer augmentation and friction penalty.

The superior performance at r/R = 1.25 is associated with a more effective vortex–jet interaction and controlled suppression of mixed-vortex interference. At $\alpha \approx 120°$, the wake region behind the tube is significantly weakened, promoting enhanced near-wall momentum exchange and boundary-layer disruption. Such overlapping vortex configurations signal a shift towards a more intensified turbulent regime [39], which is known to strengthen convective heat transfer mechanisms [40].

Although larger radial spacing intensifies vortex structures, it also increases flow resistance, thereby reducing the overall TEF, despite higher local heat transfer rates. The combined trends of

Nu/Nu_0 and f/f_0 confirm that optimal thermo-hydraulic performance is governed by the synergy between vortex positioning, jet reinforcement and wake suppression rather than vortex strength alone.

The combined analysis of Nu/Nu_0 and f/f_0 (Figs. 5–12) supports this behaviour. Increasing hole width reduces f, thereby mitigating the pressure drop, consistent with previous findings [41]. The jet streams generated by the CRW-VGs alleviate stagnant flow regions, particularly between 30° and 90°, while beyond 105°, the interaction between intensified vortices and wake dynamics temporarily elevates the pressure drop before stabilising near 120°. The temperature contours further confirm that higher angular positions weaken the recirculation zone and enhance thermal mixing.

Overall, the TEF distribution in Fig. 14 demonstrates that thermo-hydraulic optimisation is governed not only by vortex strength but also by the synergy between vortex positioning, jet reinforcement and wake suppression. The peak performance at r/R = 1.25 and α = 120° highlights the importance of geometric tuning to achieve maximum heat transfer enhancement with controlled hydraulic losses. These findings provide deeper physical insight into jet-assisted vortex dynamics and offer practical guidance for optimising VG placement in compact heat exchanger applications.

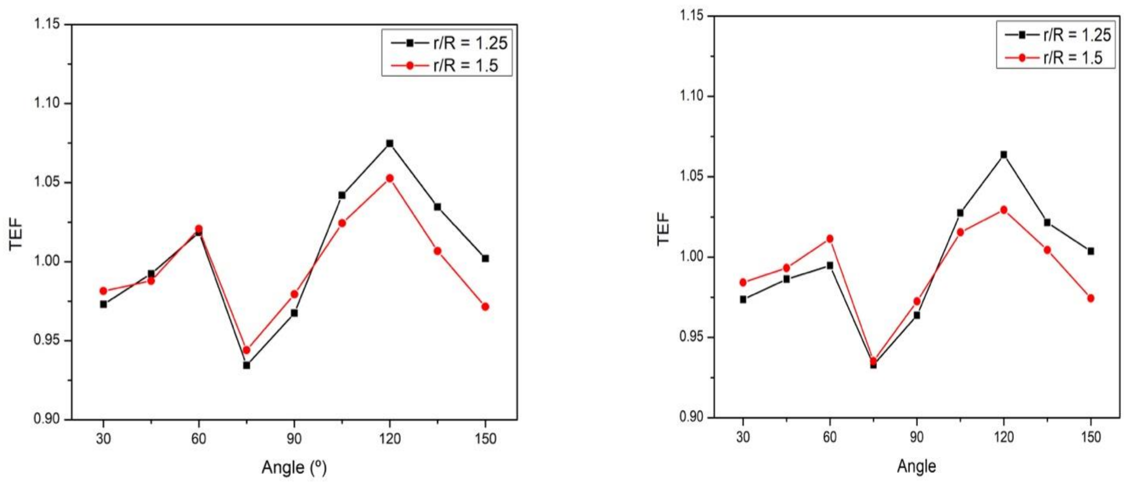

(a) (b)

Fig. 14. Thermal enhancement factor graph (a) RWVGs hole width 0.25*H* (b) RWVGs hole width 0.5*H*

3.4 Economic and Practical Implications of Thermal Enhancement Factor

The maximum TEF obtained in the present study is approximately 1.075, corresponding to a net thermo-hydraulic improvement of about 7%–8% under constant fan power conditions. Although this enhancement may appear moderate compared with some studies reporting TEF values in the range of 1.2–1.5 [42], [43], [44], it is important to recognise that such higher values are often associated with substantial pressure penalties or aggressive vortex geometries that may not be suitable for practical air-side applications. In fin–tube heat exchangers operating with low-density air, even a 5%–10% improvement in overall performance is practically meaningful, as it can reduce the required heat transfer surface area for a given thermal duty, improve compactness or lower long-term fan energy consumption [45], [46], [47].

From a manufacturing standpoint, the proposed perforated CRW-VGs are passive devices integrated directly with the fin structure and fabricated from thin sheet material. The addition of perforations does not introduce significant production complexity and can be implemented using conventional stamping or punching techniques commonly employed in fin manufacturing. Consequently, the incremental fabrication cost is expected to be minimal, particularly in large-scale production.

Moreover, the perforated configuration helps mitigate an excessive increase in pressure compared with solid VGs, thereby reducing aerodynamic loading on the fan system. The resulting balance between heat transfer enhancement and controlled friction penalty demonstrates that the proposed design achieves realistic thermo-hydraulic optimisation rather than maximum vortex intensity alone. Although a comprehensive life-cycle cost analysis is beyond the scope of this numerical study, the combination of TEF greater than unity, moderate pressure penalties and low manufacturing complexity supports the technical relevance and economic feasibility of the proposed configuration for practical Heating, Ventilation, and Air Conditioning and compact thermal management applications.

4. Conclusions

This study reveals that the thermo-hydraulic performance of CRW-VGs is governed by the interaction between vortex positioning, jet momentum and wake suppression rather than vortex strength alone. The results explicitly show that a shorter radial distance ($r/R = 1.25$) provides a more favourable balance between heat transfer enhancement and pressure penalty than $r/R = 1.5$. Although larger radial spacing intensifies vortex structures and increases Nu/Nu_0, the accompanying increase in f reduces the overall TEF.

The optimal angular position is identified at $\alpha = 120°$, at which the wake region behind the tube is significantly weakened. This configuration promotes a stronger near-wall momentum exchange, a more uniform boundary-layer disruption and improved thermal mixing. The TEF reaches its maximum values of 1.075 (0.25 *H*) and 1.064 (0.5 *H*) under this condition, confirming that wake restructuring plays a decisive role in thermo-hydraulic optimisation.

Furthermore, increasing the feeding hole width enhances jet strength, which intensifies turbulence and redistributes momentum more effectively. More importantly, this jet-assisted mechanism contributes not only to heat transfer augmentation but also to moderating pressure losses, demonstrating that momentum redistribution is more critical than simply increasing vortex intensity.

Overall, the findings establish that the optimal CRW-VG design requires controlled vortex suppression, strategic angular positioning and jet reinforcement to achieve maximum TEF. These results provide mechanistic insight into jet–vortex synergy and offer practical guidance for high-efficiency compact heat exchanger design.

Acknowledgement

The author extends gratitude to Office of Research UHAMKA for support for this research and to the Office of Publication of UHAMKA for their assistance in providing technical guidance. This research was not funded by any grant.

References

[1] K. Torii, K. M. Kwak, and K. Nishino, "Heat transfer enhancement accompanying pressure-loss reduction with winglet-type vortex generators for fin-tube heat exchangers," *Int. J. Heat Mass Transf.*, vol. 45, no. 18, pp. 3795–3801, Aug. 2002, doi: https://doi.org/10.1016/S0017-9310(02)00080-7.

[2] P. T. Tsilingiris, "Review and critical comparative evaluation of moist air thermophysical properties at the temperature range between 0 and 100 °C for Engineering Calculations," Mar. 01, 2018, *Elsevier Ltd*. doi: 10.1016/j.rser.2017.10.072.

[3] D. Mugisidi, O. Heriyani, P. H. Gunawan, and D. Apriani, "Performance improvement of a forced draught cooling tower using a vortex generator," *CFD Letters*, vol. 13, no. 1, pp. 45–57, 2021, doi: https://doi.org/10.37934/cfdl.13.1.4557.

[4] Syaiful, H. Nabilah, M. S. K. T. Suryo Utomo, A. Suprihanto, and M. F. Soetanto, "Numerical simulation of heat transfer enhancement from tubes surface to airflow using concave delta winglet vortex generators," *Results in Engineering*, vol. 16, p. 100710, Dec. 2022, doi: 10.1016/J.RINENG.2022.100710.

[5] M. Awais and A. A. Bhuiyan, “Heat transfer enhancement using different types of vortex generators (VGs): A review on experimental and numerical activities,” *Thermal Science and Engineering Progress*, vol. 5, pp. 524–545, Mar. 2018, doi: 10.1016/J.TSEP.2018.02.007.

[6] S. K. Sarangi and D. P. Mishra, “Effect of winglet location on heat transfer of a fin-and-tube heat exchanger,” *Appl. Therm. Eng.*, vol. 116, pp. 528–540, 2017, doi: 10.1016/j.applthermaleng.2017.01.106.

[7] K. W. Song, Z. P. Xi, M. Su, L. C. Wang, X. Wu, and L. B. Wang, “Effect of geometric size of curved delta winglet vortex generators and tube pitch on heat transfer characteristics of fin-tube heat exchanger,” *Exp. Therm. Fluid Sci.*, vol. 82, pp. 8–18, Apr. 2017, doi: 10.1016/j.expthermflusci.2016.11.002.

[8] A. Boonloi and W. Jedsadaratanachai, “Air Flow, Thermal Profile, and Thermohydraulic Performance Assessment in a Square Duct Heat Exchanger With Combined Vortex Generators: CFD Analysis,” *Journal of Engineering (United Kingdom)*, vol. 2025, no. 1, 2025, doi: 10.1155/je/4197880.

[9] H. Karkaba, T. Dbouk, C. Habchi, S. Russeil, T. Lemenand, and D. Bougeard, “Multiobjective optimization of Vortex Generators for heat transfer enhancement in turbulent flows,” *International Journal of Thermofluids*, vol. 22, May 2024, doi: 10.1016/j.ijft.2024.100633.

[10] H. Arjmandi, R. Amini, A. Ghaffari, H. Rahmani, and A. Chamkha, “Effects of baffles and vortex generators on cooling performance of a gas turbine combustion chamber: Numerical assessment,” *Alexandria Engineering Journal*, vol. 61, no. 6, pp. 4467–4478, Jun. 2022, doi: 10.1016/J.AEJ.2021.10.005.

[11] U. Kashyap, K. Das, and B. K. Debnath, “Effect of surface modification of a rectangular vortex generator on heat transfer rate from a surface to fluid: An extended study,” *International Journal of Thermal Sciences*, vol. 134, no. May, pp. 269–281, 2018, doi: 10.1016/j.ijthermalsci.2018.08.020.

[12] H. Naik and S. Tiwari, “Effect of winglet location on performance of fin-tube heat exchangers with inline tube arrangement,” *Int. J. Heat Mass Transf.*, vol. 125, pp. 248–261, 2018, doi: 10.1016/j.ijheatmasstransfer.2018.04.071.

[13] Z. Qian, Q. Wang, and J. Cheng, “Analysis of heat and resistance performance of plate fin-and-tube heat exchanger with rectangle-winglet vortex generator,” *Int. J. Heat Mass Transf.*, vol. 124, pp. 1198–1211, 2018, doi: 10.1016/j.ijheatmasstransfer.2018.04.037.

[14] K. Srivastava and R. R. Sahoo, “Effect of pitch and angle of attack on thermal performance of new envelope and delta vortex generators for TEG: An experimental and numerical approach,” *International Journal of Thermal Sciences*, vol. 195, Jan. 2024, doi: 10.1016/j.ijthermalsci.2023.108671.

[15] C. Luo, S. Wu, K. Song, L. Hua, and L. Wang, “Thermo-hydraulic performance optimization of wavy fin heat exchanger by combining delta winglet vortex generators,” *Appl. Therm. Eng.*, vol. 163, Dec. 2019, doi: 10.1016/j.applthermaleng.2019.114343.

[16] O. Heriyani, M. Djaeni, Syaiful, and A. K. Putri, “Perforated concave rectangular winglet pair vortex generators enhance the heat transfer of air flowing through heated tubes inside a channel,” *Results in Engineering*, vol. 16, p. 100705, Dec. 2022, doi: 10.1016/J.RINENG.2022.100705.

[17] M. Dogan and S. Erzincan, “Experimental investigation of thermal performance of novel type vortex generator in rectangular channel,” *International Communications in Heat and Mass Transfer*, vol. 144, May 2023, doi: 10.1016/j.icheatmasstransfer.2023.106785.

[18] Z. Ke, C. Chen, K. Li, S. Wang, and C. Chen, “Vortex dynamics and heat transfer of longitudinal vortex generators in a rectangular channel,” *Int. J. Heat Mass Transf.*, vol. 132, pp. 871–885, 2019, doi: 10.1016/j.ijheatmasstransfer.2018.12.064.

[19] H. Fu, H. Sun, L. Yang, L. Yan, Y. Luan, and F. Magagnato, “Effects of the configuration of the delta winglet longitudinal vortex generators and channel height on flow and heat transfer in minichannels,” *Appl. Therm. Eng.*, vol. 227, Jun. 2023, doi: 10.1016/j.applthermaleng.2023.120401.

[20] J. Batista, A. Trp, K. Lenic, and M. Kirincic, “The influence of geometry parameters of rectangular vortex generators on the air-to-water fin-and-tube heat exchanger efficiency enhancement,” *International Communications in Heat and Mass Transfer*, vol. 162, Mar. 2025, doi: 10.1016/j.icheatmasstransfer.2025.108647.

[21] D. Jin, S. Quan, J. Zuo, and S. Xu, “Numerical investigation of heat transfer enhancement in a solar air heater roughened by multiple V-shaped ribs,” *Renew. Energy*, vol. 134, pp. 78–88, Apr. 2019, doi: 10.1016/J.RENENE.2018.11.016.

[22] S. Pourhedayat, S. M. Pesteei, H. E. Ghalinghie, M. Hashemian, and M. A. Ashraf, "Thermal-exergetic behavior of triangular vortex generators through the cylindrical tubes," *Int. J. Heat Mass Transf.*, vol. 151, Apr. 2020, doi: 10.1016/j.ijheatmasstransfer.2020.119406.

[23] J. Wang, L. Zeng, T. Fu, S. Yu, and Y. He, "Effects of the position and perforation parameters of the delta winglet vortex generators on flow and heat transfer in minichannels," *International Journal of Thermal Sciences*, vol. 198, no. October 2023, p. 108878, 2024, doi: 10.1016/j.ijthermalsci.2023.108878.

[24] P. Promvonge and S. Skullong, "Heat transfer augmentation in solar receiver heat exchanger with hole-punched wings," *Appl. Therm. Eng.*, vol. 155, pp. 59–69, Jun. 2019, doi: 10.1016/J.APPLTHERMALENG.2019.03.132.

[25] M. E. Nakhchi, M. Hatami, and M. Rahmati, "Experimental investigation of performance improvement of double-pipe heat exchangers with novel perforated elliptic turbulators," *International Journal of Thermal Sciences*, vol. 168, p. 107057, Oct. 2021, doi: 10.1016/J.IJTHERMALSCI.2021.107057.

[26] A. J. Modi, N. A. Kalel, and M. K. Rathod, "Thermal performance augmentation of fin-and-tube heat exchanger using rectangular winglet vortex generators having circular punched holes," *Int. J. Heat Mass Transf.*, vol. 158, pp. 1–16, 2020, doi: 10.1016/j.ijheatmasstransfer.2020.119724.

[27] Z. Han, Z. Xu, and J. Wang, "Numerical simulation on heat transfer characteristics of rectangular vortex generators with a hole," *Int. J. Heat Mass Transf.*, vol. 126, pp. 993–1001, 2018, doi: 10.1016/j.ijheatmasstransfer.2018.06.081.

[28] J. Wang, T. Fu, L. Zeng, F. sang Lien, and G. Chen, "Thermal-hydraulic performance in a tube with punched delta winglets inserts in turbulent flow," *International Journal of Thermal Sciences*, vol. 172, Feb. 2022, doi: 10.1016/j.ijthermalsci.2021.107326.

[29] P. Saini and M. P. Shah, "Performance evaluation of finned tube heat exchanger using curved wavy delta winglet vortex generators with circular perforations," *International Communications in Heat and Mass Transfer*, vol. 159, Dec. 2024, doi: 10.1016/j.icheatmasstransfer.2024.108184.

[30] Y. Oh and K. Kim, "Effects of position and geometry of curved vortex generators on fin-tube heat-exchanger performance characteristics," *Appl. Therm. Eng.*, vol. 189, May 2021, doi: 10.1016/j.applthermaleng.2021.116736.

[31] M. W. Tian, S. Khorasani, H. Moria, S. Pourhedayat, and H. S. Dizaji, "Profit and efficiency boost of triangular vortex-generators by novel techniques," *Int. J. Heat Mass Transf.*, vol. 156, p. 119842, Aug. 2020, doi: 10.1016/J.IJHEATMASSTRANSFER.2020.119842.

[32] P. Knödler and V. Dreissigacker, "Fluid Dynamic Assessment and Development of Nusselt Correlations for Fischer Koch S Structures," *Energies (Basel).*, vol. 17, no. 3, Feb. 2024, doi: 10.3390/en17030688.

[33] X. Zou, S. B. Lo, R. Sevilla, O. Hassan, and K. Morgan, "The generation of tetrahedral meshes for NURBS-enhanced FEM," *Eng. Comput.*, vol. 40, no. 6, pp. 3949–3977, Dec. 2024, doi: 10.1007/s00366-024-02004-z.

[34] P. Saini, A. Dhar, and S. Powar, "Performance enhancement of fin and tube heat exchanger employing curved delta winglet vortex generator with circular punched holes," *International Journal of Thermofluids*, vol. 20, p. 100452, Nov. 2023, doi: 10.1016/J.IJFT.2023.100452.

[35] M. K. Fahad, N. F. Ifraj, S. H. Tahsin, and M. J. Hasan, "Numerical investigation of the hydrothermal performance of novel vortex generators in a rectangular channel by employing inclination and rotational angles," *International Journal of Thermofluids*, vol. 20, p. 100500, Nov. 2023, doi: 10.1016/J.IJFT.2023.100500.

[36] S. Gururatana and S. Skullong, "Heat transfer augmentation in a pipe with 3D printed wavy insert," *Case Studies in Thermal Engineering*, vol. 21, Oct. 2020, doi: 10.1016/j.csite.2020.100698.

[37] A. Sinha, H. Chattopadhyay, A. K. Iyengar, and G. Biswas, "Enhancement of heat transfer in a fin-tube heat exchanger using rectangular winglet type vortex generators," *Int. J. Heat Mass Transf.*, vol. 101, pp. 667–681, Oct. 2016, doi: 10.1016/j.ijheatmasstransfer.2016.05.032.

[38] D. L. Hu *et al.*, "Performance optimization of a wavy finned-tube heat exchanger with staggered curved vortex generators," *International Journal of Thermal Sciences*, vol. 183, Jan. 2023, doi: 10.1016/j.ijthermalsci.2022.107830.

[39] K. Srivastava and R. R. Sahoo, "Experimental and numerical study on thermal performance of new envelope and triangular vortex generators with different pitch and angle of attack," *Thermal Science and Engineering Progress*, vol. 49, Mar. 2024, doi: 10.1016/j.tsep.2024.102459.

[40] A. J. Modi and M. K. Rathod, "Experimental investigation of heat transfer enhancement and pressure drop of fin-and-circular tube heat exchangers with modified rectangular winglet vortex generator," *Int. J. Heat Mass Transf.*, vol. 189, Jun. 2022, doi: 10.1016/j.ijheatmasstransfer.2022.122742.

[41] R. B. Pérez, A. M. Pérez, and D. S. Suárez, "Influence of the punched holes on thermohydraulic performance and flow pattern of rectangular channels with a pair of perforated vortex generators," *Int. J. Heat Mass Transf.*, vol. 184, 2022, doi: 10.1016/j.ijheatmasstransfer.2021.122291.

[42] J. Wang, L. Zeng, Y. He, B. Zhao, and P. Chu, "Effect of structure parameters on thermal performance of novel punched V-shape VGs for hear exchangers: An experimental approach," *International Communications in Heat and Mass Transfer*, vol. 155, Jun. 2024, doi: 10.1016/j.icheatmasstransfer.2024.107472.

[43] J. Wang, C. Li, L. Zeng, T. Fu, and K. Liu, "Thermal performance analysis of a heat exchanger with a novel turbulator insert by using machine learning method," *Case Studies in Thermal Engineering*, vol. 72, Aug. 2025, doi: 10.1016/j.csite.2025.106412.

[44] A. Boonloi and W. Jedsadaratanachai, "Turbulent forced convection in a square duct heat exchanger (SDHX) equipped with combined vortex turbulators (CVT): A numerical investigation," *International Communications in Heat and Mass Transfer*, vol. 161, Feb. 2025, doi: 10.1016/j.icheatmasstransfer.2024.108421.

[45] W. Wei, G. Xu, Y. Wang, and E. Ding, "Study on air-side performance of air-cooled heat exchangers under large air velocity and wet conditions," *Thermal Science and Engineering Progress*, vol. 48, Feb. 2024, doi: 10.1016/j.tsep.2024.102389.

[46] P. Yang, T. Qing, X. Lei, L. Wang, and Y. Liu, "Experimental study on thermal–hydraulic performance of moist air inside flat tube of two kinds of plate-fin heat exchangers," *Appl. Therm. Eng.*, vol. 239, Feb. 2024, doi: 10.1016/j.applthermaleng.2023.122121.

[47] M. H. Alshameri, A. A. Azizuddin, A. Arshad, H. G. Mohammed, and S. Sadeq, "Experimental Analysis of Thermal and Hydraulic Performance of FiberReinforced Polymer Fins in Compact Heat Exchangers," *International Journal of Automotive and Mechanical Engineering*, vol. 22, no. 2, pp. 12496–12510, Jun. 2025, doi: 10.15282/ijame.22.2.2025.18.0955.

Nomenclature

Roman Symbols

D — Tube diameter (m)

f — Darcy friction factor (–)

f_0 — Friction factor without vortex generator (–)
H — Channel height (m)
k — Thermal conductivity of air (W m^{-1} K^{-1})
L — Tube length (m)
Nu — Nusselt number (–)
Nu_avg — Average Nusselt number (–)
Nu_0 — Nusselt number without vortex generator (–)
P — Static pressure (Pa)
P_L — Longitudinal pitch (m)
P_T — Transverse pitch (m)
r — Radial distance of vortex generator from tube center (m)
R — Tube radius (m)
T — Static temperature (K)
T_in — Inlet air temperature (K)
T_w — Tube wall temperature (K)

Greek Symbols
α — Angular position of vortex generator (degree)
μ — Dynamic viscosity (Pa s)
ϱ — Air density (kg m^{-3})

Dimensionless Parameters
r/R — Radial distance ratio (–)
Nu/Nu_0 — Nusselt number ratio (–)
f/f_0 — Friction factor ratio (–)
TEF — Thermal enhancement factor (–)

[MESI] Editor Decision

2026-04-06 04:47 AM

Dan Mugisidi, Oktarina Heriyani, Amir Khalid, Ahmed Rahmani:

We have reached a decision regarding your submission to Mechanical Engineering for Society and Industry, "Improving the Thermal Efficiency of Fin-tube Heat Exchangers by Optimizing Geometric Parameters of Curved Rectangular Winglet Vortex Generators".

Our decision is to: Accept Submission

To proceed with the copyediting and production of your article, an Article Processing Charge (APC) of USD 350 (IDR 5.962.950) is required. Please note that the payment should be completed no later than **April 13, 2026**.
Kindly make the payment to the following account:
Account Number: 1850006623299
Account Holder: UNIMMA MESI
Bank Name: Bank Mandiri
Branch: Magelang Branch
IBAN: 1850006623299
Intermediary SWIFT Code: BMRIIDJA

Once the payment is made, please send the proof of payment to mesi@unimma.ac.id for verification. If you have any questions, please don't hesitate to contact us.

APC policy: https://journal.unimma.ac.id/index.php/mesi/apc

Fungky Dyan Pertiwi

[MESI] Editor Decision

2026-04-06 04:47 AM

Dan Mugisidi, Oktarina Heriyani, Amir Khalid, Ahmed Rahmani:

We have reached a decision regarding your submission to Mechanical Engineering for Society and Industry, "Improving the Thermal Efficiency of Fin-tube Heat Exchangers by Optimizing Geometric Parameters of Curved Rectangular Winglet Vortex Generators".

Our decision is to: Accept Submission

To proceed with the copyediting and production of your article, an Article Processing Charge (APC) of USD 350 (IDR 5.962.950) is required. Please note that the payment should be completed no later than **April 13, 2026**.
Kindly make the payment to the following account:
Account Number: 1850006623299
Account Holder: UNIMMA MESI
Bank Name: Bank Mandiri
Branch: Magelang Branch
IBAN: 1850006623299
Intermediary SWIFT Code: BMRIIDJA

Once the payment is made, please send the proof of payment to mesi@unimma.ac.id for verification. If you have any questions, please don't hesitate to contact us.

APC policy: https://journal.unimma.ac.id/index.php/mesi/apc

Fungky Dyan Pertiwi

[MESI] Editor Decision

2026-04-06 04:47 AM

Dan Mugisidi, Oktarina Heriyani, Amir Khalid, Ahmed Rahmani:

We have reached a decision regarding your submission to Mechanical Engineering for Society and Industry, "Improving the Thermal Efficiency of Fin-tube Heat Exchangers by Optimizing Geometric Parameters of Curved Rectangular Winglet Vortex Generators".

Our decision is to: Accept Submission

To proceed with the copyediting and production of your article, an Article Processing Charge (APC) of USD 350 (IDR 5.962.950) is required. Please note that the payment should be completed no later than **April 13, 2026**.
Kindly make the payment to the following account:
Account Number: 1850006623299
Account Holder: UNIMMA MESI
Bank Name: Bank Mandiri
Branch: Magelang Branch
IBAN: 1850006623299
Intermediary SWIFT Code: BMRIIDJA

Once the payment is made, please send the proof of payment to mesi@unimma.ac.id for verification. If you have any questions, please don't hesitate to contact us.

APC policy: https://journal.unimma.ac.id/index.php/mesi/apc

Fungky Dyan Pertiwi

Type of contribution:
Editorial
▶ Research Paper
Case Study
Review Paper
Scientific Data
Report of Tech. Application

mesi
e-issn. 2798-5245
Mechanical Engineering for Society and Industry
Vol. 6, No. 1 (2026) pp 128-145
https://doi.org/10.31603/mesi.15393

Improving the thermal efficiency of fin-tube heat exchangers by optimizing geometric parameters of curved rectangular winglet vortex generators

Dan Mugisidi[1]*, Oktarina Heriyani[1], Amir Khalid[2], Ahmed Rahmani[3]

[1] Department of Mechanical Engineering, Faculty of Industrial and Informatics Technology, Universitas Muhammadiyah Prof DR HAMKA, Jakarta Timur 13830, **Indonesia**
[2] Faculty of Mechanical and Manufacturing Engineering, Universiti Tun Hussein Onn Malaysia, Batu Pahat, Johor, Malaysia
[3] Sustainable Development and Environmental Protection Laboratory, Larbi Ben M'hidi University, Oum El Bouaghi, 04000, **Algeria**
✉ dan.mugisidi@uhamka.ac.id

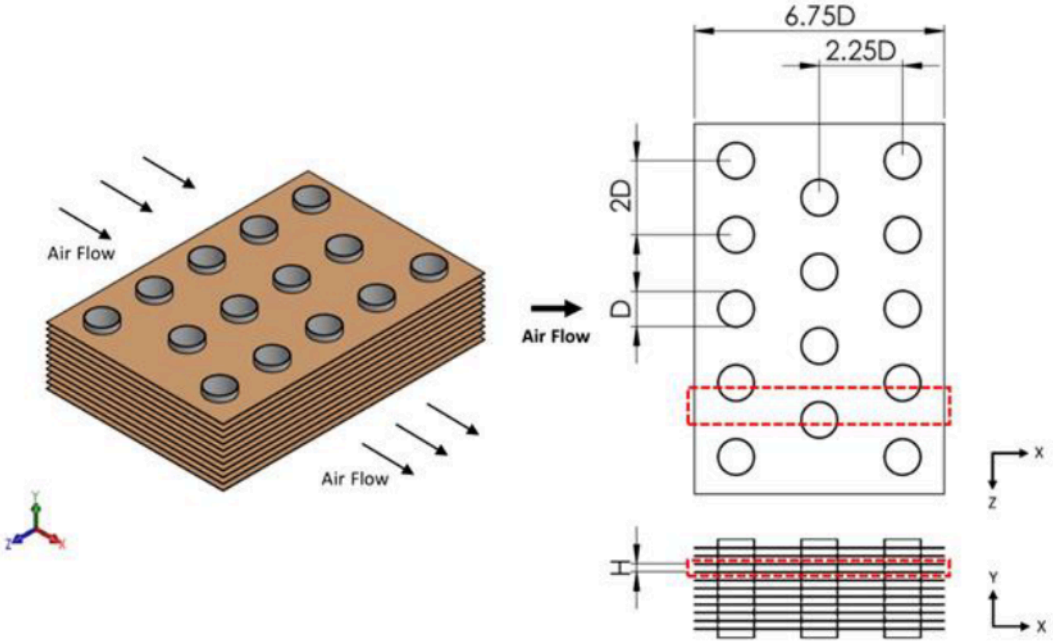

Highlights:

- Curved rectangular winglet vortex generators (CRW-VGs) were optimized to improve the thermal enhancement factor in fin–tube heat exchangers.
- Computational fluid dynamics analysis showed that radial distance, hole width, and angular position strongly influence heat transfer and pressure drop behavior.
- Smaller radial distances enhanced TEF by suppressing mixing vortices, while larger hole widths improved heat transfer through stronger jet-flow generation.
- The optimum configuration achieved a maximum TEF of 1.075 at an angular position of 120°, hole width of 0.5 H, and radial distance of 1.25.
- The findings demonstrate that proper geometric optimization of vortex generators can enhance heat transfer performance while minimizing pressure drop penalties.

Article info
Submitted: 2025-11-20
Revised: 2026-03-23
Accepted: 2026-04-06

Publisher
Universitas Muhammadiyah Magelang

Abstract

Thermal efficiency is a fundamental criterion in the design and operation of heat exchangers because it provides a clear view of the thermal behaviour and reliability of the system. Integrating vortex generators (VGs) with heat exchangers often increases turbulence and enhances the heat transfer rate but at the cost of increased pressure drops. This study aims to maximise the thermal enhancement factor (TEF) in fin–tube heat exchangers by optimising the radial distance, hole width and angular position of curved rectangular winglet vortex generators (CRW-VGs). Computational fluid dynamics analysis is utilised to investigate how variations in radial distance and hole width influence CRW-VG performance. Parameters such as TEF, Nusselt number ratio, friction factor ratio and flow regime were examined. The results show that smaller radial distances suppress mixing vortices and enhance TEF, while larger hole widths generate strong jet flows and increase heat transfer rates. The highest TEF of 1.075 is achieved at an angular position of 120°, a hole width of 0.5 H and a radial distance of 1.25. The study reveals that optimising the geometric parameters of VGs is proven satisfactory for enhancing heat transfer performance and minimising pressure drop.

Keywords: Curved rectangular winglet; Heat transfer enhancement; Hole width; Radial distance; Vortex generator

1. Introduction

Thermal efficiency is a crucial aspect in the design and operation of heat exchanger systems, playing an essential role in various industrial applications, such as power generation, cooling and chemical processing [1]. The need for better heat exchange in these systems with more compact designs has resulted in much research on this topic.

Air is the common working fluid in fin–tube heat exchangers. Similar to all gases, air has relatively poor thermophysical properties for heat transfer [2]. This limitation prompted researchers to enhance the effectiveness of heat transfer systems to increase energy efficiency while lowering production costs. Enhancing the air-side heat transfer of these equipment has been the subject of several theoretical, numerical and experimental investigations. A proven effective solution is the integration of vortex generators (VGs). These small devices are designed to enhance aerodynamic performance, flow control and heat transfer in forced draft cooling towers [3]. VGs improve thermal performance by inducing subsidiary currents, disrupting interface region development and promoting fluid dispersion near the walls. The longitudinal vortices generated by VGs allow reduced stagnation zones behind the tubes [4], increase turbulence intensity and well fluid mixing [5]. Increasing turbulence often enhances the heat transfer rate but at the cost of increased pressure drops. Therefore, optimising heat transfer and reducing fluid flow resistance have become the primary focus.

Previous studies have demonstrated that both the placement and geometric configuration of VGs significantly influence the thermal–hydraulic performance of fin–tube heat exchangers. Positioning VGs near the centre of the tube has been shown to provide more effective heat transfer enhancement compared with inlet or outlet placements, primarily due to the stronger interaction between the generated vortices and the tube wake region [6], [7]. In addition, smaller VG geometries operating at lower Reynolds numbers have been reported to further improve heat exchange performance [8].

Geometric optimisation of the heat exchanger structure also plays an important role in determining overall performance. The optimal combination of a larger fin pitch and a smaller tube diameter has been experimentally identified as providing improved fluid flow characteristics [9]. However, increasing the fin pitch can reduce the Nusselt number (Nu) and the wall friction factor (f) because of weakened vorticity formation and enhanced turbulent energy dissipation [10]. Furthermore, numerical investigations have shown that combining concave and convex VG surfaces generates stronger longitudinal vortices, resulting in an enhancement of the heat transfer rate of approximately 14.4% [11].

Operational parameters, such as VG location and angle of attack (AoA), further determine heat transfer effectiveness. Higher attack angles, particularly when VGs are positioned farther from the tube, can substantially increase heat transfer rates [12]. Conversely, smaller angles may be advantageous in certain configurations by directing colder fluid towards weak wake regions [13]. An AoA of 45° has consistently been identified as providing superior thermal enhancement compared with other angles [14], [15]. Furthermore, increasing the number of staggered VGs enhances the thermal enhancement factor (TEF) by accelerating flow and promoting fluid mixing in the wake region [16], [17]. These configurations are commonly arranged in common flow up, common flow down (CFD) or hybrid arrangements to optimise performance.

In rectangular channel systems, geometric parameters, such as winglet aspect ratio and channel height (H), have been identified as the dominant factors affecting heat transfer performance [18], [19]. Increasing duct height significantly alters vortex development, especially when VGs are mounted on opposing walls, thereby enhancing overall flow dynamics and heat transfer efficiency. Heat exchange performance is also highly sensitive to VG position and geometry

[20], with even minor geometric changes producing noticeable variations in performance [21], [22].

Among the various structural innovations, perforated VGs have emerged as a promising approach for improving thermal performance [23]. Perforated rectangular winglets have been reported to increase the Nu by approximately 3.91–5.52 times, achieving a maximum thermal performance factor of 2.01 [24]. Similarly, double perforated inclined elliptic turbulators have demonstrated Nu enhancements of up to 217.4% [25]. These improvements are attributed to jet flows generated through perforations, which disrupt recirculation zones and intensify fluid mixing, thereby enhancing thermal exchange efficiency [26], [27], [28].

Despite these substantial advancements, existing studies predominantly emphasise external geometric modifications, placement strategies and angle of attack variations. Although perforating the VG surface can either enhance or deteriorate heat transfer performance, depending on the hole size, number and placement, because it changes the vortex strength and the pressure drop [29], systematic investigations of hollow rectangular winglet VGs remain limited. More importantly, the geometric perforation parameter (hole width) and the positional parameter (radial distance from the tube) have largely been examined independently. Consequently, the coupled interaction between these two design variables and their combined influence on thermal–hydraulic performance has not been comprehensively evaluated. This lack of integrated parametric analysis restricts the development of optimised hollow VG configurations capable of simultaneously maximising heat transfer enhancement and minimising pressure drop penalties. To overcome this limitation, this study proposes a performance-based geometric optimisation framework for circular ring winglet vortex generators (CRW-VGs) in fin–tube heat exchangers, focusing on radial distance and hole width as key design variables.

The coupled effects of radial distance (r/R = 1.25 and 1.5) and hole width (0.25 H and 0.5 H) are systematically analysed using high-fidelity CFD simulations. Performance is evaluated through integrated metrics, including the TEF, Nu/Nu_0, friction factor ratio (f/f_0) and flow structure characterisation. By integrating geometric sensitivity analysis with unified thermo-hydraulic evaluation and mechanistic interpretation of vortex dynamics, this study identifies the optimal configuration that maximises heat transfer while minimising pressure drop, providing both quantitative assessment and mechanistic insight for a compact heat exchanger design.

2. Methodology

2.1. Physics Model

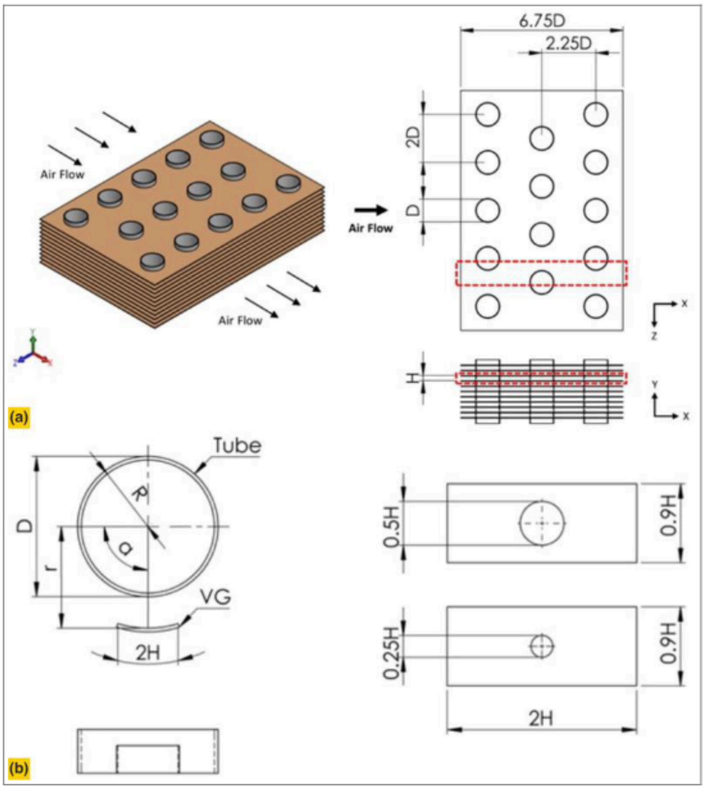

Figure 1. Schematic illustration and the main dimensions of the studied VG: (a) The overall configuration of the fin–tube heat exchanger; (b) Detailed geometry of the CRW-VG

Figure 1 shows the geometric details of a heat exchanger with three rows of staggered tubes. The VGs employed in this study take the form of a rectangular curved winglet design characterised by the geometry depicted in Figure 1. Figure 1a presents the overall configuration of the fin–tube heat exchanger and the computational domain employed in the CFD simulations. The three-dimensional (3D) schematic depicts the staggered tube arrangement and the direction of airflow. The top view specifies the tube pitches: the transverse pitch, PT = 2.25 D and the longitudinal pitch, PL = 6.75 D, where D denotes the outer tube diameter. The side view defines H as the vertical distance between two adjacent fins. The dashed rectangular region marks the representative segment selected from the complete heat exchanger geometry for numerical modelling. The tube radius, R = D/2, serves as the reference length for positioning analysis. Figure 1b shows the detailed geometry of the CRW-VG. The winglet length in the streamwise direction is 2 H, which is twice that of H. The winglet height is 0.9 H, providing a small clearance from the fin surface to prevent excessive blockage. Perforated configurations use circular holes with diameters of 0.5 *H* and *0.25 H*, representing the large, medium and small perforation cases, respectively, examined in the parametric study. All geometric dimensions are normalised by H for geometric similarity and scalable comparison.

This model serves as a pivotal component in our experimental setup, aimed at investigating its effects on enhancing fluid dynamics and heat transfer processes. The geometry of the VGs, as illustrated in the figure, showcases its distinctive features and potential to induce vortices and modify the flow field. Due to its efficacy in improving the performance of various thermal systems, such VG configurations have been widely studied [19], making them ideal candidates for our research endeavours. By using this specific design, this study aims to elucidate the VGs' impact on the efficiency and effectiveness of heat transfer mechanisms within our experimental apparatus.

The main dimensions refer to Oh and Kim's previous investigation [30]: diameter *D* = 32 mm, length *L* = 6.75, longitudinal pitch *P_L* = 2.25*D*, transverse pitch (*P_T*) = 2*D*, *H* = 7 mm, length of the section with radius 2 *H* and corner radius 60°. The hole widths of the CRW-VGs are 0.25 *H* and 0.5 *H*, with a VG height of 0.9 *H*. The angular position (α) indicates the angle measured in an anticlockwise manner from the lengthwise orientation of the tube to the line linking the CRW-VGs to the central point of the tube, (*r*) denotes the distance measured radially from this central point, and *R* represents the radius of the tube. The investigation of these parameters was carried out using variations in position angles (α): 30°, 45°, 60°, 75°, 90°, 105°, 120°, 135° and 150° with *r*/*R* = 1.25 and 1.5.

2.2. Governing Equation

The flow conditions in the system under investigation are assumed to be incompressible, indicating that changes in density due to pressure variations are negligible and do not significantly alter the fluid's behaviour. In the fin tube heat exchanger, a Newtonian fluid with a constant stream is employed. The conservation equations for mass, momentum and energy are expressed as follows:

$$\nabla \cdot \vec{V} = 0 \tag{1}$$

$$\rho(\vec{V} \cdot \nabla)\vec{V} = -\nabla p + \mu \nabla^2 \vec{V} \tag{2}$$

$$\rho \vec{V} \cdot \nabla h = \nabla \cdot (k \nabla T) \tag{3}$$

The notation in the equation above equations, namely $\vec{V}$, ρ, p, h, k, μ, and T involved are the velocity vector, air density, static pressure, thermal conductivity of air, dynamic viscosity, and static temperature, respectively.

The heat transfer performance (TEF) is formulated as follows [31],

$$TEF = (Nu/Nu_0)/(f/f_0)^{1/3} \tag{4}$$

where the Nusselt number (*Nu*) and friction factor (*f*) are formulated as follows.

$$Nu = hL_c/k \tag{5}$$

$$f = 2\Delta pH/(\rho U_c^2 L) \tag{6}$$

2.3. Computational Domain and Boundary Conditions

Figure 2 illustrates the computational domain of the fin–tube heat exchanger equipped with CRW-VGs. The domain represents the lateral arrangement, flow direction and fin pitch orientation. Owing to geometric uniformity and cyclic configuration, the computational region is defined as half of the transverse pitch (P_T/2) in the x-direction and one full pitch length in the z-direction. This periodic simplification significantly reduces computational costs while preserving the essential flow and heat transfer characteristics.

To ensure an accurate representation of the physical system, steady-state and incompressible flow assumptions are adopted. The domain is extended sufficiently in the streamwise direction to allow proper flow development and to avoid undesirable numerical or physical instabilities.

2.3.1. Boundary conditions

At the inlet, a uniform velocity profile and a constant temperature are specified:

$$\mathrm{u} = (u_{in}, 0{,}0), T = T_{in} \tag{7}$$

where u is the velocity vector, u_{in} is the inlet air velocity, and T_{in} is the inlet air temperature.

At the outlet, a constant reference pressure is prescribed:

$$p = p_{out} \tag{8}$$

together with zero-gradient conditions for velocity and temperature:

$$\frac{\partial \mathrm{u}}{\partial n} = 0, \frac{\partial T}{\partial n} = 0 \tag{9}$$

where n denotes the outward normal direction to the outlet boundary.

For all solid surfaces, including the tube, fins, and CRW-VGs, the no-slip condition is applied:

$$\mathrm{u} = 0 \tag{10}$$

A constant wall temperature is imposed on the tube surface:

$$T = T_w \tag{11}$$

where $T_w$is the prescribed tube wall temperature.

Due to the periodicity of the geometry in the transverse and spanwise directions, periodic boundary conditions are employed:

$$\phi(x, y, z) = \phi(x, y, z + P) \tag{12}$$

where ϕ represents the dependent flow variables (velocity components, pressure and temperature), and Pdenotes the periodic pitch length.

These boundary conditions ensure physically consistent flow development and reliable prediction of heat transfer and fluid flow characteristics within the computational domain.

Matching boundary conditions are established in the *x* orientation amid the algorithmic region, while cyclic restrictions are established on both the higher and lower surfaces in the upriver and downriver orientations. The wing region incorporated into the CRW-VGs serves as a barrier, and the tube is subjected to constraints at this enclosure. These conditions ensure stable flow patterns within the algorithmic region, preventing undesired turbulence or instability. Moreover, the no-slip conditions and consistent surface temperature facilitate precise control and optimise the flow dynamics around the wing region and tube enclosure.

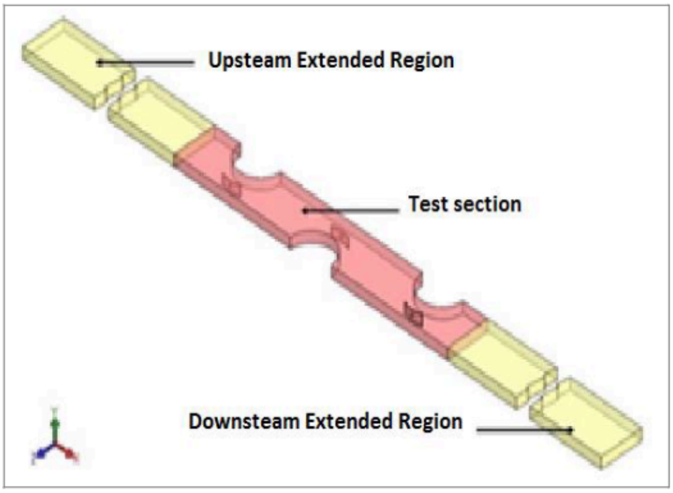

Figure 2. Computational domain

2.4. Convergence Assessment

The convergence of the numerical solution was assessed using a combination of residual-based, physical-based and grid-independence criteria to ensure numerical accuracy and physical reliability.

The normalised residuals of the governing equations were monitored during the iterative process. Convergence was assumed when the residuals of the continuity and momentum equations decreased below 10^{-6}, while a stricter threshold of 10^{-8} was imposed for the energy equation due to the heat transfer-oriented nature of the present study.

In addition to residual monitoring, several global physical quantities were continuously tracked, including the average Nusselt number (Nu_{-avg}), f and outlet bulk temperature (T_{out}). The solution was considered physically converged only when the relative variation in these parameters over 500 successive iterations was satisfied:

$$\left| \frac{\phi^{(n)} - \phi^{(n-500)}}{\phi^{(n)}} \right| < 0.1\% \tag{13}$$

where ϕrepresents Nu_{-avg}, f, or T_{out}, and $n$denotes the iteration number.

Furthermore, a grid independence study was conducted using four progressively refined meshes ranging from 600,641 to 915,422 elements. The relative deviations of Nu_{-avg} and f between the two finest meshes were below 0.1%, confirming mesh independence. This value is well within the commonly accepted convergence range of 1%–2% [32]. Thus, the grid with 822,157 elements was adopted for all subsequent simulations to achieve an optimal balance between numerical accuracy and computational efficiency.

2.5. Grid Independence Test

A grid independence test was carried out for numerical analysis. The computational grid was bifurcated into two parts, specifically the region adjacent to the VGs and the rest of the area. The non-conformal interface approach was implemented between these two zones. To ensure accuracy in analysis and attain optimal grid quality, grid generation employed inflation techniques in the tube vicinity and VGs. As illustrated in Figure 3, the cell geometry utilised around the VGs is tetrahedral because the element can precisely capture arbitrary flow around the complex geometry of the VG [33] and is directly relevant to finely detailed VGs. Four different grid sizes are considered in Table 1 to list the number of cells.

Table 1. Grid independence test

Number of grids	*Nu_avg*	*f*
600,641	16.55447	0.09671
715,421	16.70175	0.09603
822,157	16.79783	0.09551
915,422	16.80972	0.09549

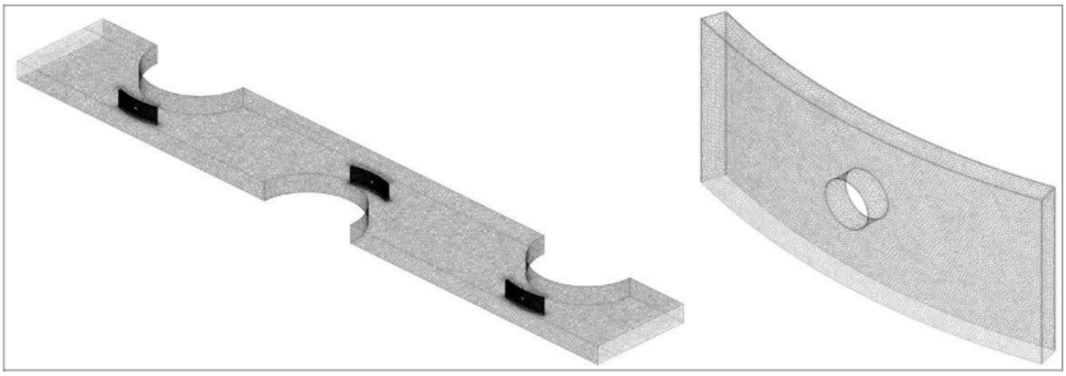

Figure 3. Computational grid test

2.6. Numerical Solution Methodology

Numerical simulations were performed under steady-state conditions using the finite volume method to solve the 3D governing equations of mass, momentum and energy. Airflow was assumed to be incompressible, Newtonian and turbulent, with constant thermophysical properties.

Turbulence effects were modelled using the shear stress transport (SST) k–ωmodel, which combines the robustness of the k–ωformulation near the wall with the freestream independence of the k–εmodel in the outer region. This model is particularly suitable for predicting adverse pressure gradients and flow separation occurring in fin–tube heat exchangers equipped with CRW-VGs.

The governing equations were discretised using a second-order upwind scheme for the convective terms of momentum and energy equations to enhance numerical accuracy. Pressure–velocity coupling was achieved using the SIMPLE algorithm. Spatial discretisation was applied consistently across the computational domain to ensure numerical stability.

A non-uniform computational grid was employed, with mesh refinement and inflation layers applied near the tube and VG surfaces to accurately capture velocity and thermal boundary layers. A grid independence study was conducted using four mesh resolutions, as detailed in Table 1. The variation in Nu_avg and f between the two finest meshes was less than 0.1%, indicating mesh-independent results. Consequently, the mesh with 822,157 cells was selected for all simulations as an optimal compromise between accuracy and computational cost.

2.7. Validation

The convergence of the numerical solution was ensured by monitoring the normalised residuals of the governing equations. The convergence criteria were set to $10^{-5}$for continuity and momentum equations and 10^{-6} for the energy equation. In addition to residual reduction, global quantities, such as Nu_avg and pressure drop, were monitored to confirm the physical convergence of the solution.

The simulation model adopted in this study was based on a previously validated configuration [30], which serves as a reference case for assessing the reliability of the numerical method. Turbulent flow was modelled using the k–ω SST model in conjunction with the governing Eq. (1) to Eq. (3). This model is well known for accurately predicting adverse pressure gradients and flow separation, making it suitable for complex flow simulations in fin–tube heat exchangers equipped with curved VGs.

The numerical results were validated against published experimental data [30], as illustrated in **Figure 4**. The comparison showed good agreement, with deviations of 2%–6% for Nu and 4%–8% for f, and an overall error below 9%. These results confirm the reliability of the present numerical methodology for predicting heat exchanger performance.

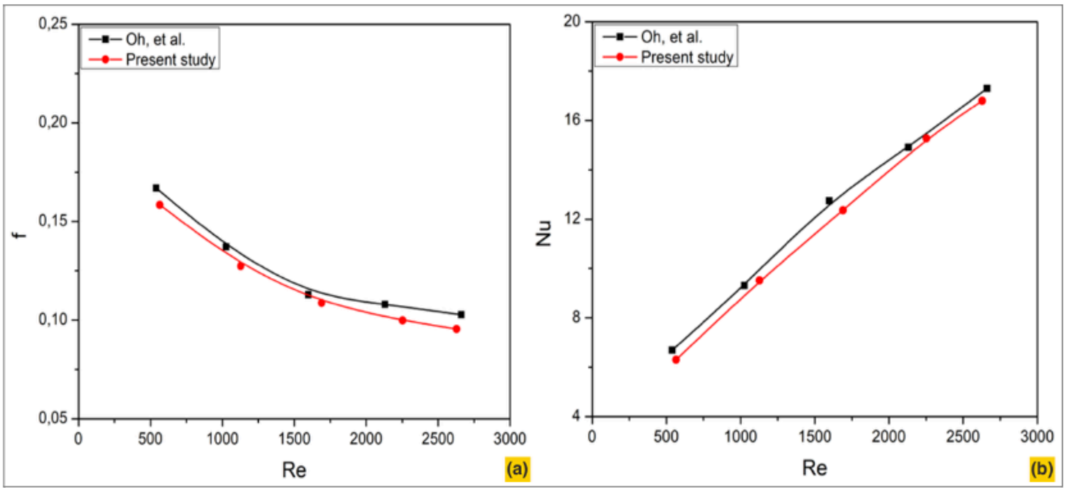

Figure 4. Numerical validation results: (a) *f*; (b) *Nu*

3. Results

3.1. Influence of Geometry and Radial Distance on the $\mathrm{Nu}/\mathrm{Nu_o}$ and $\mathrm{f}/\mathrm{f_o}$ Values

The assessment of heat transfer performance can be observed from the resulting Nu/Nu_o value. The comparison between Nu and Nu_o (Nusselt number under reference conditions) provides insight into heat transfer efficiency. Deviations in Nu/Nu_o signify alterations in the thermal performance of the observed system, as shown in **Figure 5** (i.e. (a) is 0.25 *H* and (b) is 0.5 *H*). **Figure 5** and **Figure 6** demonstrate the coupled relationship between heat transfer enhancement and flow resistance as a function of the attack angle, hole width and radial position of the CRW-VGs. As shown in **Figure 5**, the variation in Nu/Nu_o strongly depends on vortex stability and secondary flow development. At lower angles (30°–60°), moderate longitudinal vortices are generated, resulting in limited boundary layer disruption and moderate heat transfer enhancement. However, as indicated in **Figure 6**, this regime is accompanied by only a slight increase in f, reflecting a moderate disturbance level within the flow field.

When the angle approaches 75°–90°, both Nu/Nu_o (**Figure 5**) and f/f_o (**Figure 6**) reach relatively low values. This behaviour indicates a weakened and less coherent vortex structure, in which reduced mixing leads to minimal heat transfer enhancement and lowered flow resistance. The reduction in heat transfer in this region is mainly attributed to the reduced effective contact area for heat transfer, intensified rotational motion and the formation of lateral vortices on the surface of the perforated VGs [34], which dissipate energy without significantly enhancing boundary layer thinning.

A significant change occurs at 120°: a maximum Nu/Nu_0 (**Figure 5**) and a pronounced increase in f/f_0 (**Figure 6**). This correspondence confirms that strong and stable longitudinal vortices are formed at this angle, intensifying cross-stream mixing and effectively thinning the thermal boundary layer. However, enhanced vortex strength also increases shear stress and energy dissipation, leading to higher pressure penalties. This regime represents a high-disturbance, high-enhancement condition in which heat transfer improvement is achieved at the expense of increased friction losses.

At larger angles (135°–150°), both Nu/Nu_0 and f/f_0 decrease, suggesting vortex breakdown and excessive flow separation. Although flow disturbance remains present, the loss of vortex coherence reduces effective mixing and pressure buildup.

The influence of hole width and radial distance further clarifies the thermo-hydraulic interaction. The smaller hole width (0.25 *H*) produces more concentrated vortices and sharper enhancement peaks in **Figure 5** and relatively controlled friction increases in **Figure 6**. By contrast, the larger hole width (0.5 *H*) allows partial flow penetration through the perforation, promoting distributed secondary flows that increase energy dissipation and friction levels while slightly moderating heat transfer gains. Similarly, increasing the radial distance to r/R = 1.5 strengthens the vortex–wake interaction, enhancing Nu/Nu_0 but also elevating f/f_0 because of the intensified momentum exchange.

Overall, the combined analysis of **Figure 5** and **Figure 6** confirms that the thermo-hydraulic performance is governed by the balance between vortex intensity, boundary layer disruption and flow resistance. The angle of 120° emerges as the most effective configuration in terms of heat transfer enhancement, although its practical suitability must be evaluated through an integrated metric, such as the TEF, to ensure that the gain in heat transfer justifies the associated pressure penalty.

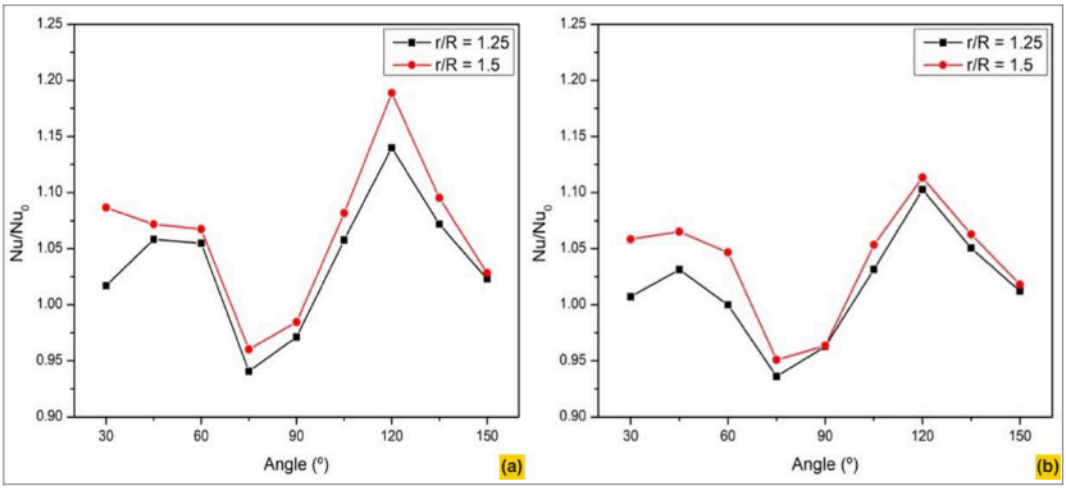

Figure 5. The effect Nu/Nu_o: (a) Hole width CRW-VGs 0.25*H*; (b) Hole width CRW-VGs 0.5*H*

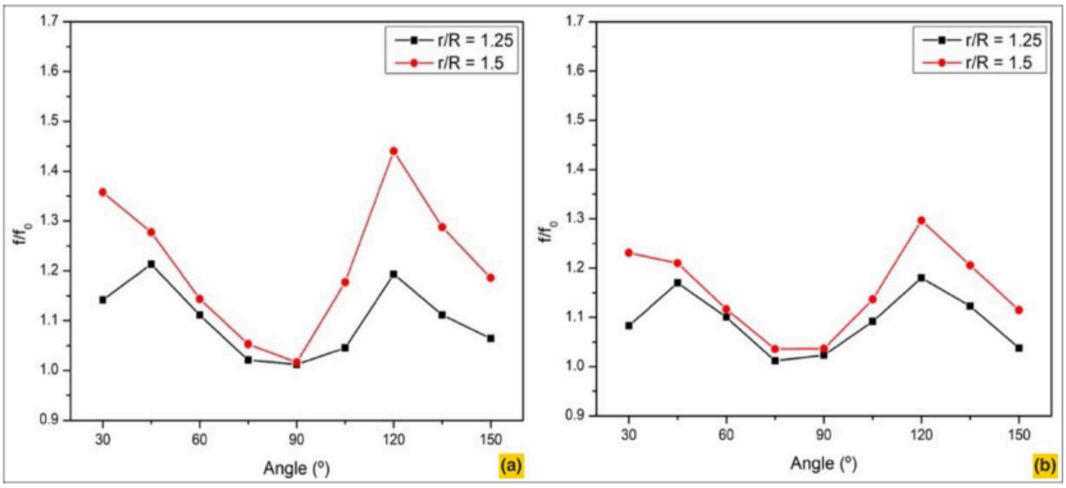

Figure 6. The effect of position angle on the friction factor: (a) Hole width CRW-VGs 0.25*H*; (b) Hole width CRW-VGs 0.5*H*

3.2. Flow Field and Thermal Field Interpretation

Reducing *f* with an increase in *Nu* using holes can reduce the pressure drop. As *Nu* and *f* are parameters of the TEF, the heat transfer performance can be determined, as discussed above, by looking at the contour changes in speed, temperature and pressure in Figure 7 to Figure 12. Figure 7 to Figure 12 reveal that the thermo-hydraulic performance of the CRW-VGs is governed not merely by geometric variation but primarily by the stability regime of the generated longitudinal vortices. Three distinct flow regimes can be identified as the attack angle (α) increases: (i) weak vortex regime (30°–60°), (ii) coherent vortex amplification regime (75°–120°) and (iii) vortex breakdown regime (135°–150°).

In the weak vortex regime, velocity contours (Figure 7 and Figure 8) indicate limited secondary flow development and only a partial disruption of the boundary layer. The generated vortices are insufficient to induce the deep penetration of core flow towards the heated surface.

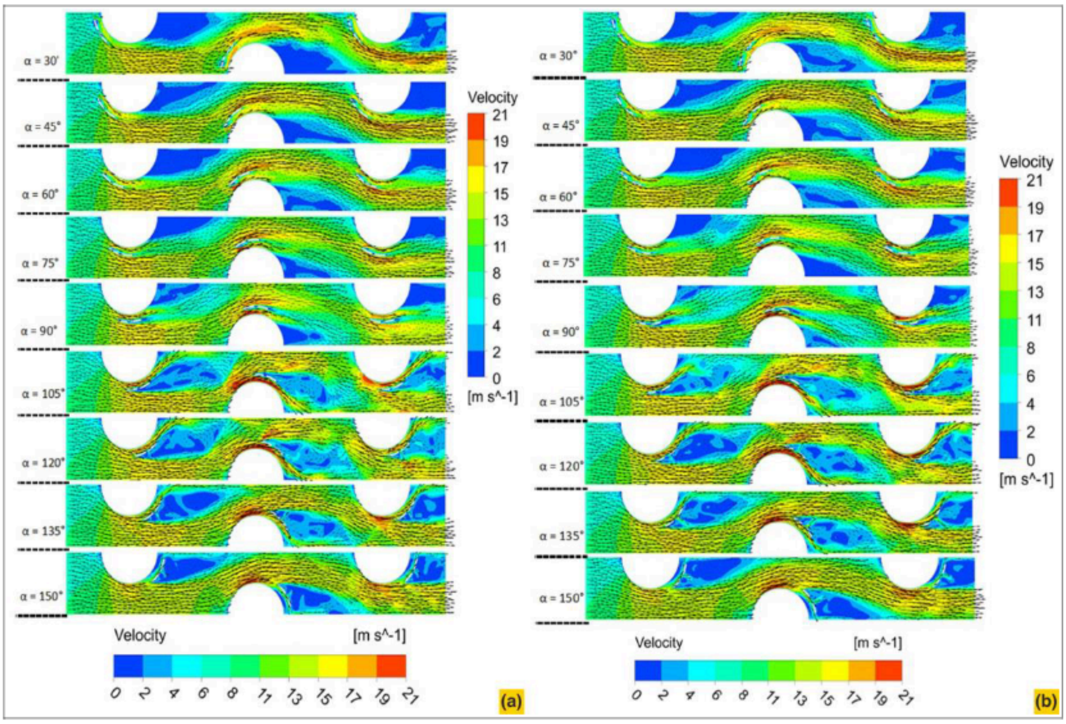

Figure 7. Velocity contour r/R 1.25: (a) Hole width 0.25H; (b) Hole width 0.5H

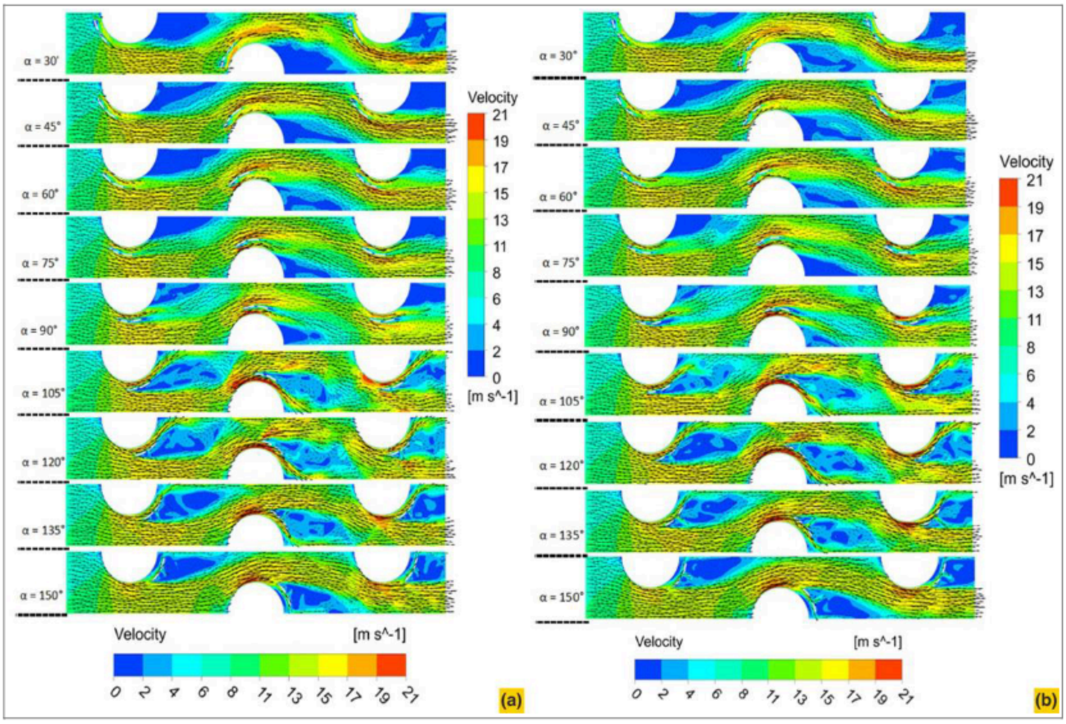

Figure 8. Velocity contour r/R 1.5: (a) Hole width 0.25H; (b) Hole width 0.5H

Consequently, the temperature contours (Figure 11 and Figure 12) show a relatively thick thermal boundary layer and non-uniform temperature stratification. The pressure contours (Figure 9 and Figure 10) display moderate upstream–downstream gradients, indicating limited energy dissipation and relatively small pressure penalties. However, as fluids move swiftly, they have fewer opportunities for prolonged interaction, resulting in smaller pressure drops [35]. This explains why lower attack angles, despite smoother flow behaviour, do not generate substantial convective enhancement.

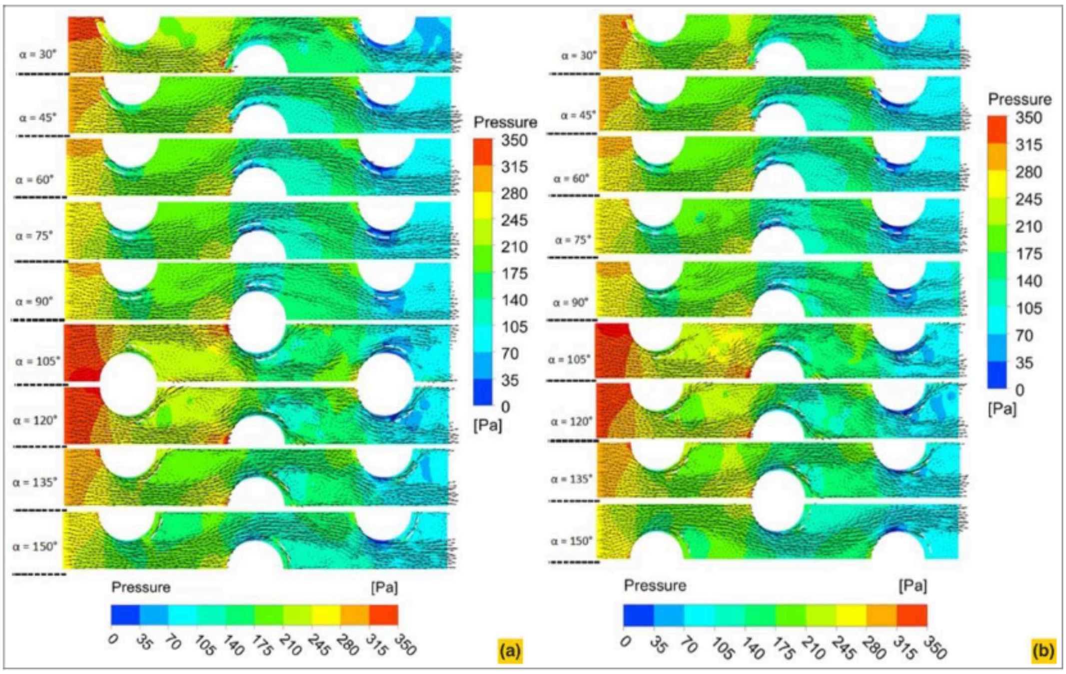

Figure 9. Pressure drop contour *r/R* 1.25: (a) Hole width 0.25*H*; (b) Hole width 0.5*H*

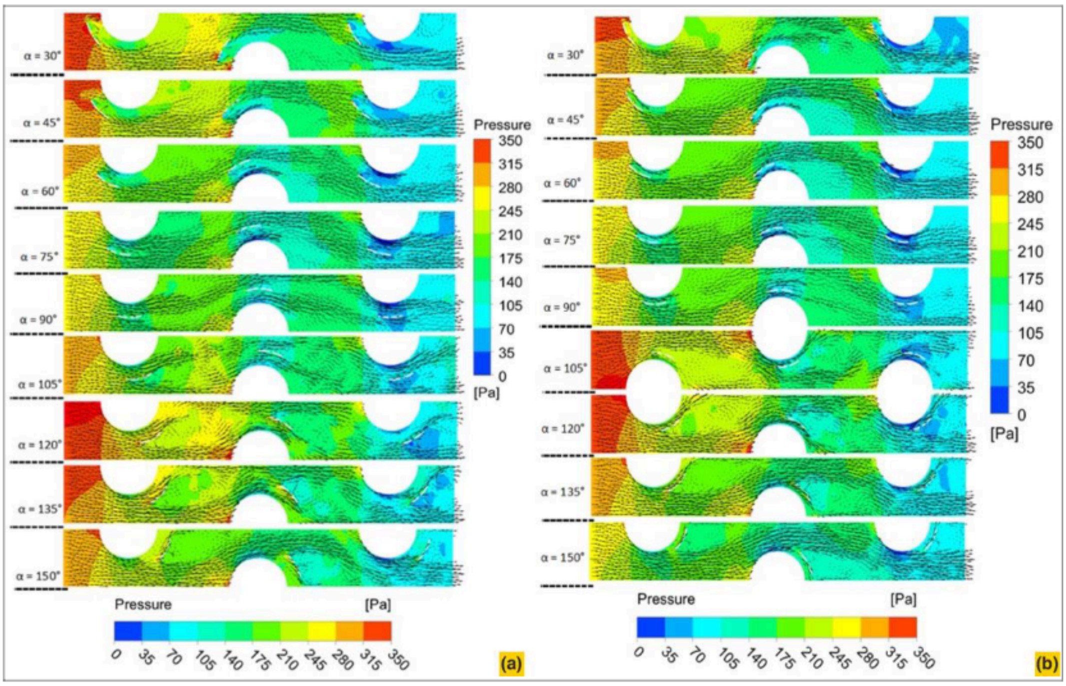

Figure 10. Pressure drop contour *r/R* 1.5: (a) Hole width 0.25*H*; (b) Hole width 0.5*H*

A fundamentally different behaviour emerges in the coherent vortex amplification regime (α ≈ 105°–120°). In this range, the velocity field exhibits highly organised longitudinal vortices with an intensified cross-stream momentum exchange. The vortices transport high-momentum core fluid towards the heated wall while ejecting low-momentum near-wall fluid outward, significantly thinning the thermal boundary layer. The temperature distribution becomes more uniform, thus confirming enhanced convective transport. Simultaneously, the pressure field exhibits the most pronounced gradients, reflecting maximal shear production and vortex strength.

Nevertheless, the perforated configuration introduces an additional mechanism. As depicted in **Figure 9** and **Figure 10**, the jet stream emanating from the orifice of the CRW-VGs has the potential to alleviate stagnation flow, consequently reducing the pressure drop [36], [37], [38]. This jet-induced acceleration redistributes local pressure peaks and mitigates excessive recirculation behind the VG, thereby partially compensating for the pressure penalty associated with strong vortex generation. Therefore, this regime represents a critical transition state in which vortex strength and structural coherence are maximised, while perforation-induced jet flow moderates stagnation-related losses.

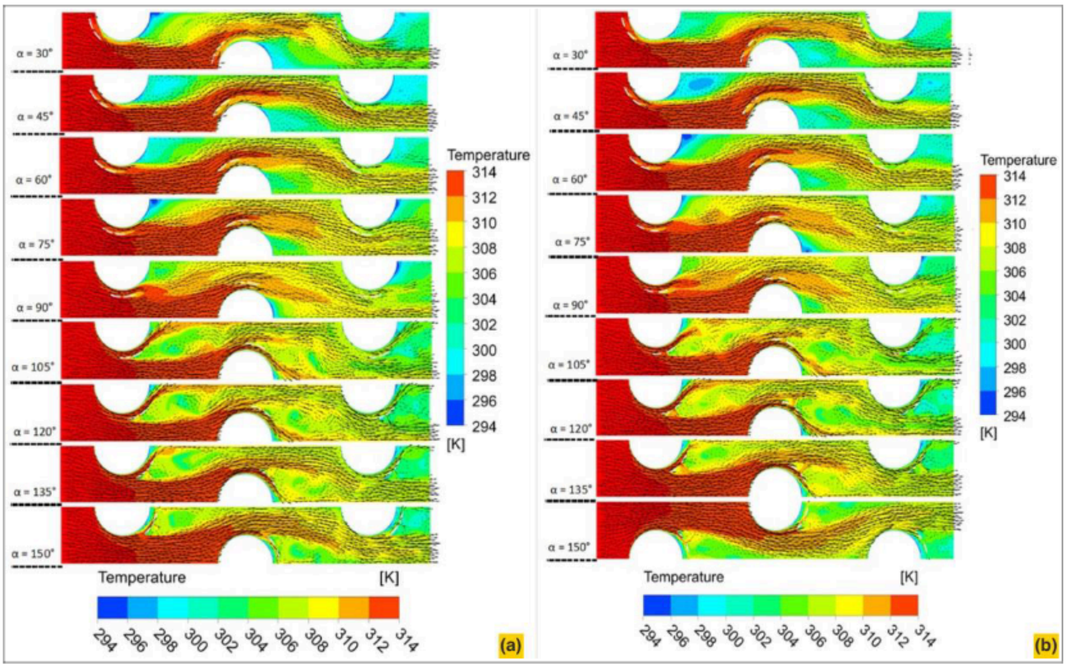

Figure 11. Temperature contour r/R 1.25: (a) Hole width 0.25H; (b) Hole width 0.5H

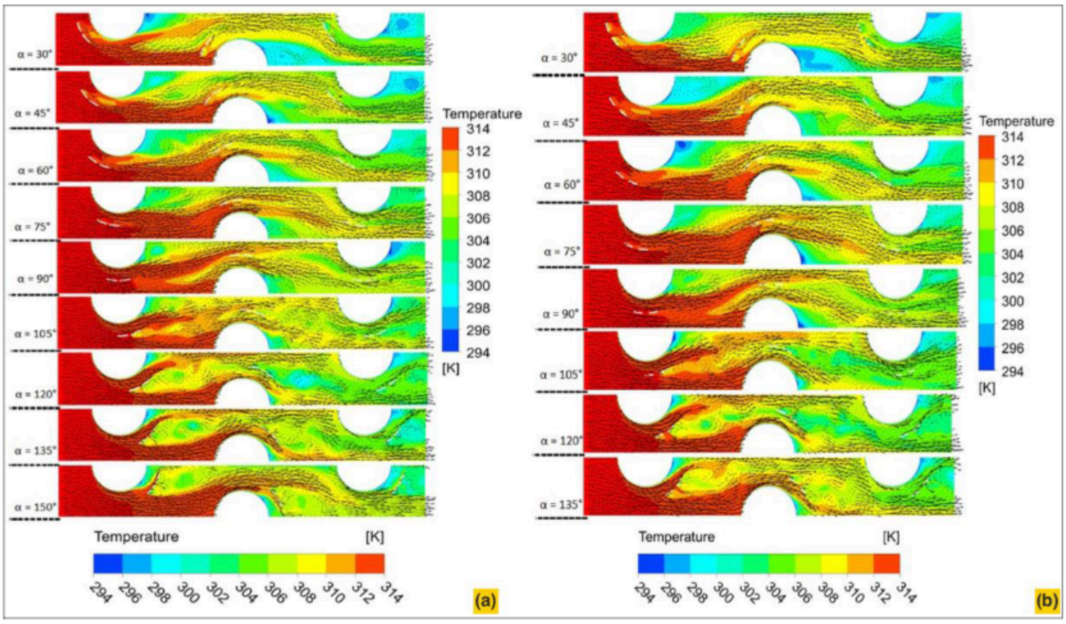

Figure 12. Temperature contour r/R 1.5: (a) Hole width 0.25H; (b) Hole width 0.5H

When α ≥ 135°, the system enters a vortex breakdown regime. Although apparent disturbance increases, velocity contours reveal fragmented and unstable vortical structures. The pressure distribution becomes spatially irregular, indicating that kinetic energy is increasingly dissipated through chaotic separation rather than organised secondary motion. As a result, temperature contours show reduced effectiveness in boundary layer thinning, despite intensified disturbance. This demonstrates that excessive geometric forcing shifts the system from a structured convective enhancement to instability-driven dissipation.

The geometric parameters further modulate these mechanisms. An increasing radial position to r/R = 1.5 enhances the wake–vortex interaction and prolongs vortex persistence, intensifying the heat transfer but also elevating the pressure penalties. Similarly, a smaller hole width (0.25 H) generates concentrated vortices and sharper shear layers, thereby promoting a stronger boundary layer disruption. By contrast, a larger hole width (0.5 H) allows for greater flow penetration through the perforation, redistributing vortex energy and stabilising the pressure field, thereby offering a more balanced thermo-hydraulic response.

Overall, the results demonstrate that thermo-hydraulic optimization is governed by vortex coherence rather than vortex magnitude alone. The optimal configuration ($\alpha \approx 105°–120°$) corresponds to the condition where organized secondary flow production is maximized, stagnation effects are partially mitigated by jet-induced flow through perforations, and instability-driven energy dissipation has not yet dominated the system. This mechanistic interpretation advances the understanding of perforated vortex generators by identifying vortex stability and jet–wake interaction as the primary control parameters governing performance. As illustrated in **Figure 13**, the streamline and velocity contours reveal a coherent high-velocity core developing along the inner wall of the curved channel, accompanied by jet-induced momentum injection from the perforations into the wake region. This mechanism promotes thermal boundary layer thinning through enhanced near-wall acceleration while simultaneously suppressing large-scale recirculation that would otherwise increase frictional losses. The interaction between curvature-driven Dean vortices and the longitudinal vortices generated by the VG further intensifies transverse momentum exchange, improving convective transport uniformity along the heated surface. Consequently, the heat transfer augmentation achieved within the optimal angular range is not merely a function of vortex strength, but rather of sustained vortex organization and controlled jet–wake stabilization, which collectively ensure enhanced Nusselt number performance with moderated pressure penalties.

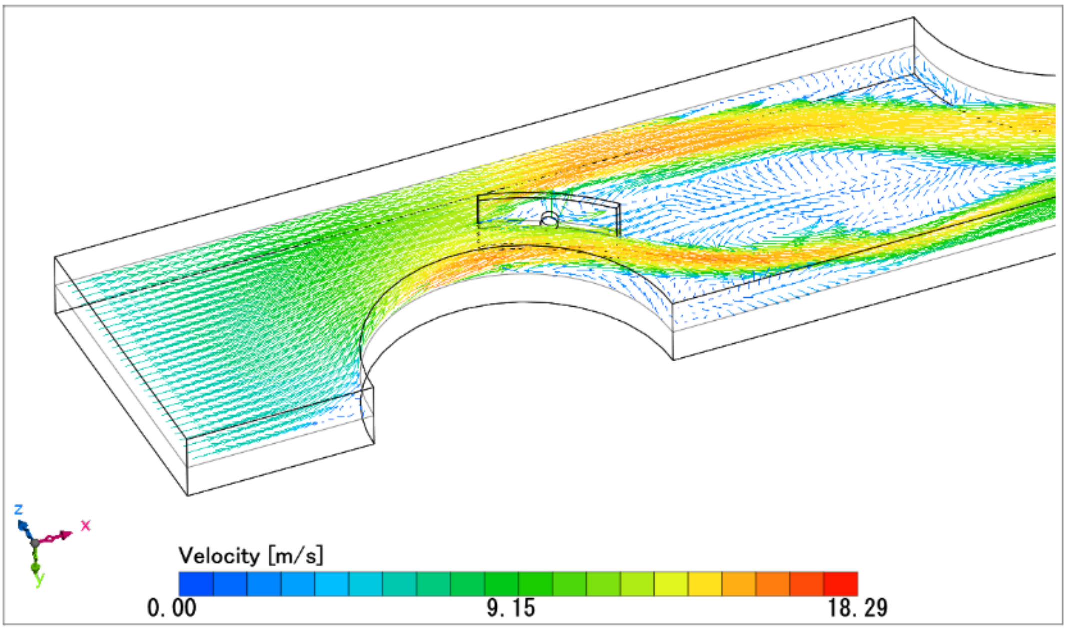

Figure 13. Streamline velocity α = 120°, r/R = 1.25, hole width = 0.5H

3.3. Influence of Geometry and Radial Distance on Thermal Enhancement Factor

The variation in the TEF with the r/R ratio at different angular positions is presented in **Figure 14a** and **Figure 14b** for hole widths of 0.25 *H* and 0.5 *H*, respectively. For both configurations, r/R = 1.25 consistently produces higher TEF values than r/R = 1.5, with the most pronounced improvement occurring at α = 120°. The maximum TEF reaches 1.075 for 0.25 *H* and 1.064 for 0.5 *H*. This trend indicates that a shorter radial distance provides a more favourable balance between heat transfer augmentation and friction penalty.

The superior performance at r/R = 1.25 is associated with a more effective vortex–jet interaction and controlled suppression of mixed-vortex interference. At $\alpha \approx 120°$, the wake region behind the tube is significantly weakened, promoting enhanced near-wall momentum exchange and boundary-layer disruption. Such overlapping vortex configurations signal a shift towards a more intensified turbulent regime [39], which is known to strengthen convective heat transfer mechanisms [40].

Although larger radial spacing intensifies vortex structures, it also increases flow resistance, thereby reducing the overall TEF, despite higher local heat transfer rates. The combined trends of Nu/Nu_0 and f/f_0 confirm that optimal thermo-hydraulic performance is governed by the synergy between vortex positioning, jet reinforcement and wake suppression rather than vortex strength alone.

The combined analysis of Nu/Nu_0 and f/f_0 (Figure 5 and Figure 12) supports this behaviour. Increasing hole width reduces f, thereby mitigating the pressure drop, consistent with previous findings [41]. The jet streams generated by the CRW-VGs alleviate stagnant flow regions, particularly between 30° and 90°, while beyond 105°, the interaction between intensified vortices and wake dynamics temporarily elevates the pressure drop before stabilising near 120°. The temperature contours further confirm that higher angular positions weaken the recirculation zone and enhance thermal mixing.

Overall, the TEF distribution in Figure 14 demonstrates that thermo-hydraulic optimisation is governed not only by vortex strength but also by the synergy between vortex positioning, jet reinforcement and wake suppression. The peak performance at r/R = 1.25 and α = 120° highlights the importance of geometric tuning to achieve maximum heat transfer enhancement with controlled hydraulic losses. These findings provide deeper physical insight into jet-assisted vortex dynamics and offer practical guidance for optimising VG placement in compact heat exchanger applications.

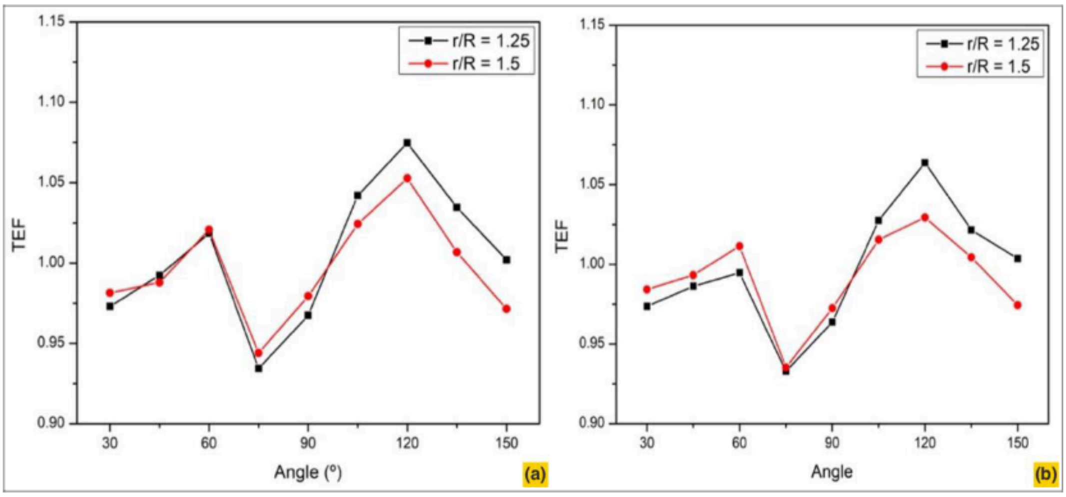

Figure 14. Thermal enhancement factor graph: (a) RWVGs hole width 0.25*H*; (b) RWVGs hole width 0.5*H*

3.4. Economic and Practical Implications of Thermal Enhancement Factor

The maximum TEF obtained in the present study is approximately 1.075, corresponding to a net thermo-hydraulic improvement of about 7%–8% under constant fan power conditions. Although this enhancement may appear moderate compared with some studies reporting TEF values in the range of 1.2–1.5 [42], [43], [44], it is important to recognise that such higher values are often associated with substantial pressure penalties or aggressive vortex geometries that may not be suitable for practical air-side applications. In fin–tube heat exchangers operating with low-density air, even a 5%–10% improvement in overall performance is practically meaningful, as it can reduce the required heat transfer surface area for a given thermal duty, improve compactness or lower long-term fan energy consumption [45], [46], [47].

From a manufacturing standpoint, the proposed perforated CRW-VGs are passive devices integrated directly with the fin structure and fabricated from thin sheet material. The addition of perforations does not introduce significant production complexity and can be implemented using conventional stamping or punching techniques commonly employed in fin manufacturing. Consequently, the incremental fabrication cost is expected to be minimal, particularly in large-scale production.

Moreover, the perforated configuration helps mitigate an excessive increase in pressure compared with solid VGs, thereby reducing aerodynamic loading on the fan system. The resulting balance between heat transfer enhancement and controlled friction penalty demonstrates that the proposed design achieves realistic thermo-hydraulic optimisation rather than maximum vortex intensity alone. Although a comprehensive life-cycle cost analysis is beyond the scope of this numerical study, the combination of TEF greater than unity, moderate pressure penalties and low manufacturing complexity supports the technical relevance and economic feasibility of the proposed configuration for practical Heating, Ventilation, and Air Conditioning and compact thermal management applications.

4. Conclusions

This study reveals that the thermo-hydraulic performance of CRW-VGs is governed by the interaction between vortex positioning, jet momentum and wake suppression rather than vortex strength alone. The results explicitly show that a shorter radial distance (r/R = 1.25) provides a more favourable balance between heat transfer enhancement and pressure penalty than r/R = 1.5. Although larger radial spacing intensifies vortex structures and increases Nu/Nu_0, the accompanying increase in f reduces the overall TEF.

The optimal angular position is identified at α = 120°, at which the wake region behind the tube is significantly weakened. This configuration promotes a stronger near-wall momentum exchange, a more uniform boundary-layer disruption and improved thermal mixing. The TEF reaches its maximum values of 1.075 (0.25 *H*) and 1.064 (0.5 *H*) under this condition, confirming that wake restructuring plays a decisive role in thermo-hydraulic optimisation.

Furthermore, increasing the feeding hole width enhances jet strength, which intensifies turbulence and redistributes momentum more effectively. More importantly, this jet-assisted mechanism contributes not only to heat transfer augmentation but also to moderating pressure losses, demonstrating that momentum redistribution is more critical than simply increasing vortex intensity.

Overall, the findings establish that the optimal CRW-VG design requires controlled vortex suppression, strategic angular positioning and jet reinforcement to achieve maximum TEF. These results provide mechanistic insight into jet–vortex synergy and offer practical guidance for high-efficiency compact heat exchanger design.

Acknowledgements

The author extends gratitude to Office of Research UHAMKA for support for this research and to the Office of Publication of UHAMKA for their assistance in providing technical guidance. This research was not funded by any grant.

Authors' Declaration

Authors' contributions and responsibilities – The authors made substantial contributions to the conception and design of the study. The authors took responsibility for data analysis, interpretation and discussion of results. The authors read and approved the final manuscript.

Funding – This research was not funded by any grant.

Availability of data and materials – All data is available from the authors.

Competing interests – The authors declare no competing interests.

Additional information – No additional information from the authors.

Nomenclature			
D	: Tube diameter (m)	r	: Radial distance of VG from tube center (m)
f	: Darcy friction factor (–)	R	: Tube radius (m)
f_0	: Friction factor without vortex generator (–)	T	: Static temperature (K)
H	: Channel height (m)	T_{in}	: Inlet air temperature (K)
k	: Thermal conductivity of air (W m^{-1} K^{-1})	T_w	: Tube wall temperature (K)
L	: Tube length (m)	α	: Angular position of vortex generator (degree)
N_u	: Nusselt number (–)	μ	: Dynamic viscosity (Pa s)
Nu_{avg}	: Average Nusselt number (–)	ρ	: Air density (kg m^{-3})
Nu_0	: Nusselt number without vortex generator (–)	r/R	: Radial distance ratio (–)
P	: Static pressure (Pa)	Nu/Nu_0	: Nusselt number ratio (–)
P_L	: Longitudinal pitch (m)	f/f_0	: Friction factor ratio (–)
P_T	: Transverse pitch (m)	TEF	: Thermal enhancement factor (–)

References

[1] K. Torii, K. M. Kwak, and K. Nishino, “Heat transfer enhancement accompanying pressure-loss reduction with winglet-type vortex generators for fin-tube heat exchangers,” *International Journal of Heat and Mass Transfer*, vol. 45, no. 18, pp. 3795–3801, Aug. 2002, doi: 10.1016/S0017-9310(02)00080-7.

[2] P. T. Tsilingiris, “Review and critical comparative evaluation of moist air thermophysical properties at the temperature range between 0 and 100 °C for Engineering Calculations,” *Renewable and Sustainable Energy Reviews*, vol. 83, pp. 50–63, Mar. 2018, doi: 10.1016/j.rser.2017.10.072.

[3] Dan Mugisidi, Oktarina Heriyani, Pancatatva Hesti Gunawan, and Dwi Apriani, “Performance Improvement of a Forced Draught Cooling Tower Using a Vortex Generator,” *CFD Letters*, vol. 13, no. 1, pp. 45–57, Jan. 2021, doi: 10.37934/cfdl.13.1.4557.

[4] Syaiful, H. Nabilah, M. S. K. T. Suryo Utomo, A. Suprihanto, and M. F. Soetanto, “Numerical simulation of heat transfer enhancement from tubes surface to airflow using concave delta winglet vortex generators,” *Results in Engineering*, vol. 16, p. 100710, Dec. 2022, doi: 10.1016/j.rineng.2022.100710.

[5] M. Awais and A. A. Bhuiyan, “Heat transfer enhancement using different types of vortex generators (VGs): A review on experimental and numerical activities,” *Thermal Science and Engineering Progress*, vol. 5, pp. 524–545, Mar. 2018, doi: 10.1016/j.tsep.2018.02.007.

[6] S. K. Sarangi and D. P. Mishra, “Effect of winglet location on heat transfer of a fin-and-tube heat exchanger,” *Applied Thermal Engineering*, vol. 116, pp. 528–540, Apr. 2017, doi: 10.1016/j.applthermaleng.2017.01.106.

[7] K. Song, Z. Xi, M. Su, L. Wang, X. Wu, and L. Wang, “Effect of geometric size of curved delta winglet vortex generators and tube pitch on heat transfer characteristics of fin-tube heat exchanger,” *Experimental Thermal and Fluid Science*, vol. 82, pp. 8–18, Apr. 2017, doi: 10.1016/j.expthermflusci.2016.11.002.

[8] A. Boonloi and W. Jedsadaratanachai, “Air Flow, Thermal Profile, and Thermohydraulic Performance Assessment in a Square Duct Heat Exchanger With Combined Vortex Generators: CFD Analysis,” *Journal of Engineering*, vol. 2025, no. 1, Jan. 2025, doi: 10.1155/je/4197880.

[9] H. Karkaba, T. Dbouk, C. Habchi, S. Russeil, T. Lemenand, and D. Bougeard, “Multiobjective optimization of Vortex Generators for heat transfer enhancement in turbulent flows,” *International Journal of Thermofluids*, vol. 22, p. 100633, May 2024, doi: 10.1016/j.ijft.2024.100633.

[10] H. Arjmandi, R. Amini, A. Ghaffari, H. Rahmani, and A. Chamkha, “Effects of baffles and vortex generators on cooling performance of a gas turbine combustion chamber: Numerical assessment,” *Alexandria Engineering Journal*, vol. 61, no. 6, pp. 4467–4478, Jun. 2022, doi: 10.1016/j.aej.2021.10.005.

[11] U. Kashyap, K. Das, and B. K. Debnath, “Effect of surface modification of a rectangular vortex generator on heat transfer rate from a surface to fluid: An extended study,” *International Journal of Thermal Sciences*, vol. 134, pp. 269–281, Dec. 2018, doi: 10.1016/j.ijthermalsci.2018.08.020.

[12] H. Naik and S. Tiwari, “Effect of winglet location on performance of fin-tube heat exchangers with inline tube arrangement,” *International Journal of Heat and Mass Transfer*, vol. 125, pp. 248–261, Oct. 2018, doi: 10.1016/j.ijheatmasstransfer.2018.04.071.

[13] Z. Qian, Q. Wang, and J. Cheng, “Analysis of heat and resistance performance of plate fin-and-tube heat exchanger with rectangle-winglet vortex generator,” *International Journal of Heat and Mass Transfer*, vol. 124, pp. 1198–1211, Sep. 2018, doi: 10.1016/j.ijheatmasstransfer.2018.04.037.

[14] K. Srivastava and R. R. Sahoo, “Effect of pitch and angle of attack on thermal performance of new envelope and delta vortex generators for TEG: An experimental and numerical approach,” *International Journal of Thermal Sciences*, vol. 195, p. 108671, Jan. 2024, doi: 10.1016/j.ijthermalsci.2023.108671.

[15] C. Luo, S. Wu, K. Song, L. Hua, and L. Wang, “Thermo-hydraulic performance optimization of wavy fin heat exchanger by combining delta winglet vortex generators,” *Applied Thermal*

Engineering, vol. 163, p. 114343, Dec. 2019, doi: 10.1016/j.applthermaleng.2019.114343.

[16] O. Heriyani, M. Djaeni, Syaiful, and A. K. Putri, "Perforated concave rectangular winglet pair vortex generators enhance the heat transfer of air flowing through heated tubes inside a channel," *Results in Engineering*, vol. 16, p. 100705, Dec. 2022, doi: 10.1016/j.rineng.2022.100705.

[17] M. Dogan and S. Erzincan, "Experimental investigation of thermal performance of novel type vortex generator in rectangular channel," *International Communications in Heat and Mass Transfer*, vol. 144, p. 106785, May 2023, doi: 10.1016/j.icheatmasstransfer.2023.106785.

[18] Z. Ke, C.-L. Chen, K. Li, S. Wang, and C.-H. Chen, "Vortex dynamics and heat transfer of longitudinal vortex generators in a rectangular channel," *International Journal of Heat and Mass Transfer*, vol. 132, pp. 871–885, Apr. 2019, doi: 10.1016/j.ijheatmasstransfer.2018.12.064.

[19] H. Fu, H. Sun, L. Yang, L. Yan, Y. Luan, and F. Magagnato, "Effects of the configuration of the delta winglet longitudinal vortex generators and channel height on flow and heat transfer in minichannels," *Applied Thermal Engineering*, vol. 227, p. 120401, Jun. 2023, doi: 10.1016/j.applthermaleng.2023.120401.

[20] J. Batista, A. Trp, K. Lenic, and M. Kirincic, "The influence of geometry parameters of rectangular vortex generators on the air-to-water fin-and-tube heat exchanger efficiency enhancement," *International Communications in Heat and Mass Transfer*, vol. 162, p. 108647, Mar. 2025, doi: 10.1016/j.icheatmasstransfer.2025.108647.

[21] D. Jin, S. Quan, J. Zuo, and S. Xu, "Numerical investigation of heat transfer enhancement in a solar air heater roughened by multiple V-shaped ribs," *Renewable Energy*, vol. 134, pp. 78–88, Apr. 2019, doi: 10.1016/j.renene.2018.11.016.

[22] S. Pourhedayat, S. M. Pesteei, H. E. Ghalinghie, M. Hashemian, and M. A. Ashraf, "Thermal-exergetic behavior of triangular vortex generators through the cylindrical tubes," *International Journal of Heat and Mass Transfer*, vol. 151, p. 119406, Apr. 2020, doi: 10.1016/j.ijheatmasstransfer.2020.119406.

[23] J. Wang, L. Zeng, T. Fu, S. Yu, and Y. He, "Effects of the position and perforation parameters of the delta winglet vortex generators on flow and heat transfer in minichannels," *International Journal of Thermal Sciences*, vol. 198, p. 108878, Apr. 2024, doi: 10.1016/j.ijthermalsci.2023.108878.

[24] P. Promvonge and S. Skullong, "Heat transfer augmentation in solar receiver heat exchanger with hole-punched wings," *Applied Thermal Engineering*, vol. 155, pp. 59–69, Jun. 2019, doi: 10.1016/j.applthermaleng.2019.03.132.

[25] M. E. Nakhchi, M. Hatami, and M. Rahmati, "Experimental investigation of performance improvement of double-pipe heat exchangers with novel perforated elliptic turbulators," *International Journal of Thermal Sciences*, vol. 168, p. 107057, Oct. 2021, doi: 10.1016/j.ijthermalsci.2021.107057.

[26] A. J. Modi, N. A. Kalel, and M. K. Rathod, "Thermal performance augmentation of fin-and-tube heat exchanger using rectangular winglet vortex generators having circular punched holes," *International Journal of Heat and Mass Transfer*, vol. 158, p. 119724, Sep. 2020, doi: 10.1016/j.ijheatmasstransfer.2020.119724.

[27] Z. Han, Z. Xu, and J. Wang, "Numerical simulation on heat transfer characteristics of rectangular vortex generators with a hole," *International Journal of Heat and Mass Transfer*, vol. 126, pp. 993–1001, Nov. 2018, doi: 10.1016/j.ijheatmasstransfer.2018.06.081.

[28] J. Wang, T. Fu, L. Zeng, F. Lien, and G. Chen, "Thermal-hydraulic performance in a tube with punched delta winglets inserts in turbulent flow," *International Journal of Thermal Sciences*, vol. 172, p. 107326, Feb. 2022, doi: 10.1016/j.ijthermalsci.2021.107326.

[29] P. Saini and M. P. Shah, "Performance evaluation of finned tube heat exchanger using curved wavy delta winglet vortex generators with circular perforations," *International Communications in Heat and Mass Transfer*, vol. 159, p. 108184, Dec. 2024, doi: 10.1016/j.icheatmasstransfer.2024.108184.

[30] Y. Oh and K. Kim, "Effects of position and geometry of curved vortex generators on fin-tube heat-exchanger performance characteristics," *Applied Thermal Engineering*, vol. 189, p. 116736, May 2021, doi: 10.1016/j.applthermaleng.2021.116736.

[31] M.-W. Tian, S. Khorasani, H. Moria, S. Pourhedayat, and H. S. Dizaji, "Profit and efficiency boost of triangular vortex-generators by novel techniques," *International Journal of Heat and Mass Transfer*, vol. 156, p. 119842, Aug. 2020, doi: 10.1016/j.ijheatmasstransfer.2020.119842.

[32] P. Knödler and V. Dreissigacker, "Fluid Dynamic Assessment and Development of Nusselt Correlations for Fischer Koch S Structures," *Energies*, vol. 17, no. 3, p. 688, Jan. 2024, doi: 10.3390/en17030688.

[33] X. Zou, S. B. Lo, R. Sevilla, O. Hassan, and K. Morgan, "The generation of tetrahedral meshes for NURBS-enhanced FEM," *Engineering with Computers*, vol. 40, no. 6, pp. 3949–3977, Dec. 2024, doi: 10.1007/s00366-024-02004-z.

[34] P. Saini, A. Dhar, and S. Powar, "Performance enhancement of fin and tube heat exchanger employing curved delta winglet vortex generator with circular punched holes," *International Journal of Thermofluids*, vol. 20, p. 100452, Nov. 2023, doi: 10.1016/j.ijft.2023.100452.

[35] M. K. Fahad, N. F. Ifraj, S. H. Tahsin, and M. J. Hasan, "Numerical investigation of the hydrothermal performance of novel vortex generators in a rectangular channel by employing inclination and rotational angles," *International Journal of Thermofluids*, vol. 20, p. 100500, Nov. 2023, doi: 10.1016/j.ijft.2023.100500.

[36] S. Gururatana and S. Skullong, "Heat transfer augmentation in a pipe with 3D printed wavy insert," *Case Studies in Thermal Engineering*, vol. 21, p. 100698, Oct. 2020, doi: 10.1016/j.csite.2020.100698.

[37] A. Sinha, H. Chattopadhyay, A. K. Iyengar, and G. Biswas, "Enhancement of heat transfer in a fin-tube heat exchanger using rectangular winglet type vortex generators," *International Journal of Heat and Mass Transfer*, vol. 101, pp. 667–681, Oct. 2016, doi: 10.1016/j.ijheatmasstransfer.2016.05.032.

[38] D. Hu *et al.*, "Performance optimization of a wavy finned-tube heat exchanger with staggered curved vortex generators," *International Journal of Thermal Sciences*, vol. 183, p. 107830, Jan. 2023, doi: 10.1016/j.ijthermalsci.2022.107830.

[39] K. Srivastava and R. R. Sahoo, "Experimental and numerical study on thermal performance of new envelope and triangular vortex generators with different pitch and angle of attack," *Thermal Science and Engineering Progress*, vol. 49, p. 102459, Mar. 2024, doi: 10.1016/j.tsep.2024.102459.

[40] A. J. Modi and M. K. Rathod, "Experimental investigation of heat transfer enhancement and pressure drop of fin-and-circular tube heat exchangers with modified rectangular winglet vortex generator," *International Journal of Heat and Mass Transfer*, vol. 189, p. 122742, Jun. 2022, doi: 10.1016/j.ijheatmasstransfer.2022.122742.

[41] R. B. Pérez, A. M. Pérez, and D. S. Suárez, "Influence of the punched holes on thermohydraulic performance and flow pattern of rectangular channels with a pair of perforated vortex generators," *International Journal of Heat and Mass Transfer*, vol. 184, p. 122291, Mar. 2022, doi: 10.1016/j.ijheatmasstransfer.2021.122291.

[42] J. Wang, L. Zeng, Y. He, B. Zhao, and P. Chu, "Effect of structure parameters on thermal performance of novel punched V-shape VGs for hear exchangers: An experimental approach," *International Communications in Heat and Mass Transfer*, vol. 155, p. 107472, Jun. 2024, doi: 10.1016/j.icheatmasstransfer.2024.107472.

[43] J. Wang, C. Li, L. Zeng, T. Fu, and K. Liu, "Thermal performance analysis of a heat exchanger with a novel turbulator insert by using machine learning method," *Case Studies in Thermal Engineering*, vol. 72, p. 106412, Aug. 2025, doi: 10.1016/j.csite.2025.106412.

[44] A. Boonloi and W. Jedsadaratanachai, "Turbulent forced convection in a square duct heat exchanger (SDHX) equipped with combined vortex turbulators (CVT): A numerical investigation," *International Communications in Heat and Mass Transfer*, vol. 161, p. 108421, Feb. 2025, doi: 10.1016/j.icheatmasstransfer.2024.108421.

[45] W. Wei, G. Xu, Y. Wang, and E. Ding, "Study on air-side performance of air-cooled heat exchangers under large air velocity and wet conditions," *Thermal Science and Engineering Progress*, vol. 48, p. 102389, Feb. 2024, doi: 10.1016/j.tsep.2024.102389.

[46] P. Yang, T. Qing, X. Lei, L. Wang, and Y. Liu, "Experimental study on thermal–hydraulic performance of moist air inside flat tube of two kinds of plate-fin heat exchangers," *Applied Thermal Engineering*, vol. 239, p. 122121, Feb. 2024, doi:

10.1016/j.applthermaleng.2023.122121.

[47] M. H. Alshameri, A. A. Azizuddin, A. Arshad, H. G. Mohammed, and S. Sadeq, “Experimental Analysis of Thermal and Hydraulic Performance of Fiber-Reinforced Polymer Fins in Compact Heat Exchangers,” *International Journal of Automotive and Mechanical Engineering*, vol. 22, no. 2, pp. 12496–12510, Jun. 2025, doi: 10.15282/ijame.22.2.2025.18.0955.

Layanan Perpustakaan Uhamka

Dan Mugisidi - Improving the thermal efficiency of fin-tube heat exchangers by optimizing geometric parameters of curve...

Dan Mugisidi (GB)

Document Details

Submission ID

trn:oid:::3618:144257484

Submission Date

Jun 26, 2026, 9:02 AM GMT+7

Download Date

Jun 26, 2026, 9:14 AM GMT+7

File Name

8_15393_Dan+Mugisidi (1).pdf

File Size

2.6 MB

18 Pages

8,296 Words

47,441 Characters

17% Overall Similarity

The combined total of all matches, including overlapping sources, for each database.

Filtered from the Report

- Bibliography

Exclusions

- 5 Excluded Sources
- 27 Excluded Matches

Match Groups

- **118** Not Cited or Quoted 17%
  Matches with neither in-text citation nor quotation marks
- **1** Missing Quotations 0%
  Matches that are still very similar to source material
- **0** Missing Citation 0%
  Matches that have quotation marks, but no in-text citation
- **0** Cited and Quoted 0%
  Matches with in-text citation present, but no quotation marks

Top Sources

8%	Internet sources
14%	Publications
10%	Submitted works (Student Papers)

Integrity Flags

0 Integrity Flags for Review

Our system's algorithms look deeply at a document for any inconsistencies that would set it apart from a normal submission. If we notice something strange, we flag it for you to review.

A Flag is not necessarily an indicator of a problem. However, we'd recommend you focus your attention there for further review.

Match Groups

- **118** Not Cited or Quoted 17%
  Matches with neither in-text citation nor quotation marks
- **1** Missing Quotations 0%
  Matches that are still very similar to source material
- **0** Missing Citation 0%
  Matches that have quotation marks, but no in-text citation
- **0** Cited and Quoted 0%
  Matches with in-text citation present, but no quotation marks

Top Sources

8% Internet sources
14% Publications
10% Submitted works (Student Papers)

Top Sources

The sources with the highest number of matches within the submission. Overlapping sources will not be displayed.

1	Publication	Yeongtaek Oh, Kuisoon Kim. "Effects of position and geometry of curved vortex g...	1%
2	Publication	Dheeraj Kumar, Amaresh Dalal. "Computational investigation of heat transfer an...	<1%
3	Internet	hal.science	<1%
4	Publication	Amnart Boonloi, Withada Jedsadaratanachai. "Numerical investigation of therma...	<1%
5	Internet	semarakilmu.com.my	<1%
6	Internet	www.mdpi.com	<1%
7	Publication	Wei Dang, Wenqiang Deng, Jian Song, Kewei Song. "Heat transfer enhancement o...	<1%
8	Publication	Shailesh Kumar Sarangi, Dipti Prasad Mishra. "A comprehensive review on vortex...	<1%
9	Publication	Bekir Dogan. "Numerical investigation of conjugate heat transfer in circular pipe...	<1%
10	Internet	iieta.org	<1%

11	Publication	
	Prashant Saini, Atul Dhar, Satvasheel Powar. "Performance Enhancement of Fin a...	<1%
12	Internet	
	www.researchgate.net	<1%
13	Publication	
	M. Ramanipriya, S. Suresh Kumar Raju, S. Anitha. "Influence of porosity and inclin...	<1%
14	Student papers	
	Swinburne University of Technology on 2020-11-21	<1%
15	Internet	
	pphmjopenaccess.com	<1%
16	Publication	
	Mehmet Gürdal, Muhammed Tan, Aziz Hakan Altun, Emrehan Gürsoy, Adnan Ber...	<1%
17	Publication	
	Yonggang Lei, Fang Zheng, Chongfang Song, Yongkang Lyu. "Improving the ther...	<1%
18	Internet	
	c.coek.info	<1%
19	Internet	
	www.tandfonline.com	<1%
20	Publication	
	Mallikarjuna Veerabhadrappa Bidari, P. B. Nagaraj, Gururaj Lalagi. "Influence of d...	<1%
21	Internet	
	gcris.iyte.edu.tr	<1%
22	Internet	
	pmc.ncbi.nlm.nih.gov	<1%
23	Publication	
	K. S. N. Raju. "Fluid Mechanics, Heat Transfer, and Mass Transfer", Wiley, 2011	<1%
24	Publication	
	Leandro Oliveira Salviano. "Optimization of vortex generators positions and angl...	<1%

25 Student papers

Mansoura University on 2019-04-02 <1%

26 Internet

univ-pau.hal.science <1%

27 Student papers

Indian Institute of Technology, Kanpur on 2014-07-12 <1%

28 Student papers

Minerva_LTI on 2026-03-31 <1%

29 Student papers

University of Western Sydney on 2026-06-05 <1%

30 Internet

pubmed.ncbi.nlm.nih.gov <1%

31 Publication

Abdussamet Subasi, Kasim Erdem. "An integrated optimization methodology for ... <1%

32 Publication

Amit Arora, P.M.V. Subbarao. "Geometric parametrization of toe-out type vortex ... <1%

33 Publication

Jiangbo Wang, Liangcai Zeng, Sheng Yu, Yuting He, Junhao Tang. "Experimental a... <1%

34 Publication

M. Behfard, A. Sohankar. "Numerical investigation for finding the appropriate de... <1%

35 Internet

escholarship.org <1%

36 Internet

umpir.ump.edu.my <1%

37 Student papers

Griffth University on 2026-06-07 <1%

38 Publication

Muhammad Reshaeel, Mostafa M. Abdelsamie, Mohamed I. Hassan Ali. "A critical ... <1%

39 Publication

Roytor Charoensin-O-Larn, Boonchai Lertnuwat. "Impact of Leading and Trailing-... <1%

40 Publication

S.C. Mohapatra, Z.C. Liu, C. Guedes Soares. "Motion response of a flexible floater ... <1%

41 Student papers

The Scientific & Technological Research Council of Turkey (TUBITAK) on 2023-03-27 <1%

42 Student papers

University of Auckland on 2024-05-26 <1%

43 Internet

www.sid.ir <1%

44 Student papers

Asia e University on 2023-03-24 <1%

45 Publication

Josip Batista, Anica Trp, Kristian Lenic. "Experimentally validated numerical mode... <1%

46 Publication

Kartik Srivastava, Rashmi Rekha Sahoo. "Thermoelectric performance enhancem... <1%

47 Student papers

University of Florida on 2019-06-16 <1%

48 Publication

Xiao Li. "Industrialized Construction in the Age of AI and Robotics", Routledge, 20... <1%

49 Publication

Zhaoqing Ke, Chung-Lung Chen, Kuojiang Li, Sheng Wang, Chien-Hua Chen. "Vort... <1%

50 Internet

autodocbox.com <1%

51 Internet

eprints.nottingham.ac.uk <1%

52 Internet

www.isteonline.in <1%

53 Publication

"Theoretical, Computational, and Experimental Solutions to Thermo-Fluid System... <1%

54 Student papers

Cranfield University on 2024-04-23 <1%

55 Publication

Crystal, Roland Virgil. "Enhancement of Air-Side Heat Transfer in Crossflow Heat E... <1%

56 Publication

Gökhan Sevilgen, Muhsin Kiliç, Mehmet Aktaş. "Dual-separated cooling channel p... <1%

57 Publication

Hüseyin Zahit Demirağ. "Innovative approach for longitudinal vortex generator d... <1%

58 Publication

KeWei Song, Toshio Tagawa, ZhongHao Chen, Qiang Zhang. "Heat transfer charac... <1%

59 Student papers

Queen Mary and Westfield College on 2013-05-07 <1%

60 Student papers

SUNY, Maritime College on 2021-03-06 <1%

61 Publication

Samer Ali, Talib Dbouk, Mahmoud Khaled, Jalal Faraj, Dimitris Drikakis. "Morphin... <1%

62 Publication

Shailesh Kumar Sarangi, Dipti Prasad Mishra, Praveen Mishra. "Numerical Analysi... <1%

63 Publication

Taha Tuna Göksu, Rasim Behçet. "Experimental investigation of the effect of a no... <1%

64 Publication

Tamna, Sombat, Sompol Skullong, Chinaruk Thianpong, and Pongjet Promvonge. ... <1%

65 Internet

eprints.cihanuniversity.edu.iq <1%

66 Internet

gala.gre.ac.uk <1%

67 Internet

psecommunity.org <1%

68 Internet

tsl.energy.hust.edu.cn <1%

69 Internet

www.paperpublications.org <1%

70 Student papers

Al-Qasim Green University on 2024-01-04 <1%

71 Publication

Mingjie Li, Jingguo Qu, Jianfei Zhang, Jinjia Wei, Wenquan Tao. "Air side heat tran... <1%

72 Student papers

Universiti Teknologi Malaysia on 2016-08-30 <1%

73 Student papers

University of New South Wales on 2026-04-24 <1%

74 Publication

Withada Jedsadaratanachai, Amnart Boonloi. "Thermal performance assessment ... <1%

75 Student papers

Amity University on 2019-08-07 <1%

76 Publication

Ashish J. Modi, Manish K. Rathod. "Experimental investigation of heat transfer en... <1%

77 Publication

Ralph L. Webb, Nae-Hyun Kim. "Principles of Enhanced Heat Transfer", Taylor & Fr... <1%

78 Student papers

University of Anbar on 2023-06-04 <1%

79 Student papers

University of Bedfordshire on 2024-05-16 <1%

80 Publication

Xinchao Wu, Ting Fu, Jiangbo Wang, Liangcai Zeng, Feng Zhang. "A comparative s... <1%

81 Publication

Yongrui Bian, Zhenfei Feng, Yuxiang Liang, Yuetong Li, Xu Lu, Xinghong Li, Yuliu ... **<1%**

Type of contribution:
Editorial
▶ Research Paper
Case Study
Review Paper
Scientific Data
Report of Tech. Application

mesi
e-issn. 2798-5245
Mechanical Engineering for Society and Industry
Vol. 6, No. 1 (2026) pp 128-145
https://doi.org/10.31603/mesi.15393

Improving the thermal efficiency of fin-tube heat exchangers by optimizing geometric parameters of curved rectangular winglet vortex generators

Dan Mugisidi[1]*, Oktarina Heriyani[1], Amir Khalid[2], Ahmed Rahmani[3]

[1] Department of Mechanical Engineering, Faculty of Industrial and Informatics Technology, Universitas Muhammadiyah Prof DR HAMKA, Jakarta Timur 13830, **Indonesia**
[2] Faculty of Mechanical and Manufacturing Engineering, Universiti Tun Hussein Onn Malaysia, Batu Pahat, Johor, Malaysia
[3] Sustainable Development and Environmental Protection Laboratory, Larbi Ben M'hidi University, Oum El Bouaghi, 04000, **Algeria**
✉ dan.mugisidi@uhamka.ac.id

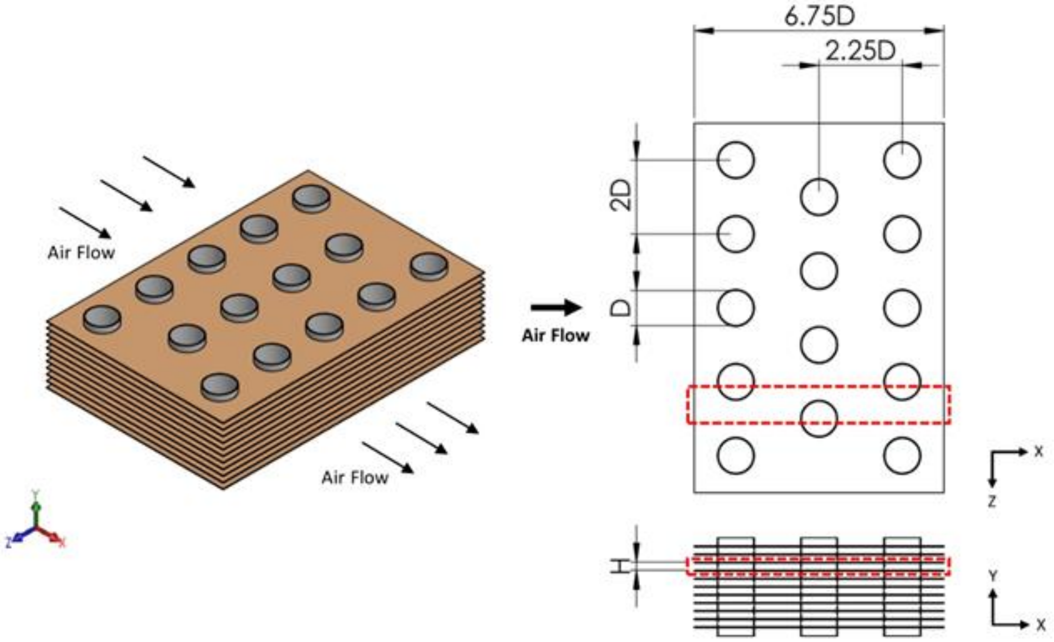

Highlights:

- Curved rectangular winglet vortex generators (CRW-VGs) were optimized to improve the thermal enhancement factor in fin–tube heat exchangers.
- Computational fluid dynamics analysis showed that radial distance, hole width, and angular position strongly influence heat transfer and pressure drop behavior.
- Smaller radial distances enhanced TEF by suppressing mixing vortices, while larger hole widths improved heat transfer through stronger jet-flow generation.
- The optimum configuration achieved a maximum TEF of 1.075 at an angular position of 120°, hole width of 0.5 H, and radial distance of 1.25.
- The findings demonstrate that proper geometric optimization of vortex generators can enhance heat transfer performance while minimizing pressure drop penalties.

Article info
Submitted:
2025-11-20
Revised:
2026-03-23
Accepted:
2026-04-06

Publisher
Universitas Muhammadiyah Magelang

Abstract

Thermal efficiency is a fundamental criterion in the design and operation of heat exchangers because it provides a clear view of the thermal behaviour and reliability of the system. Integrating vortex generators (VGs) with heat exchangers often increases turbulence and enhances the heat transfer rate but at the cost of increased pressure drops. This study aims to maximise the thermal enhancement factor (TEF) in fin–tube heat exchangers by optimising the radial distance, hole width and angular position of curved rectangular winglet vortex generators (CRW-VGs). Computational fluid dynamics analysis is utilised to investigate how variations in radial distance and hole width influence CRW-VG performance. Parameters such as TEF, Nusselt number ratio, friction factor ratio and flow regime were examined. The results show that smaller radial distances suppress mixing vortices and enhance TEF, while larger hole widths generate strong jet flows and increase heat transfer rates. The highest TEF of 1.075 is achieved at an angular position of 120°, a hole width of 0.5 H and a radial distance of 1.25. The study reveals that optimising the geometric parameters of VGs is proven satisfactory for enhancing heat transfer performance and minimising pressure drop.

Keywords: Curved rectangular winglet; Heat transfer enhancement; Hole width; Radial distance; Vortex generator

1. Introduction

Thermal efficiency is a crucial aspect in the design and operation of heat exchanger systems, playing an essential role in various industrial applications, such as power generation, cooling and chemical processing [1]. The need for better heat exchange in these systems with more compact designs has resulted in much research on this topic.

Air is the common working fluid in fin–tube heat exchangers. Similar to all gases, air has relatively poor thermophysical properties for heat transfer [2]. This limitation prompted researchers to enhance the effectiveness of heat transfer systems to increase energy efficiency while lowering production costs. Enhancing the air-side heat transfer of these equipment has been the subject of several theoretical, numerical and experimental investigations. A proven effective solution is the integration of vortex generators (VGs). These small devices are designed to enhance aerodynamic performance, flow control and heat transfer in forced draft cooling towers [3]. VGs improve thermal performance by inducing subsidiary currents, disrupting interface region development and promoting fluid dispersion near the walls. The longitudinal vortices generated by VGs allow reduced stagnation zones behind the tubes [4], increase turbulence intensity and well fluid mixing [5]. Increasing turbulence often enhances the heat transfer rate but at the cost of increased pressure drops. Therefore, optimising heat transfer and reducing fluid flow resistance have become the primary focus.

Previous studies have demonstrated that both the placement and geometric configuration of VGs significantly influence the thermal–hydraulic performance of fin–tube heat exchangers. Positioning VGs near the centre of the tube has been shown to provide more effective heat transfer enhancement compared with inlet or outlet placements, primarily due to the stronger interaction between the generated vortices and the tube wake region [6], [7]. In addition, smaller VG geometries operating at lower Reynolds numbers have been reported to further improve heat exchange performance [8].

Geometric optimisation of the heat exchanger structure also plays an important role in determining overall performance. The optimal combination of a larger fin pitch and a smaller tube diameter has been experimentally identified as providing improved fluid flow characteristics [9]. However, increasing the fin pitch can reduce the Nusselt number (Nu) and the wall friction factor (f) because of weakened vorticity formation and enhanced turbulent energy dissipation [10]. Furthermore, numerical investigations have shown that combining concave and convex VG surfaces generates stronger longitudinal vortices, resulting in an enhancement of the heat transfer rate of approximately 14.4% [11].

Operational parameters, such as VG location and angle of attack (AoA), further determine heat transfer effectiveness. Higher attack angles, particularly when VGs are positioned farther from the tube, can substantially increase heat transfer rates [12]. Conversely, smaller angles may be advantageous in certain configurations by directing colder fluid towards weak wake regions [13]. An AoA of 45° has consistently been identified as providing superior thermal enhancement compared with other angles [14], [15]. Furthermore, increasing the number of staggered VGs enhances the thermal enhancement factor (TEF) by accelerating flow and promoting fluid mixing in the wake region [16], [17]. These configurations are commonly arranged in common flow up, common flow down (CFD) or hybrid arrangements to optimise performance.

In rectangular channel systems, geometric parameters, such as winglet aspect ratio and channel height (H), have been identified as the dominant factors affecting heat transfer performance [18], [19]. Increasing duct height significantly alters vortex development, especially when VGs are mounted on opposing walls, thereby enhancing overall flow dynamics and heat transfer efficiency. Heat exchange performance is also highly sensitive to VG position and geometry

[20], with even minor geometric changes producing noticeable variations in performance [21], [22].

Among the various structural innovations, perforated VGs have emerged as a promising approach for improving thermal performance [23]. Perforated rectangular winglets have been reported to increase the Nu by approximately 3.91–5.52 times, achieving a maximum thermal performance factor of 2.01 [24]. Similarly, double perforated inclined elliptic turbulators have demonstrated Nu enhancements of up to 217.4% [25]. These improvements are attributed to jet flows generated through perforations, which disrupt recirculation zones and intensify fluid mixing, thereby enhancing thermal exchange efficiency [26], [27], [28].

Despite these substantial advancements, existing studies predominantly emphasise external geometric modifications, placement strategies and angle of attack variations. Although perforating the VG surface can either enhance or deteriorate heat transfer performance, depending on the hole size, number and placement, because it changes the vortex strength and the pressure drop [29], systematic investigations of hollow rectangular winglet VGs remain limited. More importantly, the geometric perforation parameter (hole width) and the positional parameter (radial distance from the tube) have largely been examined independently. Consequently, the coupled interaction between these two design variables and their combined influence on thermal–hydraulic performance has not been comprehensively evaluated. This lack of integrated parametric analysis restricts the development of optimised hollow VG configurations capable of simultaneously maximising heat transfer enhancement and minimising pressure drop penalties. To overcome this limitation, this study proposes a performance-based geometric optimisation framework for circular ring winglet vortex generators (CRW-VGs) in fin–tube heat exchangers, focusing on radial distance and hole width as key design variables.

The coupled effects of radial distance (r/R = 1.25 and 1.5) and hole width (0.25 H and 0.5 H) are systematically analysed using high-fidelity CFD simulations. Performance is evaluated through integrated metrics, including the TEF, Nu/Nu_0, friction factor ratio (f/f_0) and flow structure characterisation. By integrating geometric sensitivity analysis with unified thermo-hydraulic evaluation and mechanistic interpretation of vortex dynamics, this study identifies the optimal configuration that maximises heat transfer while minimising pressure drop, providing both quantitative assessment and mechanistic insight for a compact heat exchanger design.

2. Methodology

2.1. Physics Model

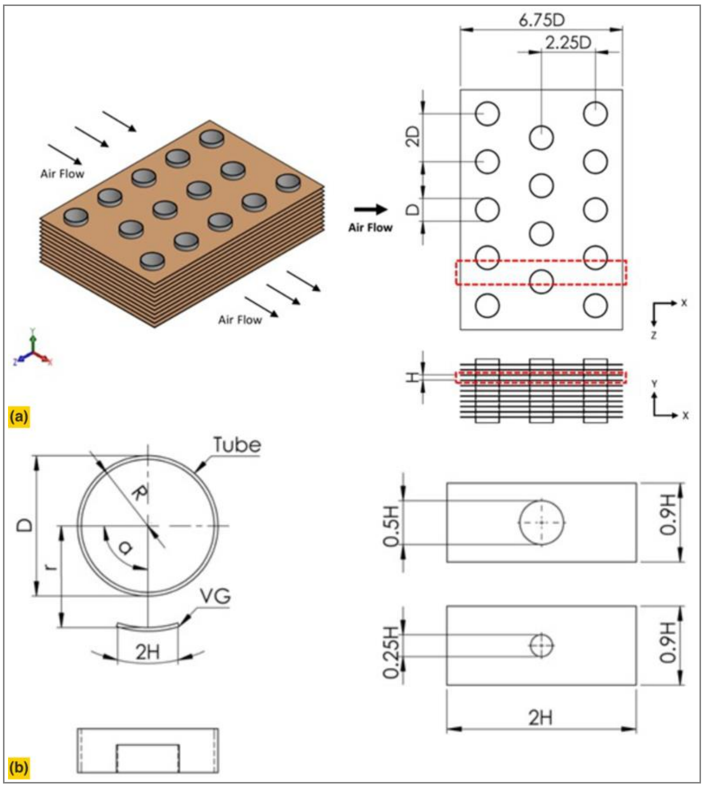

Figure 1. Schematic illustration and the main dimensions of the studied VG: (a) The overall configuration of the fin–tube heat exchanger; (b) Detailed geometry of the CRW-VG

Figure 1 shows the geometric details of a heat exchanger with three rows of staggered tubes. The VGs employed in this study take the form of a rectangular curved winglet design characterised by the geometry depicted in Figure 1. Figure 1a presents the overall configuration of the fin–tube heat exchanger and the computational domain employed in the CFD simulations. The three-dimensional (3D) schematic depicts the staggered tube arrangement and the direction of airflow. The top view specifies the tube pitches: the transverse pitch, PT = 2.25 D and the longitudinal pitch, PL = 6.75 D, where D denotes the outer tube diameter. The side view defines H as the vertical distance between two adjacent fins. The dashed rectangular region marks the representative segment selected from the complete heat exchanger geometry for numerical modelling. The tube radius, R = D/2, serves as the reference length for positioning analysis. **Figure 1b** shows the detailed geometry of the CRW-VG. The winglet length in the streamwise direction is 2 H, which is twice that of H. The winglet height is 0.9 H, providing a small clearance from the fin surface to prevent excessive blockage. Perforated configurations use circular holes with diameters of 0.5 *H* and *0.25 H*, representing the large, medium and small perforation cases, respectively, examined in the parametric study. All geometric dimensions are normalised by H for geometric similarity and scalable comparison.

This model serves as a pivotal component in our experimental setup, aimed at investigating its effects on enhancing fluid dynamics and heat transfer processes. The geometry of the VGs, as illustrated in the figure, showcases its distinctive features and potential to induce vortices and modify the flow field. Due to its efficacy in improving the performance of various thermal systems, such VG configurations have been widely studied [19], making them ideal candidates for our research endeavours. By using this specific design, this study aims to elucidate the VGs' impact on the efficiency and effectiveness of heat transfer mechanisms within our experimental apparatus.

The main dimensions refer to Oh and Kim's previous investigation [30]: diameter *D* = 32 mm, length *L* = 6.75, longitudinal pitch *P_L* = 2.25*D*, transverse pitch (*P_T*) = 2*D*, *H* = 7 mm, length of the section with radius 2 *H* and corner radius 60º. The hole widths of the CRW-VGs are 0.25 *H* and 0.5 *H*, with a VG height of 0.9 *H*. The angular position (*α*) indicates the angle measured in an anticlockwise manner from the lengthwise orientation of the tube to the line linking the CRW-VGs to the central point of the tube, (*r*) denotes the distance measured radially from this central point, and *R* represents the radius of the tube. The investigation of these parameters was carried out using variations in position angles (α): 30°, 45°, 60°, 75°, 90°, 105°, 120°, 135° and 150° with *r*/*R* = 1.25 and 1.5.

2.2. Governing Equation

The flow conditions in the system under investigation are assumed to be incompressible, indicating that changes in density due to pressure variations are negligible and do not significantly alter the fluid's behaviour. In the fin tube heat exchanger, a Newtonian fluid with a constant stream is employed. The conservation equations for mass, momentum and energy are expressed as follows:

$$\nabla \cdot \vec{V} = 0 \tag{1}$$

$$\rho(\vec{V} \cdot \nabla)\vec{V} = -\nabla p + \mu \nabla^2 \vec{V} \tag{2}$$

$$\rho \vec{V} \cdot \nabla h = \nabla \cdot (k \nabla T) \tag{3}$$

The notation in the equation above equations, namely $\vec{V}$, ρ, p, h, k, μ, and T involved are the velocity vector, air density, static pressure, thermal conductivity of air, dynamic viscosity, and static temperature, respectively.

The heat transfer performance (TEF) is formulated as follows [31],

$$TEF = (Nu/Nu_0)/(f/f_0)^{1/3} \tag{4}$$

where the Nusselt number (*Nu*) and friction factor (*f*) are formulated as follows.

$$Nu = hL_c/k \tag{5}$$

$$f = 2\Delta pH/(\rho U_c^2\ L) \tag{6}$$

2.3. Computational Domain and Boundary Conditions

Figure 2 illustrates the computational domain of the fin–tube heat exchanger equipped with CRW-VGs. The domain represents the lateral arrangement, flow direction and fin pitch orientation. Owing to geometric uniformity and cyclic configuration, the computational region is defined as half of the transverse pitch (P_T/2) in the x-direction and one full pitch length in the z-direction. This periodic simplification significantly reduces computational costs while preserving the essential flow and heat transfer characteristics.

To ensure an accurate representation of the physical system, steady-state and incompressible flow assumptions are adopted. The domain is extended sufficiently in the streamwise direction to allow proper flow development and to avoid undesirable numerical or physical instabilities.

2.3.1. Boundary conditions

At the inlet, a uniform velocity profile and a constant temperature are specified:

$$\mathrm{u} = (u_{in}, 0, 0), T = T_{in} \tag{7}$$

where u is the velocity vector, u_{in} is the inlet air velocity, and T_{in} is the inlet air temperature.

At the outlet, a constant reference pressure is prescribed:

$$p = p_{out} \tag{8}$$

together with zero-gradient conditions for velocity and temperature:

$$\frac{\partial \mathrm{u}}{\partial n} = 0, \frac{\partial T}{\partial n} = 0 \tag{9}$$

where n denotes the outward normal direction to the outlet boundary.

For all solid surfaces, including the tube, fins, and CRW-VGs, the no-slip condition is applied:

$$\mathrm{u} = 0 \tag{10}$$

A constant wall temperature is imposed on the tube surface:

$$T = T_w \tag{11}$$

where T_w is the prescribed tube wall temperature.

Due to the periodicity of the geometry in the transverse and spanwise directions, periodic boundary conditions are employed:

$$\phi(x, y, z) = \phi(x, y, z + P) \tag{12}$$

where ϕ represents the dependent flow variables (velocity components, pressure and temperature), and P denotes the periodic pitch length.

These boundary conditions ensure physically consistent flow development and reliable prediction of heat transfer and fluid flow characteristics within the computational domain.

Matching boundary conditions are established in the x orientation amid the algorithmic region, while cyclic restrictions are established on both the higher and lower surfaces in the upriver and downriver orientations. The wing region incorporated into the CRW-VGs serves as a barrier, and the tube is subjected to constraints at this enclosure. These conditions ensure stable flow patterns within the algorithmic region, preventing undesired turbulence or instability. Moreover, the no-slip conditions and consistent surface temperature facilitate precise control and optimise the flow dynamics around the wing region and tube enclosure.

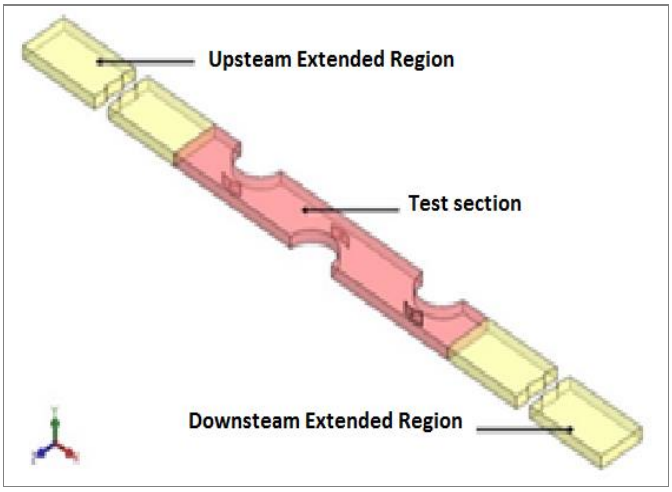

Figure 2. Computational domain

2.4. Convergence Assessment

The convergence of the numerical solution was assessed using a combination of residual-based, physical-based and grid-independence criteria to ensure numerical accuracy and physical reliability.

The normalised residuals of the governing equations were monitored during the iterative process. Convergence was assumed when the residuals of the continuity and momentum equations decreased below 10^{-6}, while a stricter threshold of 10^{-8} was imposed for the energy equation due to the heat transfer-oriented nature of the present study.

In addition to residual monitoring, several global physical quantities were continuously tracked, including the average Nusselt number ($Nu_{\_avg}$), f and outlet bulk temperature (T_{out}). The solution was considered physically converged only when the relative variation in these parameters over 500 successive iterations was satisfied:

$$\left| \frac{\phi^{(n)} - \phi^{(n-500)}}{\phi^{(n)}} \right| < 0.1\% \quad (13)$$

where ϕrepresents $Nu_{\_avg}$, f, or T_{out}, and $n$denotes the iteration number.

10 80 Furthermore, a grid independence study was conducted using four progressively refined meshes ranging from 600,641 to 915,422 elements. The relative deviations of $Nu_{\_avg}$ and f between the two finest meshes were below 0.1%, confirming mesh independence. This value is well within the commonly accepted convergence range of 1%–2% [32]. Thus, the grid with 822,157
13 elements was adopted for all subsequent simulations to achieve an optimal balance between numerical accuracy and computational efficiency.

25 2.5. Grid Independence Test

A grid independence test was carried out for numerical analysis. The computational grid was bifurcated into two parts, specifically the region adjacent to the VGs and the rest of the area. The non-conformal interface approach was implemented between these two zones. To ensure accuracy in analysis and attain optimal grid quality, grid generation employed inflation techniques in the tube vicinity and VGs. As illustrated in Figure 3, the cell geometry utilised around the VGs is tetrahedral because the element can precisely capture arbitrary flow around the complex geometry of the VG [33] and is directly relevant to finely detailed VGs. Four different grid sizes are considered in Table 1 to list the
78 number of cells.

Table 1. Grid independence test

Number of grids	*Nu_avg*	*f*
600,641	16.55447	0.09671
715,421	16.70175	0.09603
822,157	16.79783	0.09551
915,422	16.80972	0.09549

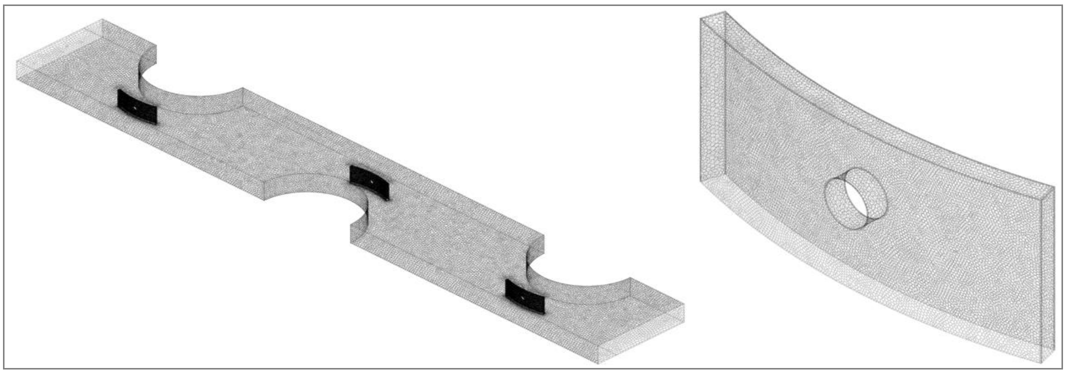

Figure 3. Computational grid test

2.6. Numerical Solution Methodology

12 10 Numerical simulations were performed under steady-state conditions using the finite volume method to solve the 3D governing equations of mass, momentum and energy. Airflow was assumed to be incompressible, Newtonian and turbulent, with constant thermophysical properties.

3 Turbulence effects were modelled using the shear stress transport (SST) k–ωmodel, which combines the robustness of the k–ωformulation near the wall with the freestream independence of the k–εmodel in the outer region. This model is particularly suitable for predicting adverse
54 pressure gradients and flow separation occurring in fin–tube heat exchangers equipped with CRW-VGs.

26 9 The governing equations were discretised using a second-order upwind scheme for the convective terms of momentum and energy equations to enhance numerical accuracy. Pressure–velocity coupling was achieved using the SIMPLE algorithm. Spatial discretisation was applied consistently across the computational domain to ensure numerical stability.

A non-uniform computational grid was employed, with mesh refinement and inflation layers applied near the tube and VG surfaces to accurately capture velocity and thermal boundary layers.
28 A grid independence study was conducted using four mesh resolutions, as detailed in Table 1. The
39 variation in Nu_avg and f between the two finest meshes was less than 0.1%, indicating mesh-

9 independent results. Consequently, the mesh with 822,157 cells was selected for all simulations as an optimal compromise between accuracy and computational cost.

2.7. Validation

The convergence of the numerical solution was ensured by monitoring the normalised
21 residuals of the governing equations. The convergence criteria were set to 10^{-5} for continuity and momentum equations and 10^{-6} for the energy equation. In addition to residual reduction, global quantities, such as Nu_avg and pressure drop, were monitored to confirm the physical convergence of the solution.

The simulation model adopted in this study was based on a previously validated configuration
1 [30], which serves as a reference case for assessing the reliability of the numerical method. Turbulent flow was modelled using the k–ω SST model in conjunction with the governing Eq. (1) to
1 Eq. (3). This model is well known for accurately predicting adverse pressure gradients and flow
76 separation, making it suitable for complex flow simulations in fin–tube heat exchangers equipped with curved VGs.

42 The numerical results were validated against published experimental data [30], as illustrated
7 in Figure 4. The comparison showed good agreement, with deviations of 2%–6% for Nu and 4%–8%
18 for f, and an overall error below 9%. These results confirm the reliability of the present numerical methodology for predicting heat exchanger performance.

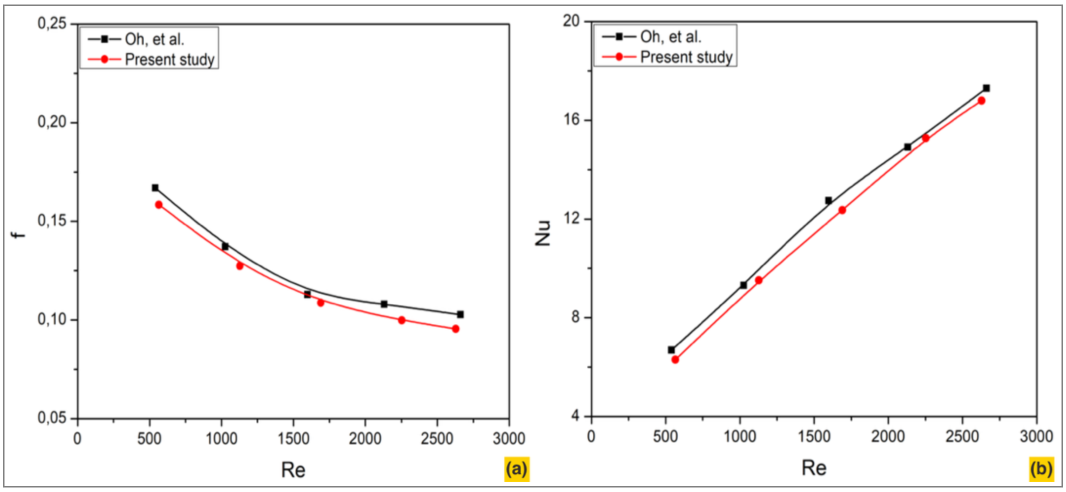

Figure 4. Numerical validation results: (a) *f*; (b) *Nu*

3. Results

3.1. Influence of Geometry and Radial Distance on the $\mathrm{Nu/Nu_o}$ and $\mathrm{f/f_o}$ Values

53 The assessment of heat transfer performance can be observed from the resulting Nu/Nu_o value. The comparison between Nu and Nu_o (Nusselt number under reference conditions) provides insight into heat transfer efficiency. Deviations in Nu/Nu_o signify alterations in the
48 thermal performance of the observed system, as shown in Figure 5 (i.e. (a) is 0.25 *H* and (b) is 0.5
43 *H*). Figure 5 and Figure 6 demonstrate the coupled relationship between heat transfer enhancement and flow resistance as a function of the attack angle, hole width and radial position of the CRW-VGs. As shown in Figure 5, the variation in Nu/Nu_o strongly depends on vortex stability and secondary flow development. At lower angles (30°–60°), moderate longitudinal vortices are
62 generated, resulting in limited boundary layer disruption and moderate heat transfer enhancement. However, as indicated in Figure 6, this regime is accompanied by only a slight increase in f, reflecting a moderate disturbance level within the flow field.

When the angle approaches 75°–90°, both Nu/Nu_o (Figure 5) and f/f_o (Figure 6) reach relatively low values. This behaviour indicates a weakened and less coherent vortex structure, in which
18 reduced mixing leads to minimal heat transfer enhancement and lowered flow resistance. The reduction in heat transfer in this region is mainly attributed to the reduced effective contact area
11 for heat transfer, intensified rotational motion and the formation of lateral vortices on the surface of the perforated VGs [34], which dissipate energy without significantly enhancing boundary layer thinning.

A significant change occurs at 120°: a maximum Nu/Nu$_0$ (**Figure 5**) and a pronounced increase in *f/f$_0$* (**Figure 6**). This correspondence confirms that strong and stable longitudinal vortices are formed at this angle, intensifying cross-stream mixing and effectively thinning the thermal boundary layer. However, enhanced vortex strength also increases shear stress and energy dissipation, leading to higher pressure penalties. This regime represents a high-disturbance, high-
63 enhancement condition in which heat transfer improvement is achieved at the expense of increased friction losses.

77 At larger angles (135°–150°), both Nu/Nu$_0$ and *f/f$_0$* decrease, suggesting vortex breakdown and excessive flow separation. Although flow disturbance remains present, the loss of vortex coherence reduces effective mixing and pressure buildup.

The influence of hole width and radial distance further clarifies the thermo-hydraulic interaction. The smaller hole width (0.25 *H*) produces more concentrated vortices and sharper enhancement peaks in **Figure 5** and relatively controlled friction increases in **Figure 6**. By contrast, the larger hole width (0.5 *H*) allows partial flow penetration through the perforation, promoting distributed secondary flows that increase energy dissipation and friction levels while slightly moderating heat transfer gains. Similarly, increasing the radial distance to r/R = 1.5 strengthens the vortex–wake interaction, enhancing Nu/Nu$_0$ but also elevating *f/f$_0$* because of the intensified momentum exchange.

15 Overall, the combined analysis of **Figure 5** and **Figure 6** confirms that the thermo-hydraulic performance is governed by the balance between vortex intensity, boundary layer disruption and
6 flow resistance. The angle of 120° emerges as the most effective configuration in terms of heat transfer enhancement, although its practical suitability must be evaluated through an integrated
16 metric, such as the TEF, to ensure that the gain in heat transfer justifies the associated pressure penalty.

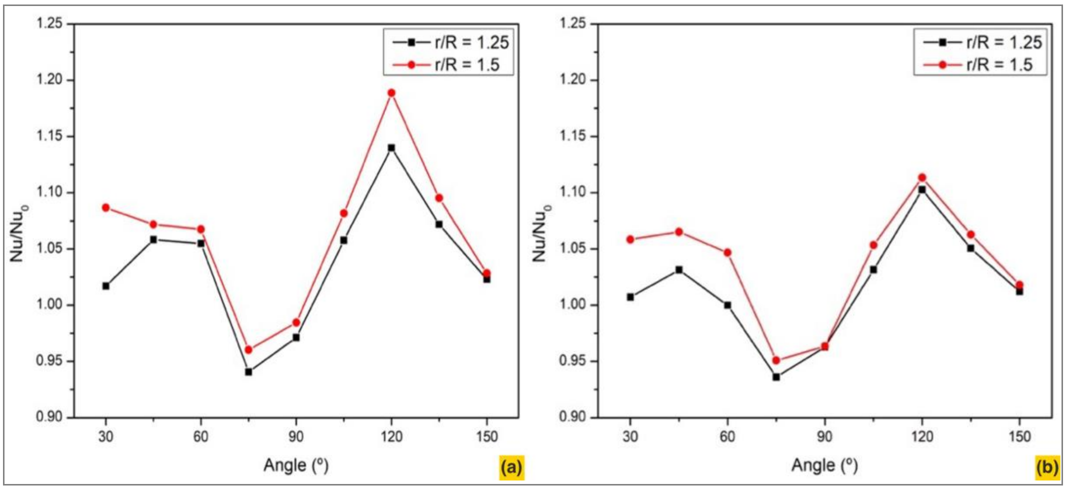

Figure 5. The effect Nu/Nu_o: (a) Hole width CRW-VGs 0.25*H*; (b) Hole width CRW-VGs 0.5*H*

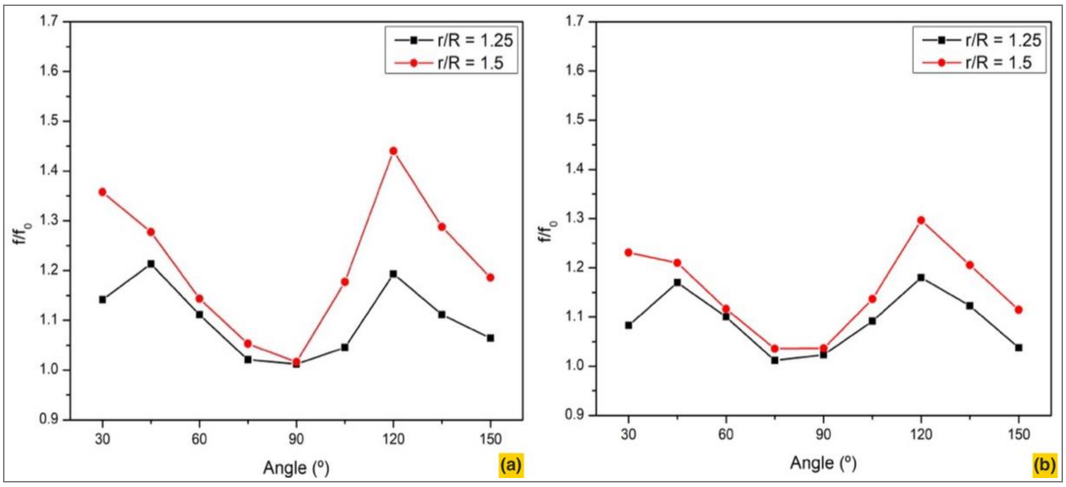

Figure 6. 66 The effect of position angle on the friction factor: (a) Hole width CRW-VGs 0.25*H*; (b) Hole width CRW-VGs 0.5*H*

3.2. Flow Field and Thermal Field Interpretation

27 Reducing *f* with an increase in *Nu* using holes can reduce the pressure drop. As *Nu* and *f* are
27 parameters of the TEF, the heat transfer performance can be determined, as discussed above, by

looking at the contour changes in speed, temperature and pressure in Figure 7 to Figure 12. Figure 7 to Figure 12 reveal that the thermo-hydraulic performance of the CRW-VGs is governed not merely by geometric variation but primarily by the stability regime of the generated longitudinal vortices. Three distinct flow regimes can be identified as the attack angle (α) increases: (i) weak vortex regime (30°–60°), (ii) coherent vortex amplification regime (75°–120°) and (iii) vortex breakdown regime (135°–150°).

In the weak vortex regime, velocity contours (Figure 7 and Figure 8) indicate limited secondary flow development and only a partial disruption of the boundary layer. The generated vortices are insufficient to induce the deep penetration of core flow towards the heated surface.

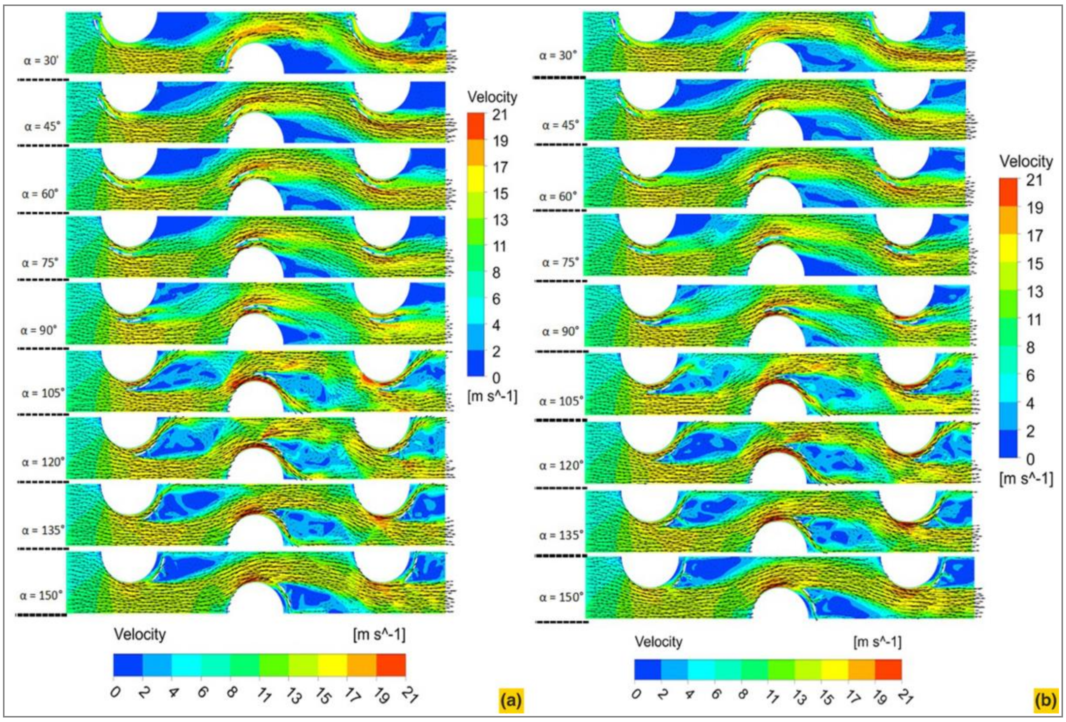

Figure 7. Velocity contour r/R 1.25: (a) Hole width 0.25H; (b) Hole width 0.5H

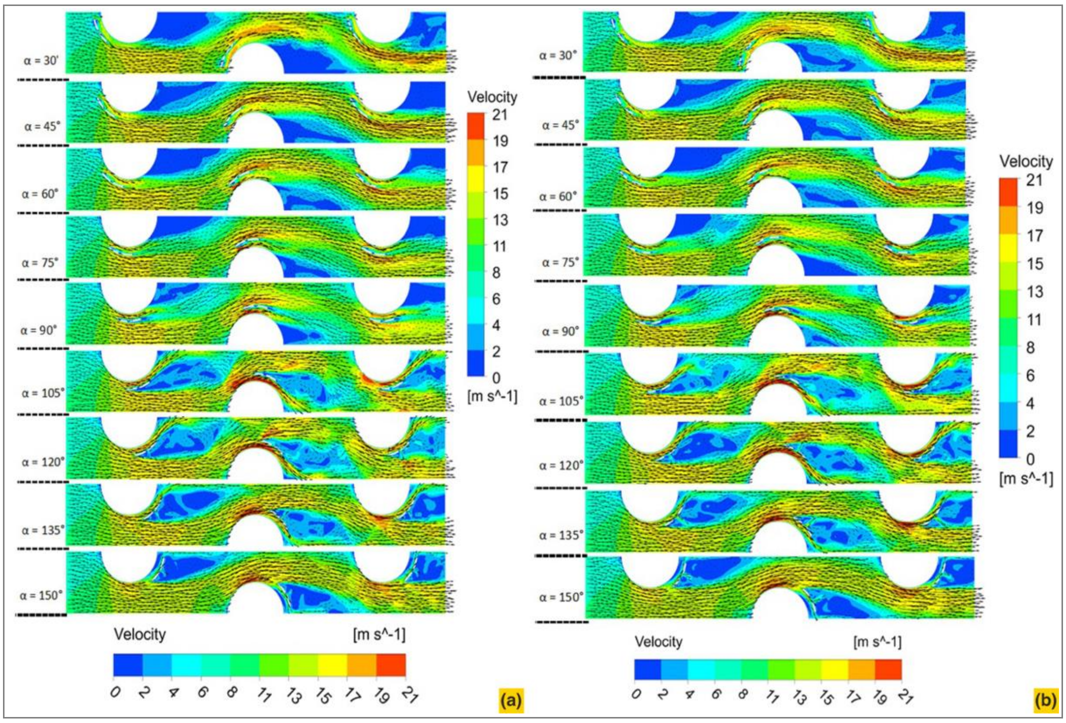

Figure 8. Velocity contour r/R 1.5: (a) Hole width 0.25H; (b) Hole width 0.5H

Consequently, the temperature contours (Figure 11 and Figure 12) show a relatively thick thermal boundary layer and non-uniform temperature stratification. The pressure contours (Figure 9 and Figure 10) display moderate upstream–downstream gradients, indicating limited energy dissipation and relatively small pressure penalties. However, as fluids move swiftly, they have fewer opportunities for prolonged interaction, resulting in smaller pressure drops [35]. This explains why lower attack angles, despite smoother flow behaviour, do not generate substantial convective enhancement.

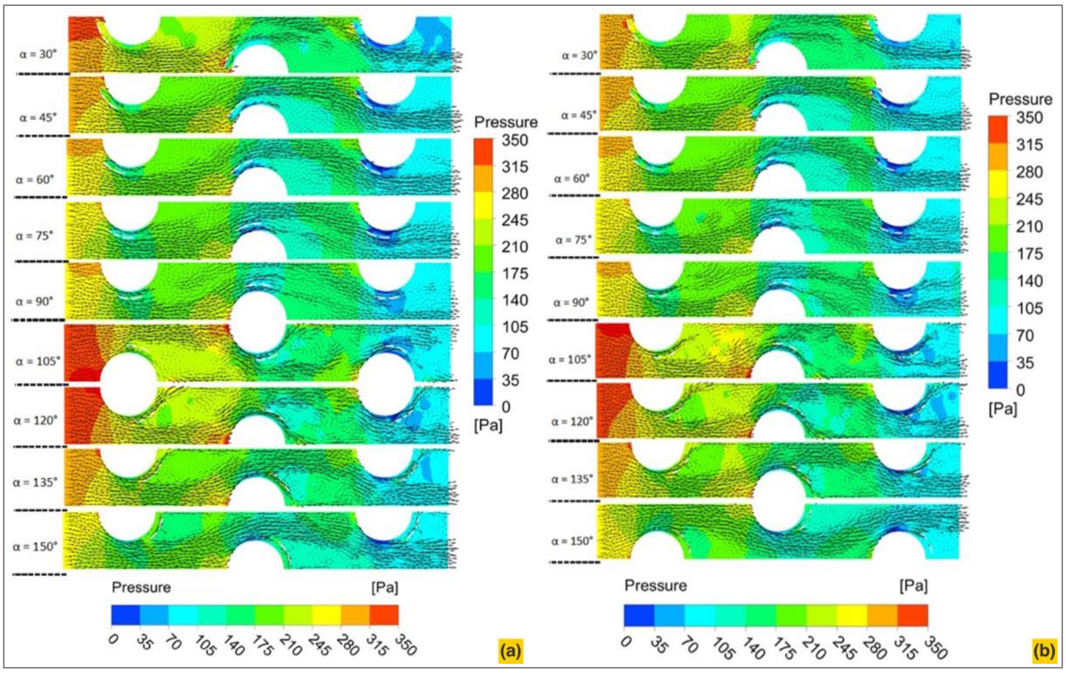

Figure 9. Pressure drop contour *r/R* 1.25: (a) Hole width 0.25*H*; (b) Hole width 0.5*H*

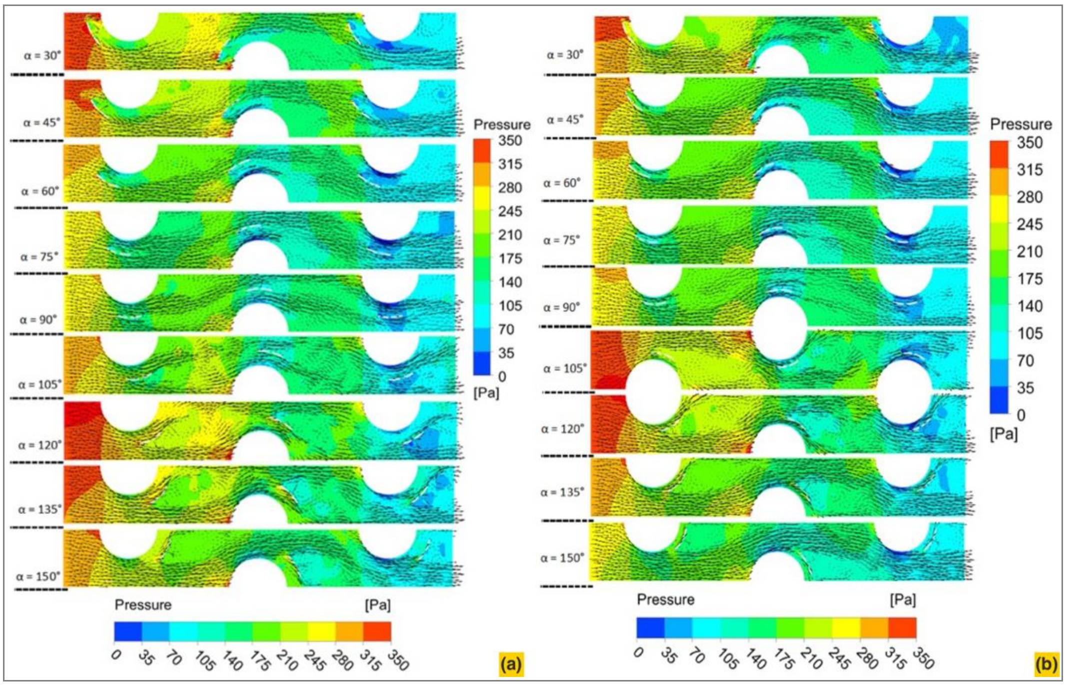

Figure 10. Pressure drop contour *r/R* 1.5: (a) Hole width 0.25*H*; (b) Hole width 0.5*H*

A fundamentally different behaviour emerges in the coherent vortex amplification regime (α ≈ 105°–120°). In this range, the velocity field exhibits highly organised longitudinal vortices with an intensified cross-stream momentum exchange. The vortices transport high-momentum core fluid towards the heated wall while ejecting low-momentum near-wall fluid outward, significantly thinning the thermal boundary layer. The temperature distribution becomes more uniform, thus confirming enhanced convective transport. Simultaneously, the pressure field exhibits the most pronounced gradients, reflecting maximal shear production and vortex strength.

47

Nevertheless, the perforated configuration introduces an additional mechanism. As depicted in **Figure 9** and **Figure 10**, the jet stream emanating from the orifice of the CRW-VGs has the potential to alleviate stagnation flow, consequently reducing the pressure drop [36], [37], [38]. This jet-induced acceleration redistributes local pressure peaks and mitigates excessive recirculation behind the VG, thereby partially compensating for the pressure penalty associated with strong vortex generation. Therefore, this regime represents a critical transition state in which vortex strength and structural coherence are maximised, while perforation-induced jet flow moderates stagnation-related losses.

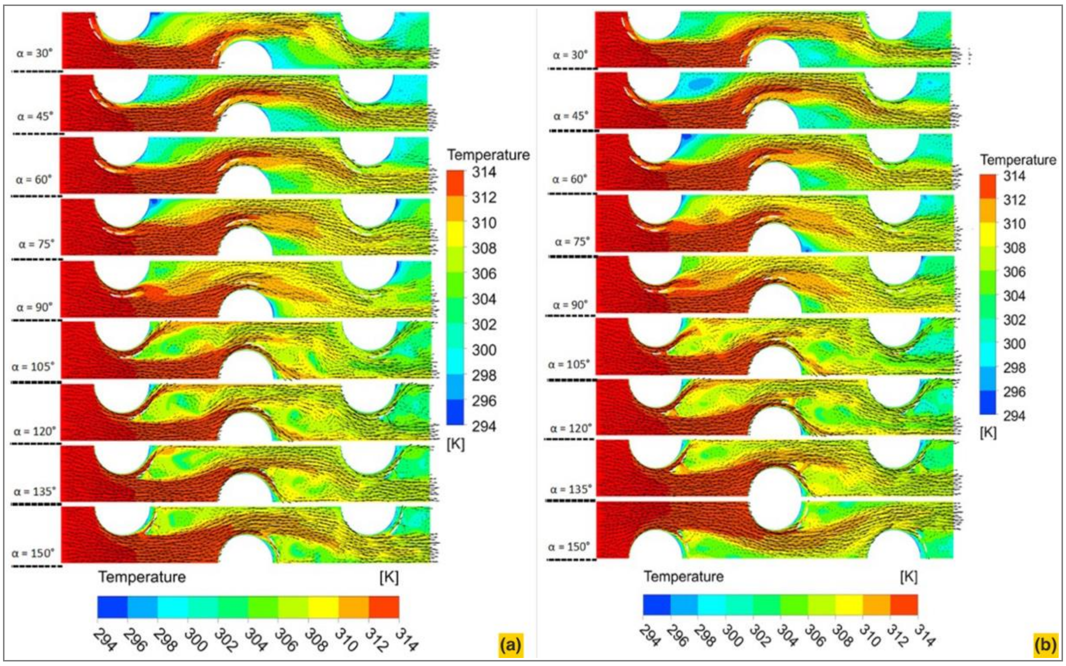

Figure 11. Temperature contour *r/R* 1.25: (a) Hole width 0.25*H*; (b) Hole width 0.5*H*

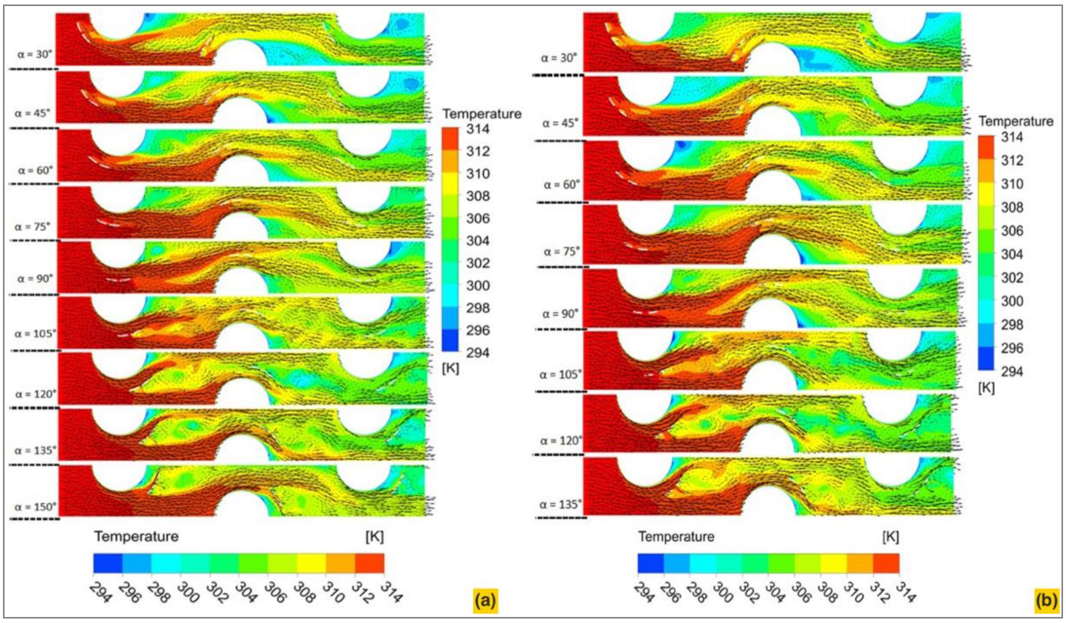

Figure 12. Temperature contour *r/R* 1.5: (a) Hole width 0.25*H*; (b) Hole width 0.5*H*

When α ≥ 135°, the system enters a vortex breakdown regime. Although apparent disturbance increases, velocity contours reveal fragmented and unstable vortical structures. The pressure distribution becomes spatially irregular, indicating that kinetic energy is increasingly dissipated through chaotic separation rather than organised secondary motion. As a result, temperature contours show reduced effectiveness in boundary layer thinning, despite intensified disturbance. This demonstrates that excessive geometric forcing shifts the system from a structured convective enhancement to instability-driven dissipation.

The geometric parameters further modulate these mechanisms. An increasing radial position to r/R = 1.5 enhances the wake–vortex interaction and prolongs vortex persistence, intensifying the heat transfer but also elevating the pressure penalties. Similarly, a smaller hole width (0.25 *H*) generates concentrated vortices and sharper shear layers, thereby promoting a stronger boundary layer disruption. By contrast, a larger hole width (0.5 *H*) allows for greater flow penetration through the perforation, redistributing vortex energy and stabilising the pressure field, thereby offering a more balanced thermo-hydraulic response.

Overall, the results demonstrate that thermo-hydraulic optimization is governed by vortex coherence rather than vortex magnitude alone. The optimal configuration (α ≈ 105°–120°) corresponds to the condition where organized secondary flow production is maximized, stagnation effects are partially mitigated by jet-induced flow through perforations, and instability-driven energy dissipation has not yet dominated the system. This mechanistic interpretation advances the understanding of perforated vortex generators by identifying vortex stability and jet–wake interaction as the primary control parameters governing performance. As illustrated in **Figure 13**, the streamline and velocity contours reveal a coherent high-velocity core developing along the inner wall of the curved channel, accompanied by jet-induced momentum injection from the perforations into the wake region. This mechanism promotes thermal boundary layer thinning through enhanced near-wall acceleration while simultaneously suppressing large-scale recirculation that would otherwise increase frictional losses. The interaction between curvature-driven Dean vortices and the longitudinal vortices generated by the VG further intensifies transverse momentum exchange, improving convective transport uniformity along the heated surface. Consequently, the heat transfer augmentation achieved within the optimal angular range is not merely a function of vortex strength, but rather of sustained vortex organization and controlled jet–wake stabilization, which collectively ensure enhanced Nusselt number performance with moderated pressure penalties.

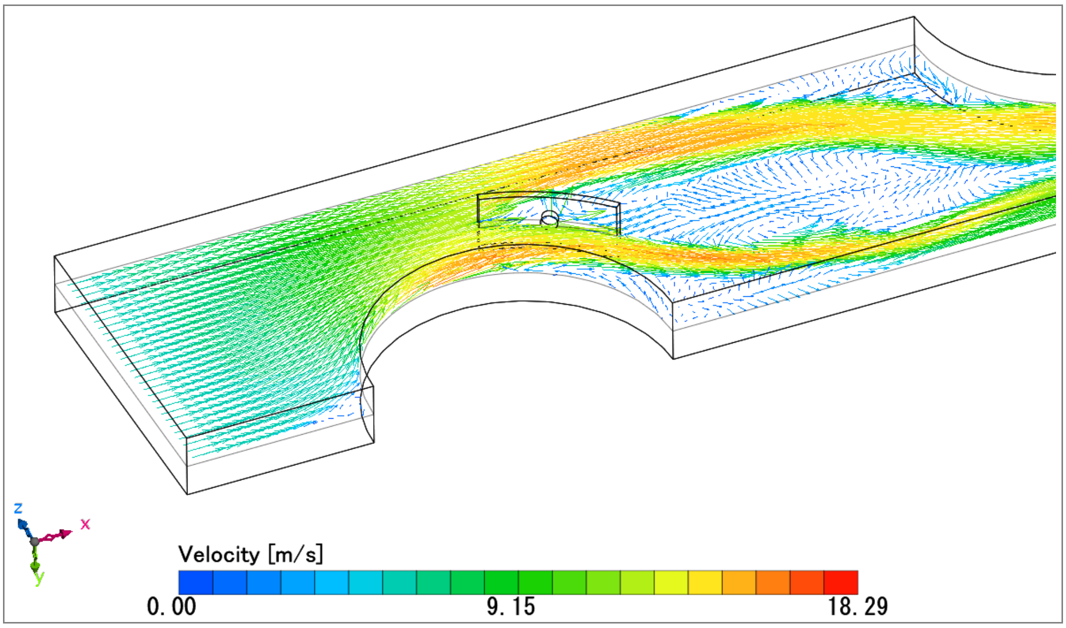

Figure 13. Streamline velocity α = 120°, *r/R* = 1.25, hole width = 0.5*H*

3.3. Influence of Geometry and Radial Distance on Thermal Enhancement Factor

The variation in the TEF with the r/R ratio at different angular positions is presented in **Figure 14a** and **Figure 14b** for hole widths of 0.25 *H* and 0.5 *H*, respectively. For both configurations, r/R = 1.25 consistently produces higher TEF values than r/R = 1.5, with the most pronounced improvement occurring at α = 120°. The maximum TEF reaches 1.075 for 0.25 *H* and 1.064 for 0.5 *H*. This trend indicates that a shorter radial distance provides a more favourable balance between heat transfer augmentation and friction penalty.

The superior performance at r/R = 1.25 is associated with a more effective vortex–jet interaction and controlled suppression of mixed-vortex interference. At α ≈ 120°, the wake region behind the tube is significantly weakened, promoting enhanced near-wall momentum exchange and boundary-layer disruption. Such overlapping vortex configurations signal a shift towards a more intensified turbulent regime [39], which is known to strengthen convective heat transfer mechanisms [40].

Although larger radial spacing intensifies vortex structures, it also increases flow resistance, thereby reducing the overall TEF, despite higher local heat transfer rates. The combined trends of Nu/Nu_0 and f/f_0 confirm that optimal thermo-hydraulic performance is governed by the synergy between vortex positioning, jet reinforcement and wake suppression rather than vortex strength alone.

4 The combined analysis of Nu/Nu$_0$ and f/f_0 (**Figure 5** and **Figure 12**) supports this behaviour. Increasing hole width reduces f, thereby mitigating the pressure drop, consistent with previous findings [41]. The jet streams generated by the CRW-VGs alleviate stagnant flow regions, particularly between 30° and 90°, while beyond 105°, the interaction between intensified vortices and wake dynamics temporarily elevates the pressure drop before stabilising near 120°. The temperature contours further confirm that higher angular positions weaken the recirculation zone and enhance thermal mixing.

Overall, the TEF distribution in **Figure 14** demonstrates that thermo-hydraulic optimisation is governed not only by vortex strength but also by the synergy between vortex positioning, jet reinforcement and wake suppression. The peak performance at r/R = 1.25 and α = 120° highlights the importance of geometric tuning to achieve maximum heat transfer enhancement with controlled hydraulic losses. These findings provide deeper physical insight into jet-assisted vortex dynamics and offer practical guidance for optimising VG placement in compact heat exchanger applications.

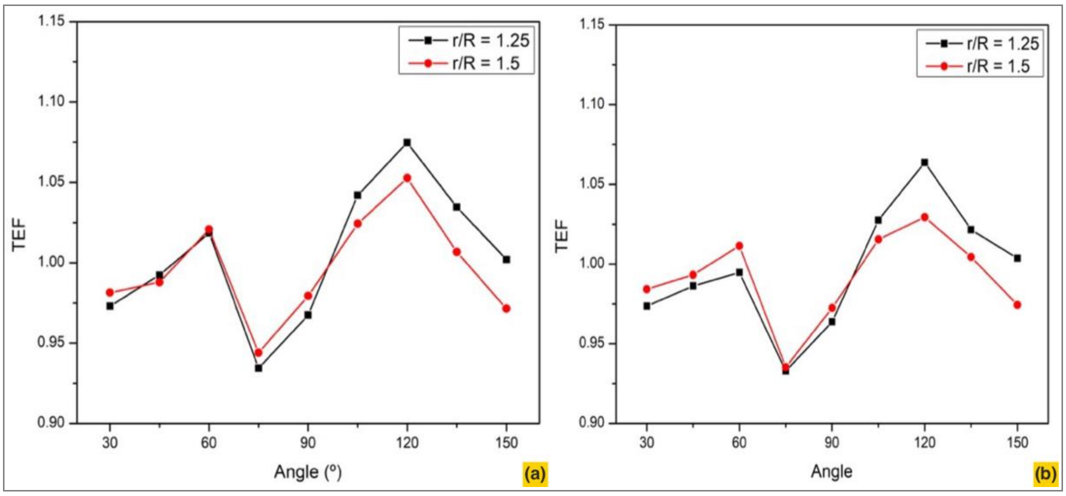

Figure 14. Thermal enhancement factor graph: (a) RWVGs hole width 0.25*H*; (b) RWVGs hole width 0.5*H*

12 3.4. Economic and Practical Implications of Thermal Enhancement Factor

The maximum TEF obtained in the present study is approximately 1.075, corresponding to a net thermo-hydraulic improvement of about 7%–8% under constant fan power conditions. Although this enhancement may appear moderate compared with some studies reporting TEF values in the range of 1.2–1.5 [42], [43], [44], it is important to recognise that such higher values are often associated with substantial pressure penalties or aggressive vortex geometries that may
29 not be suitable for practical air-side applications. In fin–tube heat exchangers operating with low-density air, even a 5%–10% improvement in overall performance is practically meaningful, as it can
50 reduce the required heat transfer surface area for a given thermal duty, improve compactness or lower long-term fan energy consumption [45], [46], [47].

From a manufacturing standpoint, the proposed perforated CRW-VGs are passive devices integrated directly with the fin structure and fabricated from thin sheet material. The addition of perforations does not introduce significant production complexity and can be implemented using conventional stamping or punching techniques commonly employed in fin manufacturing. Consequently, the incremental fabrication cost is expected to be minimal, particularly in large-scale production.

Moreover, the perforated configuration helps mitigate an excessive increase in pressure compared with solid VGs, thereby reducing aerodynamic loading on the fan system. The resulting
68 balance between heat transfer enhancement and controlled friction penalty demonstrates that the proposed design achieves realistic thermo-hydraulic optimisation rather than maximum vortex intensity alone. Although a comprehensive life-cycle cost analysis is beyond the scope of this numerical study, the combination of TEF greater than unity, moderate pressure penalties and low manufacturing complexity supports the technical relevance and economic feasibility of the

proposed configuration for practical Heating, Ventilation, and Air Conditioning and compact thermal management applications.

4. Conclusions

15 37 This study reveals that the thermo-hydraulic performance of CRW-VGs is governed by the interaction between vortex positioning, jet momentum and wake suppression rather than vortex strength alone. The results explicitly show that a shorter radial distance (r/R = 1.25) provides a more favourable balance between heat transfer enhancement and pressure penalty than r/R = 1.5. Although larger radial spacing intensifies vortex structures and increases Nu/Nu_0, the accompanying increase in f reduces the overall TEF.

7 73 The optimal angular position is identified at α = 120°, at which the wake region behind the tube is significantly weakened. This configuration promotes a stronger near-wall momentum exchange, a more uniform boundary-layer disruption and improved thermal mixing. The TEF reaches its maximum values of 1.075 (0.25 *H*) and 1.064 (0.5 *H*) under this condition, confirming that wake restructuring plays a decisive role in thermo-hydraulic optimisation.

64 Furthermore, increasing the feeding hole width enhances jet strength, which intensifies turbulence and redistributes momentum more effectively. More importantly, this jet-assisted mechanism contributes not only to heat transfer augmentation but also to moderating pressure losses, demonstrating that momentum redistribution is more critical than simply increasing vortex intensity.

Overall, the findings establish that the optimal CRW-VG design requires controlled vortex suppression, strategic angular positioning and jet reinforcement to achieve maximum TEF. These results provide mechanistic insight into jet–vortex synergy and offer practical guidance for high-efficiency compact heat exchanger design.

Acknowledgements

5 The author extends gratitude to Office of Research UHAMKA for support for this research and to the Office of Publication of UHAMKA for their assistance in providing technical guidance. This research was not funded by any grant.

Authors' Declaration

Authors' contributions and responsibilities – The authors made substantial contributions to the conception and design of the study. The authors took responsibility for data analysis, interpretation and discussion of results. The authors read and approved the final manuscript.

5 **Funding** – This research was not funded by any grant.

Availability of data and materials – All data is available from the authors.

Competing interests – The authors declare no competing interests.

Additional information – No additional information from the authors.

Nomenclature

D	: Tube diameter (m)	r	: Radial distance of VG from tube center (m)
f	: Darcy friction factor (–)	R	: Tube radius (m)
f_0	: Friction factor without vortex generator (–)	T	: Static temperature (K)
H	: Channel height (m)	T_{in}	: Inlet air temperature (K)
k	: Thermal conductivity of air (W m^{-1} K^{-1})	T_w	: Tube wall temperature (K)
L	: Tube length (m)	α	: Angular position of vortex generator (degree)
N_u	: Nusselt number (–)	μ	: Dynamic viscosity (Pa s)
Nu_{avg}	: Average Nusselt number (–)	ρ	: Air density (kg m^{-3})
Nu_0	: Nusselt number without vortex generator (–)	r/R	: Radial distance ratio (–)
P	: Static pressure (Pa)	Nu/Nu_0	: Nusselt number ratio (–)
P_L	: Longitudinal pitch (m)	f/f_0	: Friction factor ratio (–)
P_T	: Transverse pitch (m)	TEF	: Thermal enhancement factor (–)

References

[1] K. Torii, K. M. Kwak, and K. Nishino, "Heat transfer enhancement accompanying pressure-loss reduction with winglet-type vortex generators for fin-tube heat exchangers," *International Journal of Heat and Mass Transfer*, vol. 45, no. 18, pp. 3795–3801, Aug. 2002, doi: 10.1016/S0017-9310(02)00080-7.

[2] P. T. Tsilingiris, "Review and critical comparative evaluation of moist air thermophysical properties at the temperature range between 0 and 100 °C for Engineering Calculations," *Renewable and Sustainable Energy Reviews*, vol. 83, pp. 50–63, Mar. 2018, doi: 10.1016/j.rser.2017.10.072.

[3] Dan Mugisidi, Oktarina Heriyani, Pancatatva Hesti Gunawan, and Dwi Apriani, "Performance Improvement of a Forced Draught Cooling Tower Using a Vortex Generator," *CFD Letters*, vol. 13, no. 1, pp. 45–57, Jan. 2021, doi: 10.37934/cfdl.13.1.4557.

[4] Syaiful, H. Nabilah, M. S. K. T. Suryo Utomo, A. Suprihanto, and M. F. Soetanto, "Numerical simulation of heat transfer enhancement from tubes surface to airflow using concave delta winglet vortex generators," *Results in Engineering*, vol. 16, p. 100710, Dec. 2022, doi: 10.1016/j.rineng.2022.100710.

[5] M. Awais and A. A. Bhuiyan, "Heat transfer enhancement using different types of vortex generators (VGs): A review on experimental and numerical activities," *Thermal Science and Engineering Progress*, vol. 5, pp. 524–545, Mar. 2018, doi: 10.1016/j.tsep.2018.02.007.

[6] S. K. Sarangi and D. P. Mishra, "Effect of winglet location on heat transfer of a fin-and-tube heat exchanger," *Applied Thermal Engineering*, vol. 116, pp. 528–540, Apr. 2017, doi: 10.1016/j.applthermaleng.2017.01.106.

[7] K. Song, Z. Xi, M. Su, L. Wang, X. Wu, and L. Wang, "Effect of geometric size of curved delta winglet vortex generators and tube pitch on heat transfer characteristics of fin-tube heat exchanger," *Experimental Thermal and Fluid Science*, vol. 82, pp. 8–18, Apr. 2017, doi: 10.1016/j.expthermflusci.2016.11.002.

[8] A. Boonloi and W. Jedsadaratanachai, "Air Flow, Thermal Profile, and Thermohydraulic Performance Assessment in a Square Duct Heat Exchanger With Combined Vortex Generators: CFD Analysis," *Journal of Engineering*, vol. 2025, no. 1, Jan. 2025, doi: 10.1155/je/4197880.

[9] H. Karkaba, T. Dbouk, C. Habchi, S. Russeil, T. Lemenand, and D. Bougeard, "Multiobjective optimization of Vortex Generators for heat transfer enhancement in turbulent flows," *International Journal of Thermofluids*, vol. 22, p. 100633, May 2024, doi: 10.1016/j.ijft.2024.100633.

[10] H. Arjmandi, R. Amini, A. Ghaffari, H. Rahmani, and A. Chamkha, "Effects of baffles and vortex generators on cooling performance of a gas turbine combustion chamber: Numerical assessment," *Alexandria Engineering Journal*, vol. 61, no. 6, pp. 4467–4478, Jun. 2022, doi: 10.1016/j.aej.2021.10.005.

[11] U. Kashyap, K. Das, and B. K. Debnath, "Effect of surface modification of a rectangular vortex generator on heat transfer rate from a surface to fluid: An extended study," *International Journal of Thermal Sciences*, vol. 134, pp. 269–281, Dec. 2018, doi: 10.1016/j.ijthermalsci.2018.08.020.

[12] H. Naik and S. Tiwari, "Effect of winglet location on performance of fin-tube heat exchangers with inline tube arrangement," *International Journal of Heat and Mass Transfer*, vol. 125, pp. 248–261, Oct. 2018, doi: 10.1016/j.ijheatmasstransfer.2018.04.071.

[13] Z. Qian, Q. Wang, and J. Cheng, "Analysis of heat and resistance performance of plate fin-and-tube heat exchanger with rectangle-winglet vortex generator," *International Journal of Heat and Mass Transfer*, vol. 124, pp. 1198–1211, Sep. 2018, doi: 10.1016/j.ijheatmasstransfer.2018.04.037.

[14] K. Srivastava and R. R. Sahoo, "Effect of pitch and angle of attack on thermal performance of new envelope and delta vortex generators for TEG: An experimental and numerical approach," *International Journal of Thermal Sciences*, vol. 195, p. 108671, Jan. 2024, doi: 10.1016/j.ijthermalsci.2023.108671.

[15] C. Luo, S. Wu, K. Song, L. Hua, and L. Wang, "Thermo-hydraulic performance optimization of wavy fin heat exchanger by combining delta winglet vortex generators," *Applied Thermal*

Engineering, vol. 163, p. 114343, Dec. 2019, doi: 10.1016/j.applthermaleng.2019.114343.

[16] O. Heriyani, M. Djaeni, Syaiful, and A. K. Putri, "Perforated concave rectangular winglet pair vortex generators enhance the heat transfer of air flowing through heated tubes inside a channel," *Results in Engineering*, vol. 16, p. 100705, Dec. 2022, doi: 10.1016/j.rineng.2022.100705.

[17] M. Dogan and S. Erzincan, "Experimental investigation of thermal performance of novel type vortex generator in rectangular channel," *International Communications in Heat and Mass Transfer*, vol. 144, p. 106785, May 2023, doi: 10.1016/j.icheatmasstransfer.2023.106785.

[18] Z. Ke, C.-L. Chen, K. Li, S. Wang, and C.-H. Chen, "Vortex dynamics and heat transfer of longitudinal vortex generators in a rectangular channel," *International Journal of Heat and Mass Transfer*, vol. 132, pp. 871–885, Apr. 2019, doi: 10.1016/j.ijheatmasstransfer.2018.12.064.

[19] H. Fu, H. Sun, L. Yang, L. Yan, Y. Luan, and F. Magagnato, "Effects of the configuration of the delta winglet longitudinal vortex generators and channel height on flow and heat transfer in minichannels," *Applied Thermal Engineering*, vol. 227, p. 120401, Jun. 2023, doi: 10.1016/j.applthermaleng.2023.120401.

[20] J. Batista, A. Trp, K. Lenic, and M. Kirincic, "The influence of geometry parameters of rectangular vortex generators on the air-to-water fin-and-tube heat exchanger efficiency enhancement," *International Communications in Heat and Mass Transfer*, vol. 162, p. 108647, Mar. 2025, doi: 10.1016/j.icheatmasstransfer.2025.108647.

[21] D. Jin, S. Quan, J. Zuo, and S. Xu, "Numerical investigation of heat transfer enhancement in a solar air heater roughened by multiple V-shaped ribs," *Renewable Energy*, vol. 134, pp. 78–88, Apr. 2019, doi: 10.1016/j.renene.2018.11.016.

[22] S. Pourhedayat, S. M. Pesteei, H. E. Ghalinghie, M. Hashemian, and M. A. Ashraf, "Thermal-exergetic behavior of triangular vortex generators through the cylindrical tubes," *International Journal of Heat and Mass Transfer*, vol. 151, p. 119406, Apr. 2020, doi: 10.1016/j.ijheatmasstransfer.2020.119406.

[23] J. Wang, L. Zeng, T. Fu, S. Yu, and Y. He, "Effects of the position and perforation parameters of the delta winglet vortex generators on flow and heat transfer in minichannels," *International Journal of Thermal Sciences*, vol. 198, p. 108878, Apr. 2024, doi: 10.1016/j.ijthermalsci.2023.108878.

[24] P. Promvonge and S. Skullong, "Heat transfer augmentation in solar receiver heat exchanger with hole-punched wings," *Applied Thermal Engineering*, vol. 155, pp. 59–69, Jun. 2019, doi: 10.1016/j.applthermaleng.2019.03.132.

[25] M. E. Nakhchi, M. Hatami, and M. Rahmati, "Experimental investigation of performance improvement of double-pipe heat exchangers with novel perforated elliptic turbulators," *International Journal of Thermal Sciences*, vol. 168, p. 107057, Oct. 2021, doi: 10.1016/j.ijthermalsci.2021.107057.

[26] A. J. Modi, N. A. Kalel, and M. K. Rathod, "Thermal performance augmentation of fin-and-tube heat exchanger using rectangular winglet vortex generators having circular punched holes," *International Journal of Heat and Mass Transfer*, vol. 158, p. 119724, Sep. 2020, doi: 10.1016/j.ijheatmasstransfer.2020.119724.

[27] Z. Han, Z. Xu, and J. Wang, "Numerical simulation on heat transfer characteristics of rectangular vortex generators with a hole," *International Journal of Heat and Mass Transfer*, vol. 126, pp. 993–1001, Nov. 2018, doi: 10.1016/j.ijheatmasstransfer.2018.06.081.

[28] J. Wang, T. Fu, L. Zeng, F. Lien, and G. Chen, "Thermal-hydraulic performance in a tube with punched delta winglets inserts in turbulent flow," *International Journal of Thermal Sciences*, vol. 172, p. 107326, Feb. 2022, doi: 10.1016/j.ijthermalsci.2021.107326.

[29] P. Saini and M. P. Shah, "Performance evaluation of finned tube heat exchanger using curved wavy delta winglet vortex generators with circular perforations," *International Communications in Heat and Mass Transfer*, vol. 159, p. 108184, Dec. 2024, doi: 10.1016/j.icheatmasstransfer.2024.108184.

[30] Y. Oh and K. Kim, "Effects of position and geometry of curved vortex generators on fin-tube heat-exchanger performance characteristics," *Applied Thermal Engineering*, vol. 189, p. 116736, May 2021, doi: 10.1016/j.applthermaleng.2021.116736.

[31] M.-W. Tian, S. Khorasani, H. Moria, S. Pourhedayat, and H. S. Dizaji, "Profit and efficiency boost of triangular vortex-generators by novel techniques," *International Journal of Heat and Mass Transfer*, vol. 156, p. 119842, Aug. 2020, doi: 10.1016/j.ijheatmasstransfer.2020.119842.

[32] P. Knödler and V. Dreissigacker, "Fluid Dynamic Assessment and Development of Nusselt Correlations for Fischer Koch S Structures," *Energies*, vol. 17, no. 3, p. 688, Jan. 2024, doi: 10.3390/en17030688.

[33] X. Zou, S. B. Lo, R. Sevilla, O. Hassan, and K. Morgan, "The generation of tetrahedral meshes for NURBS-enhanced FEM," *Engineering with Computers*, vol. 40, no. 6, pp. 3949–3977, Dec. 2024, doi: 10.1007/s00366-024-02004-z.

[34] P. Saini, A. Dhar, and S. Powar, "Performance enhancement of fin and tube heat exchanger employing curved delta winglet vortex generator with circular punched holes," *International Journal of Thermofluids*, vol. 20, p. 100452, Nov. 2023, doi: 10.1016/j.ijft.2023.100452.

[35] M. K. Fahad, N. F. Ifraj, S. H. Tahsin, and M. J. Hasan, "Numerical investigation of the hydrothermal performance of novel vortex generators in a rectangular channel by employing inclination and rotational angles," *International Journal of Thermofluids*, vol. 20, p. 100500, Nov. 2023, doi: 10.1016/j.ijft.2023.100500.

[36] S. Gururatana and S. Skullong, "Heat transfer augmentation in a pipe with 3D printed wavy insert," *Case Studies in Thermal Engineering*, vol. 21, p. 100698, Oct. 2020, doi: 10.1016/j.csite.2020.100698.

[37] A. Sinha, H. Chattopadhyay, A. K. Iyengar, and G. Biswas, "Enhancement of heat transfer in a fin-tube heat exchanger using rectangular winglet type vortex generators," *International Journal of Heat and Mass Transfer*, vol. 101, pp. 667–681, Oct. 2016, doi: 10.1016/j.ijheatmasstransfer.2016.05.032.

[38] D. Hu *et al.*, "Performance optimization of a wavy finned-tube heat exchanger with staggered curved vortex generators," *International Journal of Thermal Sciences*, vol. 183, p. 107830, Jan. 2023, doi: 10.1016/j.ijthermalsci.2022.107830.

[39] K. Srivastava and R. R. Sahoo, "Experimental and numerical study on thermal performance of new envelope and triangular vortex generators with different pitch and angle of attack," *Thermal Science and Engineering Progress*, vol. 49, p. 102459, Mar. 2024, doi: 10.1016/j.tsep.2024.102459.

[40] A. J. Modi and M. K. Rathod, "Experimental investigation of heat transfer enhancement and pressure drop of fin-and-circular tube heat exchangers with modified rectangular winglet vortex generator," *International Journal of Heat and Mass Transfer*, vol. 189, p. 122742, Jun. 2022, doi: 10.1016/j.ijheatmasstransfer.2022.122742.

[41] R. B. Pérez, A. M. Pérez, and D. S. Suárez, "Influence of the punched holes on thermohydraulic performance and flow pattern of rectangular channels with a pair of perforated vortex generators," *International Journal of Heat and Mass Transfer*, vol. 184, p. 122291, Mar. 2022, doi: 10.1016/j.ijheatmasstransfer.2021.122291.

[42] J. Wang, L. Zeng, Y. He, B. Zhao, and P. Chu, "Effect of structure parameters on thermal performance of novel punched V-shape VGs for hear exchangers: An experimental approach," *International Communications in Heat and Mass Transfer*, vol. 155, p. 107472, Jun. 2024, doi: 10.1016/j.icheatmasstransfer.2024.107472.

[43] J. Wang, C. Li, L. Zeng, T. Fu, and K. Liu, "Thermal performance analysis of a heat exchanger with a novel turbulator insert by using machine learning method," *Case Studies in Thermal Engineering*, vol. 72, p. 106412, Aug. 2025, doi: 10.1016/j.csite.2025.106412.

[44] A. Boonloi and W. Jedsadaratanachai, "Turbulent forced convection in a square duct heat exchanger (SDHX) equipped with combined vortex turbulators (CVT): A numerical investigation," *International Communications in Heat and Mass Transfer*, vol. 161, p. 108421, Feb. 2025, doi: 10.1016/j.icheatmasstransfer.2024.108421.

[45] W. Wei, G. Xu, Y. Wang, and E. Ding, "Study on air-side performance of air-cooled heat exchangers under large air velocity and wet conditions," *Thermal Science and Engineering Progress*, vol. 48, p. 102389, Feb. 2024, doi: 10.1016/j.tsep.2024.102389.

[46] P. Yang, T. Qing, X. Lei, L. Wang, and Y. Liu, "Experimental study on thermal–hydraulic performance of moist air inside flat tube of two kinds of plate-fin heat exchangers," *Applied Thermal Engineering*, vol. 239, p. 122121, Feb. 2024, doi:

10.1016/j.applthermaleng.2023.122121.

[47] M. H. Alshameri, A. A. Azizuddin, A. Arshad, H. G. Mohammed, and S. Sadeq, "Experimental Analysis of Thermal and Hydraulic Performance of Fiber-Reinforced Polymer Fins in Compact Heat Exchangers," *International Journal of Automotive and Mechanical Engineering*, vol. 22, no. 2, pp. 12496–12510, Jun. 2025, doi: 10.15282/ijame.22.2.2025.18.0955.